AGARD-AG-295

AGARD

ADVISORY GROUP FOR AEROSPACE RESEARCH & DEVELOPMENT

7 RUE ANCELLE 92200 NEUILLY SUR SEINE FRANCE

AGARDograph No.295

The Aerodynamics of Parachutes

NORTH ATLANTIC TREATY ORGANIZATION

AGARD-AG-295

NORTH ATLANTIC TREATY ORGANIZATION

ADVISORY GROUP FOR AEROSPACE RESEARCH AND DEVELOPMENT

(ORGANISATION DU TRAITE DE L'ATLANTIQUE NORD)

AGARDograph No.295

THE AERODYNAMICS OF PARACHUTES

by

D.J.Cockrell
Department of Engineering
The University
Leicester LE1 7RH
United Kingdom

Edited by

A.D.Young
70 Gilbert Road
Cambridge CB4 3PD
United Kingdom

This AGARDograph has been produced at the request of the Fluid Dynamics Panel of AGARD.

THE MISSION OF AGARD

The mission of AGARD is to bring together the leading personalities of the NATO nations in the fields of science and technology relating to aerospace for the following purposes:

- Exchanging of scientific and technical information;
- Continuously stimulating advances in the aerospace sciences relevant to strengthening the common defence posture;
- Improving the co-operation among member nations in aerospace research and development;
- Providing scientific and technical advice and assistance to the Military Committee in the field of aerospace research and development (with particular regard to its military application);
- Rendering scientific and technical assistance, as requested, to other NATO bodies and to member nations in connection with research and development problems in the aerospace field;
- Providing assistance to member nations for the purpose of increasing their scientific and technical potential;
- Recommending effective ways for the member nations to use their research and development capabilities for the common benefit of the NATO community.

The highest authority within AGARD is the National Delegates Board consisting of officially appointed senior representatives from each member nation. The mission of AGARD is carried out through the Panels which are composed of experts appointed by the National Delegates, the Consultant and Exchange Programme and the Aerospace Applications Studies Programme. The results of AGARD work are reported to the member nations and the NATO Authorities through the AGARD series of publications of which this is one.

Participation in AGARD activities is by invitation only and is normally limited to citizens of the NATO nations.

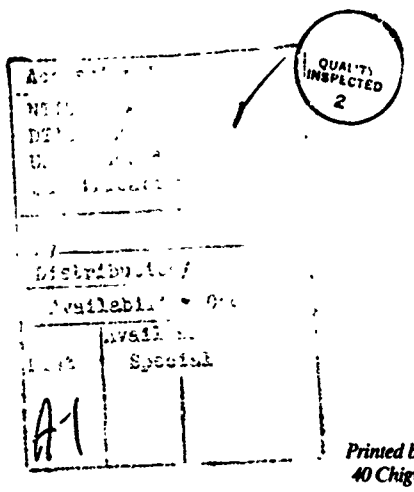

Published July 1987

ISBN 92-835-0422-4

Printed by Specialised Printing Services Limited
40 Chigwell Lane, Loughton, Essex IG10 3TZ

PREFACE

In the aftermath of the 1939–45 war, as a more scientific approach began to supplement cut-and-try as a basis for the design of parachutes, W.D.Brown first established a sound aerodynamic foundation for his subject in his book, '*Parachutes*'. Rôles which were being fulfilled by the parachutes which he described in it were firstly man-carrying for both life-saving and military applications; secondly weapon and store dropping; and thirdly deceleration of aircraft. Looking back over the 35 years that have elapsed since this publication, although their form has been greatly expanded, all of these are still essential tasks for parachutes to fulfil. However, additional ones also are now required. For example, crews of spacecraft as well as aircraft make encapsulated descents using parachutes as essential parts of their total escape systems and in addition to drag production contemporary parachutes may also need to demonstrate significant lift-producing abilities or the capability of rotation at chosen spin rates during their descent. Not ony have parachutes been used on a number of occasions to assist re-entry into the earth's atmosphere, they have also been employed in landing essential instruments on to other planets as well as on to the planet earth.

They have also had to find their place within the much wider classification of aerodynamic decelerators, in which they share a primarily decelerative task with balloons and various metallic non-inflatable devices. In his glossary in 1951, Brown defined a parachute as 'an umbrella-shaped device to produce drag, commonly used to reduce the rate of descent of a falling body'. A more precise and limiting definition is now customary. Within this broader classification of aerodynamic decelerators parachutes are now considered to be that class of drag-producing bodies whose essential characteristics include their flexibility, their inflated shape being dependent on the flow field which surrounds them.

A greater precision in definition epitomises changes taking place in many engineering fields, not only in that of parachute aerodynamics. With the availability in most design offices of powerful mainframe computers and in many situations of relatively inexpensive mini- and micro-computers, new possibilities exist for engineers to establish the relevant basic relationships and to develop their subsequent solutions. For these task to be performed adequately, basic principles must be appreciated and agreed sign conventions implemented.

It is to meet all these kinds of need that '*The Aerodynamics of Parachutes*' has been written. In the subject of parachute aerodynamics this AGARDograph is envisaged as a direct descendant of Brown's '*Parachutes*', for it has the same emphasis, that of selecting 'the principal aerodynamic characteristics of parachutes and the various known factors which affect these characteristics'. It takes into account not only many of the subsequent publications which have been summarised in the 1963 and 1978 United States Air Force Parachute Design Guides, but also the proceedings of the American Institute of Aeronautics and Astronautics Aerodynamic Decelerator Conferences which have been held every two and a half years, the Helmut G.Heinrich Decelerator Systems Engineering Short Courses which took place in 1983, 1985 and 1987 and '*The Parachute Recovery System Design Manual*', which will shortly be used by the United States Naval Weapons Center.

It has been anticipated that its main readers will be recent engineering graduates entering research establishments, parachute companies or related industries. In its preparation some appreciation on the part of the reader of basic mechanics, elementary fluid mechanics and the principles of computing has been assumed.

Apart from Karl-Friedrich Doherr and my own research associates, too many other individuals have contributed their components, criticisms and suggestions for me to mention their names individually. I can only hope that they will recognise their invaluable contributions in the publication which has resulted from all of our efforts.

David Cockrell
Leicester – 1987

* * * *

Au lendemain de la guerre de 1939–45, alors qu'un démarche plus scientifique commençait à compléter les méthodes empiriques du genre "on découpe et on essaie" comme base de la conception des parachutes, W.D.Brown fut le premier à élaborer une théorie aérodynamique saine pour ce qui faisait l'objet de son livre "Les parachutes". Les fonctions remplies par les matériels qu'il y décrivait étaient d'abord l'emport des hommes dans le double but de la sauvegarde de la vie humaine et des applications militaires, en deuxième lieu le largage d'armes et d'approvisionnements, en troisième et dernier lieu la décélération des avions à l'atterrissage. Si on étudie les 35 années qui se sont écoulées depuis cette publication, tous ces emplois sont encore essentiellement ceux que l'on attribue aux parachutes même si leur aspect extérieur s'est beaucoup diversifié. Néanmoins il en faut maintenant quelques modèles supplémentaires. Par exemple, les équipages des véhicules de l'espace comme ceux des avions font des descentes enfermé dans des capsules équipées de parachutes qui constituent la partie essentielle de l'ensemble de leur système d'évacuation; et en plus de la production d'engins basés sur la traînée, il peut aussi être demandé aux parachutes modernes de posseder des qualités de portance ou d'aptitude à tourner sur eux-mêmes à une vitesse donnée au cours de leur descente. Des parachutes ont été utilisés non seulement en de nombreuses occasions pour faciliter la rentrée dans l'atmosphere terrestre, mais aussi comme instruments essentiels d'atterrisage, qu'il s'agisse de se poser sur notre globe ou sur d'autre planètes.

Il a également fallu leur trouver un créneau dans la classe beaucoup plus vaste de décélérateurs aérodynamiques où ils remplissent, concurrement avec les ballons et divers dispositifs métalliques non gonflables, une tâche qui consiste

essentiellement à assurer un freinage. Dans son glossaire de 1951, Brown a défini le parachute comme "un dispositif en forme de parapluie, fournissant une traînée, utilisé communément pour diminuer la vitesse de descente d'un corps qui tombe". La définition courante actuelle est plus précise et plus limitative. Au sein de la catégorie très vaste des décélérateurs aérodynamiques, les parachutes sont générateurs de traînée dont une des caractéristiques essentielles est la souplesse d'emploi, car une fois gonflés, leur forme dépend de l'écoulement de l'air autour d'eux.

Cette meilleure précision dans la définition résume bien l'évolution qui s'est faite dans beaucoup de secteurs de l'industrie, et pas seulement dans l'aérodynamique des parachutes. Grâce à la présence de puissants ordinateurs centraux dans la plupart des bureaux d'étude et, dans beaucoup de cas, à l'utilisation de mini- et de micro-ordinateurs relativement peu coûteux, les ingénieurs disposent de possibilités nouvelles pour établir les formules de base voulues et développer les solutions qui en découlent en vue de la conception. Pour que ces tâches puissent être exécutées efficacement, il faut bien cerner les principes de base et appliquer les conventions de symbolique convenues.

C'est pour satisfaire tous ces besoins que l'ouvrage "Aérodynamique des parachutes" a été écrit. Dans le domaine dont il port le titre, cet "AGARDographe" est considéré comme la suite directe du livre "Les parachutes" de Brown, car il insiste sur le même thème: "les principales caractéristiques des parachutes et les divers facteurs connus qui les affectent". Il tient compte, non seulement du grand nombre de publications postérieures qui ont été répertoriées et résumées dans les "Guides de conception des parachutes" de l'armée de l'air américaine de 1963 à 1978, mais également des comptes rendus de débats des conférences de l'Institut américain d'Aéronautique et d'Astronautique ("American Institute of Aeronautics and Astronautics") sur la décélération aérodynamique qui se sont tenues tous les deux ans et demi, des cours techniques abrégés de Helmut G.Heinrich sur la technique des systèmes de décélération qu'il a donnés en 1983, 1985 et 1987, et du "Manuel de conception d'un projet de récupération par parachute" qui sera prochainement publié par le Centre des armements navals américain ("U.S. Naval Weapons Center").

On a prévu que les principaux lecteurs de cet ouvrage seraient les ingénieurs fraîchement diplômés qui sont sur les point d'entrer les établissements de recherche, les sociétés de fabrication de parachutes ou les industries qui leur sont associées. Pour préparer sa présentation, on a supposé que le lecteur possédait quelques connaissances de mécanique fondamentale, des notions élémentaires de mécanique des fluides et des principes de l'informatique.

En dehors de Karl-Friedrich Doherr et de mes propres associés en matière de recherche, les autres personnes qui ont apporté la contribution de leurs connaissances, de leurs critiques et de leurs suggestions sont trops nombreuses pour que je puisse les citer toutes individuellement. J'espère seulement qu'elles pourront reconnaître au passage les apports inestimables qu'elles ont faits à cette publication qui est l'aboutissement de tous nos efforts conjugués.

David Cockrell
Leicester — 1987

CONTENTS

1.INTRODUCTION

1.1 FUNCTION OF A PARACHUTE

The word '*parachute*' is derived from the French words *parare* , meaning to shield, or to ward off and *chute* , meaning a fall. Thus the word parachute means any natural or artificial contrivance which serves to check a fall through the air and thereby support in the air some load or store. But for present purposes this is too wide a definition. Within this AGARDograph the parachute will be considered to be one subdivision within a much larger classification of aerodynamic decelerators. Ibrahim[1.1] defines the latter as 'devices whose primary function is to maximise the drag of systems of which they form a part' and parachutes as 'flexible,elastic bodies whose inflated shapes are dependent on the flow conditions'. Because of the structural form of the rigid decelerator, the improper primary function of the flexible wing and the invariability of the ballute's inflated shape (a *ballute* is a cross between a balloon and a parachute, used as a high-speed aerodynamic decelerator) these devices are excluded from consideration as parachutes here, except as possible illustrations of certain aerodynamic principles.

Although the primary function of the parachute is the maximisation of system drag, among possible secondary rôles may be the provision of a horizontal velocity component (termed *drive*) to the system or even to be the means whereby this system acquires a lift force. Thus the distinction between parachutes and flexible wings may not be as clear cut as it first appears.

From their initial man-carrying rôle, parachutes have been required to undertake a much wider range of tasks. As well as men, stores are often decelerated by parachutes. These include weaponry as well as other supplies. Parachutes can also be used to decelerate rapidly-moving vehicles, such as aircraft and motor-cars. Sometimes, instead of an individual ejected from a malfunctioning aircraft, an entire crew-carrying module is decelerated by a parachute. As Fig. 1.1 indicates, parachutes must be capable of operation over a wide range of velocities and hence dynamic pressures, in very different environments. For example, extra-terrestrial applications may be required when instruments have to be landed on other planets. Even on the earth's surface, as natural aerodynamic decelerators such as dandelion seeds bear witness, some applications of parachutes call for unusual designs.

Fig. 1.1 PARACHUTE PERFORMANCE ENVELOPE
From Ref. 1.3

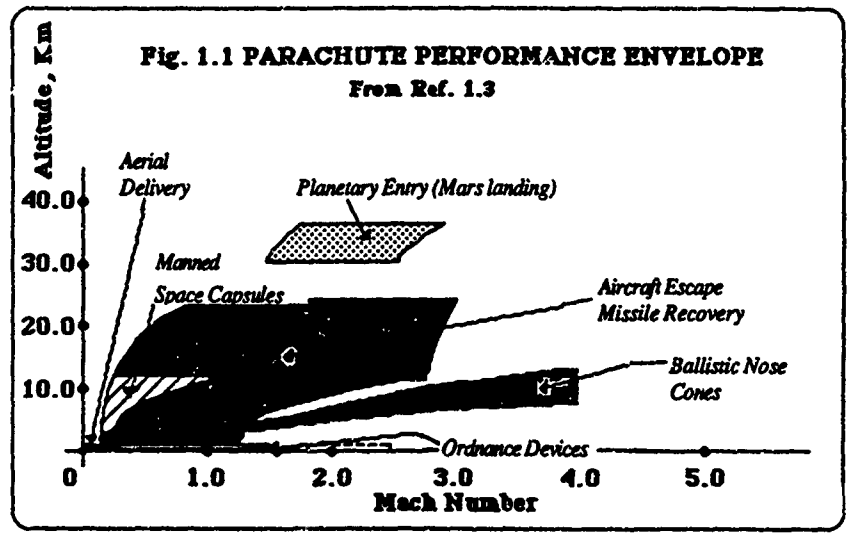

1.2 AERODYNAMICS: ONE AMONG MANY DESIGN CRITERIA

The aerodynamics of parachutes is only one aspect of their multi-faceted design. Their flexible structure must be of light weight, yet strong enough to withstand the high loads imposed during inflation. Their deployment must be both simple and reliable. They must be relatively easy to manufacture so that their cost is small compared with that of the store which they decelerate and then deliver. Parachute aerodynamics is concerned with the mechanism of inflation, the determination of flight mechanics, such as the rate of system descent in a given application, the drive and the lifting behaviour of the parachute. Included are system stability characteristics such as equilibrium angles, frequency of oscillation and the oscillation damping rates. To predict satisfactorily all these characteristics the necessary mathematical relationships must first be developed and relevant data acquired through appropriate experimental programmes. Having been acquired, these data must then be made generally available. The Parachute Design and

Performance Data Bank[1,2], established at the United States Air Force Flight Dynamics Laboratory in the period 1970-73, was a significant step in data dissemination and this AGARDograph has been written to further assist data formalisation, application and dissemination.

1.3 BRIEF HISTORICAL SURVEY (REFERENCES 1.3 TO 1.11)

Although evidence of parachute-like devices to lower both animals and humans from high towers exists in Chinese archives from as early as the 12th-century and in 1514 sketches of parachutes were made by Leonardo da Vinci, the first authenticated parachute descent was not made until October 22 1797, when André-Jacques Ganerin jumped from a balloon over Paris. Early users of parachutes were stunt men, descending from towers or from tethered balloons for the entertainment of spectators. By the early nineteenth century, exhibition parachute descents from balloons were being made all over the world and in this capacity, in 1808 a parachute first saved a human life.

At the outbreak of the 1914 world war, participants on both sides studied activities behind the enemy lines by stationing observers in baskets, slung beneath tethered hydrogen-filled balloons. As these balloons exploded if they were hit by machine-gun fire, on the approach of enemy aircraft the observers would bail out, using for this purpose cotton parachutes, some 9 - 11 metres in diameter which were tethered to their baskets. A large number of observers' lives were thus saved, there being 407 successful parachute descents in France by members of the British Balloon Wings alone and a further 125 by members of the United States Forces. For French observers a parachute system was evolved in which the entire basket was retrieved, becoming the first recorded 'encapsulated' retrieval by parachute. Similar observational practices were carried out by the German Army, with a corresponding high success rate in observer retrieval.

When aircraft entered the war the use of parachutes by aircrew was delayed. The probable reason for not using them initially was because of difficulties in egress from aircraft cockpits. Since it took valuable time to put the parachute harness on and to extract the parachute from its container which was fixed to the aircraft, often there was insufficient altitude remaining for the parachute to fully open. But eventually, the prime importance of pilots' lives was recognised, probably because of the considerable investment in training cost and time which they represented. The first recorded saving of life from an aircraft by a parachute was in 1916. At that time parachutes were opened by static lines attached to the aircraft, the opening being delayed until the parachutist was well clear of the machine.

By this stage in the war, individual aviators on the German side were equipping themselves with appropriately modified Heinecke parachutes which had originally been intended for balloon observers. As these parachutes opened they lifted the aviators clear of their cockpits. Following the development of 'packaged' or pack parachutes by Charles Broadwick and others in the early 1900's, all combatants rapidly made the necessary developments in materials and in parachute packing. On April 28 1919, Leslie L. Irvin made the first free parachute descent, from 1500 ft above the ground. By this time, parachutes were in regular use for the dropping of flares and in 1918 they were often the means by which spies were infiltrated behind enemy lines.

The first parachute designed for military personnel was standardised in 1924. After that time, first in the United States and later in Great Britain, the use of parachutes became compulsory for aircrew. By about 1930 the Soviet Army had begun to equip and train some of its units for airborne operations, using parachutes. Corresponding German units were deployed in Holland and Belgium during the early stages of the 1939-45 war.

By this stage in many countries a systematic testing and development programme had become essential. There was an over-riding need for reliability, thus for a better appreciation of parachute materials characteristics, of structural strengths, opening factors, drag characteristics and stability behaviour. Research took place in many places but increasingly in the United Kingdom and in Germany. By the outbreak of the second world war in 1939 there was considerable experience in using parachutes for weapon stabilisation, required both for impact attitude and the need to obviate high g-loading in the direction normal to that of the weapon axis, in the dropping of supplies by parachute and in paratrooping. During that war there was considerable development in all these applications as well as in the aircraft decelerator rôle, made necessary through both the advent of dive bombing and the rapid deceleration on landing required by some fighter aircraft. During the 1930's the needs for high aircraft deceleration led to the development of ribbon parachutes by Georg Madelung. At the high speeds which were necessary such parachutes were able to provide the required low opening shock loads and also exhibit stability in pitch.

These various applications were demanding differing parachute characteristics, for example a low degree of parachute stability tolerable to a member of aircrew making an emergency escape from his aircraft would be quite unacceptable to a regular parachutist such as a paratrooper, or for an aircraft decelerator system. For such ejector systems knowledge of the relevant parameters influencing parachute inflation became essential so that satisfactory predictions of the time taken for inflation and the corresponding forces which were developed could be achieved . Using parachutes, guided missiles, such as the V.1 and V.2, as well as missile components were successfully recovered in 1944 and the earliest ejector seat deceleration was made by parachute about 1944-6, the idea for so doing originating in Sweden.

During the 1939-45 war, at the various research establishments parachute sections were established. For example, at the Royal Aircraft Establishment under W.D.Brown, the British Parachute Section was established in 1942. After

this war was over, when T.F.Johns, a member of this Section, published the Report "Parachute Design", he stated that most usual requirements for parachutes were:-

(i). that they will invariably inflate;
(ii). that they will develop specified drag forces at particular descent speeds;
(iii). that they will be sufficiently strong to withstand opening at speeds which are usually higher than their descent speeds, and
(iv). that they will give specified degrees of stability to the payloads to which they are attached.

In this AGARDograph, the aerodynamic aspects of requirement (ii) are discussed in chapter 2, those of (i) in chapter 5 and (iv) in chapter 4. The aerodynamic aspects of requirement (iii) are considered in chapters 2, 3 and 4.

After the end of the second world war, in the United States the military engagements in Viet-Nam and elsewhere stimulated more parachute research into gliding parachutes such as the ram-air inflated textile wing originally proposed in 1961 by Jalbert, the emergency escape of aircrew and the airborne delivery of personnel, stores and weapons as well as into aircraft retardation and vehicle recovery over a wide dynamic pressure range. Deceleration through the deployment of a series of parachute canopies in a number of separate stages became commonplace. By the 1960's the ribbon parachutes developed for this purpose were used for the deceleration of the United States astronauts returning from the Moon in the Mercury, Gemini and Apollo spacecraft as well as those in the Soviet Union's Vostok and Soyuz space vehicles. Yuri Gagarin safely landed Vostok I by parachute in April 1961 and in February 1962 John Glenn used a ringsail ribbon parachute to land a Mercury spacecraft. In July 1976, using parachutes, successful landings of the first of two Viking spacecraft was made on the planet Mars.

REFERENCES

1.1 Ibrahim,S.K. An Overview of Munition Decelerator Technology with Recent Applications at Honeywell. *Proceedings of the AIAA 8th Aerodynamic Decelerator and Balloon Technology Conference*, Hyannis,1984

1.2 DeWeese,J.H. and McCarty,R.E. Parachute Design and Performance Data Bank. Air Force Flight Dynamics Laboratory, Wright-Patterson A.F.B. AFFDL-TD-74-45, 1975

1.3 Knacke,T.W. *Parachute Recovery System Design Manual.* Naval Weapons Center,China Lake,California NWC TP 6575. To be published in 1987. *Pre-publication copy delivered in part as reference 5.4.*

1.4 Brown,W.D. *Parachutes.* Pitman & Sons, London, 1951

1.5 Dennis,D.R. Recent Advances in Parachute Technology. *Aeronautical Journal*, pp.333-342, Nov.1983

1.6 Gold,D. Early Development of the Manually Operated Personnel Parachute, 1900-1919. *Proceedings of the AIAA 2nd Aerodynamic Deceleration Systems Conference*, 68-964, El Centro,1968

1.7 Pepper,W.B. & Maydew,R.C. Aerodynamic Decelerators-An Engineering Review. *AIAA Journal of Aircraft*, 8,1,Jan.1971

1.8 Heinrich,H.G. Some Research Efforts Related to Problems of Aerodynamic Deceleration. U.S. Wright Air Development Division WADD TN 60-276,Nov.1961

1.9 Ewing,E.G., Bixby,H.W. and Knacke,T.W. Recovery System Design Guide. AFDL-TR-78-151, December 1978

1.10 Johns,T.F. Parachute Design.U.K.Aeronautical Research Council R.& M. 2402, Dec.1946

1.11 Knacke,T.W. Technical-Historical Development of Parachutes and Their Application since World War I. AIAA-86-2423. *Proceedings of the AIAA 9th Aerodynamic Decelerator and Balloon Technology Conference*, Albuquerque, 1986.

2.STEADY-STATE AERODYNAMICS

Although it is more logical to begin by describing the deployment and the inflation of the parachute canopy, proceed with its deceleration and then to consider its behaviour in the steady state, basic aerodynamic concepts for parachutes are most readily introduced by first considering their fully-deployed steady descent.

2.1 SOME DEFINITIONS. RELEVANT DIMENSIONLESS PARAMETERS

In flight mechanics the characteristic forward direction of vehicles in motion is first determined. Then a common procedure is to establish orthogonal sets of axes which are fixed in these vehicles, passing through an origin which itself is fixed in the vehicle. Such axes are referred to as *body axes*. Customarily the axis O-x is so positioned that it points in that characteristic forward direction. As Fig. 2.1 illustrates, the *angle of attack*, α ,is the angle measured between the component in the Oxz plane of the resultant airflow V_R in that forward direction and the body axis O-x. The body axes are right-handed in direction.

As *Terms and Symbols for Flight Dynamics*[2.1] makes clear, in aeronautical parlance the term *angle of incidence* is no longer an acceptable alternative for angle of attack, α .

Like any other immersed body, when a parachute moves through a fluid *a resultant aerodynamic force* R is developed on it. Experiments can be devised by which to measure both the magnitude of this force and its moment about any specified location. Though these measurements are sufficient to define the line of action of this resultant force they do not determine the precise position of the centre of pressure, a specific point on that line of action at which the resultant aerodynamic force can be considered to act. In most aerodynamic applications the location of the centre of pressure is determined by convention. Thus, for a section of aircraft wing section or for a gliding parachute *the centre of pressure position* is defined as being at the intersection of the resultant aerodynamic force line of action with the chord line of the aerofoil section which constitutes the wing or the gliding parachute. A *gliding parachute*, such as that with a ram-air canopy described in Appendix 2B, is one which is capable of imparting a horizontal component of velocity or *drive* to the parachute and its payload. Momentarily it is possible for a system comprising a gliding parachute and payload to develop a resultant lift force. In contrast is the *conventional parachute*, possessing solely a drag-generating rôle. A number of conventional parachute canopies are illustrated in Appendix 2A. In some situations this distinction between these two types of parachute canopies becomes artificial, since conventional parachutes become gliding parachutes if appropriate panels are removed from the canopy. When this occurs either definition of parachute could be adopted, whichever is the more convenient.

In the physical appreciation of parachute behaviour, such as when formulating and solving equations of motion, it is sometimes desirable (though not essential) to know the centre of pressure location. For conventional parachutes the centre of pressure position is defined to be at the the intersection of the line of action of the resultant aerodynamic force with the parachute axis of symmetry.

Fig. 2.1 Tangential & Normal Components of Aerodynamic Force for Conventional Parachutes

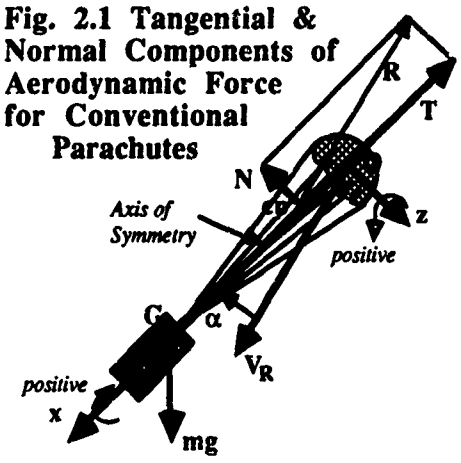

O Origin of co-ordinate System
G Centroid of Parachute System
cp Centre of Pressure of Parachute System
V_R Parachute Resultant Velocity at Origin
α Angle of Attack
R Resultant Aerodynamic Force
N Normal Component of Aerodynamic Force
T Tangential Component of Aerodynamic Force

The single most significant aerodynamic characteristic of parachutes is their *drag* D, defined in *Terms and Symbols for Flight Dynamics*, International Standards 1151[2.1] as the component of the resultant aerodynamic force in the direction of the resultant relative airflow V_R, equal and opposite to that of the parachute. In the plane of the resultant velocity the other component of the resultant aerodynamic force is its *lift*, L. Initially however, consideration will be given to the tangential and the normal components of the resultant aerodynamic force rather than to its drag and lift components. Since conventional parachutes are usually considered to be axially symmetric for present purposes a two-dimensional representation will be adequate. Three-dimensional representation is certainly desirable with gliding parachutes however, the two-dimensional conventions of high aspect ratio aircraft aerodynamics usually prevail. *Aspect ratio* denotes the ratio of the wing span to its mean chord and for the gliding parachute the resultant velocity is considered to lie in the plane of symmetry of the parachute.

The components of the resultant aerodynamic force which are parallel and normal respectively to the O-x and O-z axes and in the reverse sense to these axes are termed the *tangential force*, T and the *normal force*, N. For a conventional parachute, as shown in Fig. 2.1, the tangential component of force is parallel to the parachute's axis of symmetry. Expressed non-dimensionally they are:

$$C_T = T/(^1/_2\rho V_R^2 S_o) \qquad \text{and} \qquad C_N = N/(^1/_2\rho V_R^2 S_o) \qquad (2.1 \ \& \ 2.2)$$

where ρ is the *local air density*, V_R is the *parachute resultant velocity* at the origin of a co-ordinate system, which is fixed in the parachute and S_o is the nominal *total surface area of the canopy* that is, it represents the total canopy surface area, inclusive of any openings, slots and vent areas.

Since steady aerodynamic forces and moments developed on an immersed body such as a parachute are considered to be functions of the body shape, inclusive of its attitude in the fluid, the body size, together with its relative velocity through the fluid in which it is immersed, as well as the fluid properties density, viscosity and temperature, then by dimensional analysis:

$$C_T \text{ and } C_R = f(\alpha; Re; Ma) \qquad (2.3)$$

where $Re = V_R D_o/\nu$ is the *Reynolds number* and

$$D_o = [4S_o/\pi)]^{1/2} \qquad (2.4)$$

D_o being defined as the parachute *nominal diameter* and ν as the fluid's *kinematic viscosity*.

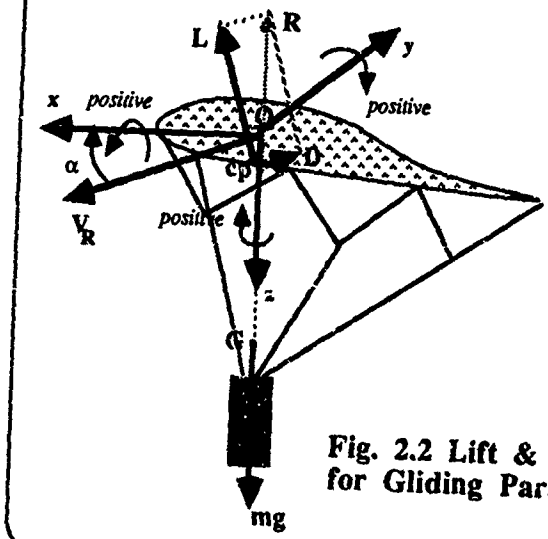

O Origin of co-ordinate System
G Centroid of Parachute System
cp Centre of Pressure of Parachute System
V_R Parachute Resultant Velocity at Origin
α Angle of Attack
R Resultant Aerodynamic Force
L Lift Component of Aerodynamic Force
D Drag Component of Aerodynamic Force

Fig. 2.2 Lift & Drag Force Components for Gliding Parachutes

Since the nominal total surface area of the canopy is not always clearly defined there can be confusion over the magnitude of the parachute's nominal diameter D_o. To avoid this confusion the term *constructed diameter*, D_c is sometimes used. The Recovery Systems Design Guide, reference 1.9, defines the constructed diameter of a parachute canopy as 'the distance measured along the radial seam between points where the maximum width of opposing gores intersects that radial seam'.

The *Mach number* Ma equals V_R/a , where a is the local speed of sound in the undisturbed fluid. The ways in which these and other aerodynamic force and moment coefficients vary with the angle of attack, Reynolds number and Mach number are described in Section 2.2.

For gliding parachutes the aerodynamic reaction R is usually expressed in terms of its two components, *lift* L and *drag* D respectively perpendicular to and parallel to the resultant airflow, as illustrated in fig.2.2 The positive direction of lift is in the opposite sense to the weight of the system and the positive direction of drag is in the opposite sense to the parachute's resultant velocity. Like tangential and normal force components, lift and drag forces are similarly expressed in terms of non-dimensional coefficients as C_L and C_D:

$$C_L = \frac{L}{\frac{1}{2}\rho V_R^2 S_o} \qquad (2.5)$$

and

$$C_D = \frac{D}{\frac{1}{2}\rho V_R^2 S_o} \qquad (2.6)$$

The non-dimensional force coefficients C_L and C_D can be expressed as functions of the angle ot attack, the Reynolds number and the Mach number in exactly the same way as were the force coefficients C_T and C_N in equation 2.3.

To avoid any confusion in determining the sense of the lift component force it is preferable to confine the use of tangential and normal force components to conventional parachutes while reserving lift and drag components for gliding parachutes. When considering flight mechanics however, the component of aerodynamic force in the direction of the relative airflow, i.e. the drag component is often required, so transformation is necessary from one set of aerodynamic force components to the other. The relationships shown in Fig.2.3 are:

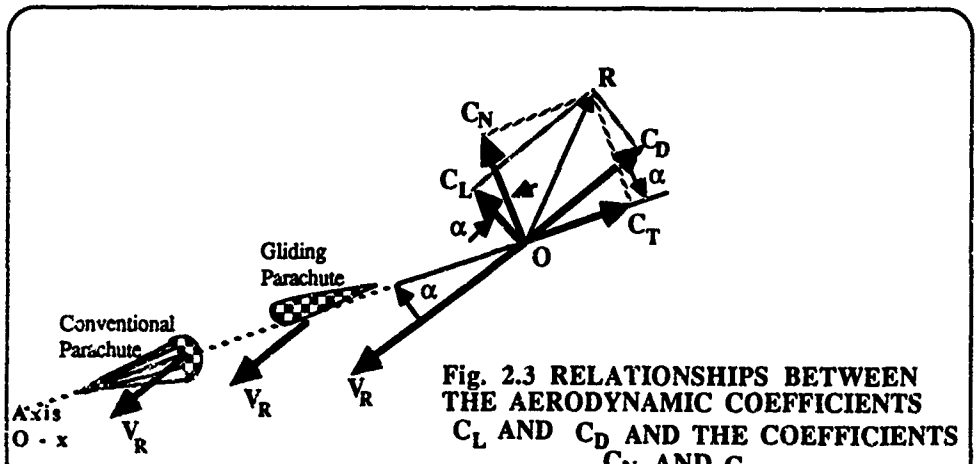

Fig. 2.3 RELATIONSHIPS BETWEEN THE AERODYNAMIC COEFFICIENTS C_L AND C_D AND THE COEFFICIENTS C_N AND C_T

$$C_D = C_T \cos\alpha + C_N \sin\alpha \qquad (2.7)$$

and

$$C_L = C_N \cos\alpha - C_T \sin\alpha \qquad (2.8)$$

Correspondingly,

$$C_T = C_D \cos\alpha - C_L \sin\alpha \qquad (2.9)$$

and $$C_N = C_L \cos\alpha + C_D \sin\alpha \quad . \qquad (2.10)$$

And since $$\tfrac{1}{2}\rho V_R^2 = \tfrac{1}{2}\rho_o[V_R^2]_E \qquad (2.11)$$

where the subscripts o and E respectively imply measurement at sea level and the equivalent air speed, the expressions for the aerodynamic force components in equations 2.1, 2.2, 2.5 and 2.6 can be written in terms of the *equivalent air speed* V_E. The latter is the appropriately-corrected speed be recorded by an air speed indicator.

2.2 SOME STEADY-STATE AERODYNAMIC CHARACTERISTICS

To illustrate the functional relationships expressed in equation 2.3, some typical aerodynamic characteristics of various canopy shapes are now considered. A list of the most common parachute canopy shapes, together with a brief account of their aerodynamic characteristics, is appended to Section 2.

2.2.1 Shape of Parachute Canopy

As explained in the Introduction, the process of parachute design is inevitably one of making compromise decisions. The shape of the parachute canopy is determined by considering all the rôles which the parachute may be required to fulfil. Some of the factors which will influence the choice of design are outlined below.

2.2.1.1 Opening Characteristics The speeds at which parachute canopies are required to deploy and to inflate strongly influence the maximum structural loads which they must be designed to withstand. On strength considerations, if inflation is required at high equivalent air speeds, ribbon parachute canopies, such as that shown in Fig.2.4, are almost exclusively chosen.

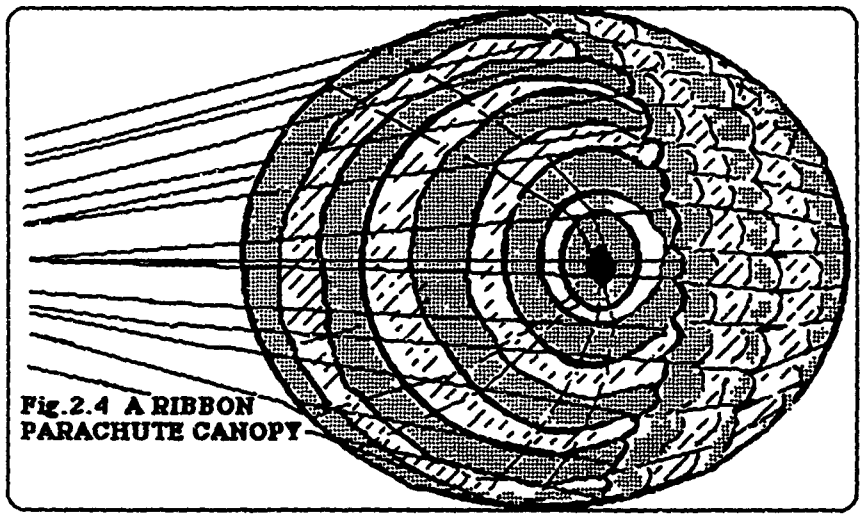

Fig.2.4 A RIBBON PARACHUTE CANOPY

2.2.1.2 Is 'Drive' Required? Drive, defined in Section 2.1, may be a stragetic requirement, as it is for airborne forces parachutes, or it may be undesirable, as would be the case for dropping stores by parachute into a confined zone. As will be outlined in Section 2.3.2, a parachute canopy possessing drive is likely to be strongly statically stable in pitch.

When drive is required, a gliding parachute canopy must be adopted. But where drive would be an undesirable characteristic a conventional parachute canopy is used instead.

Since many gliding parachutes are effectively inflatable low aspect ratio wings, their aerodynamic characteristics vary with the angle of attack and wing aspect ratio in a manner typical of these ratio wings. Gliding parachutes are limited by control considerations to a maximum aspect ratio of about 3:1, giving a gentle stall and a correspondingly slow increase in drag coefficient. The ratio of lift to drag is low; at the present state of the art about 3:1 is characteristic but higher ratios are attainable with the more advanced design of swept-wing closed-cell ram-air gliding parachutes described in Section 9.5.1. The characteristic variation of lift coefficient with angle of attack for ram-air

gliding parachute canopies having aspect ratios varying from 1:1 to 3:1 is shown in Fig. 2.5. These experimental results were quoted by Lingard[2.3] from an earlier report by Nicolaides[2.4].

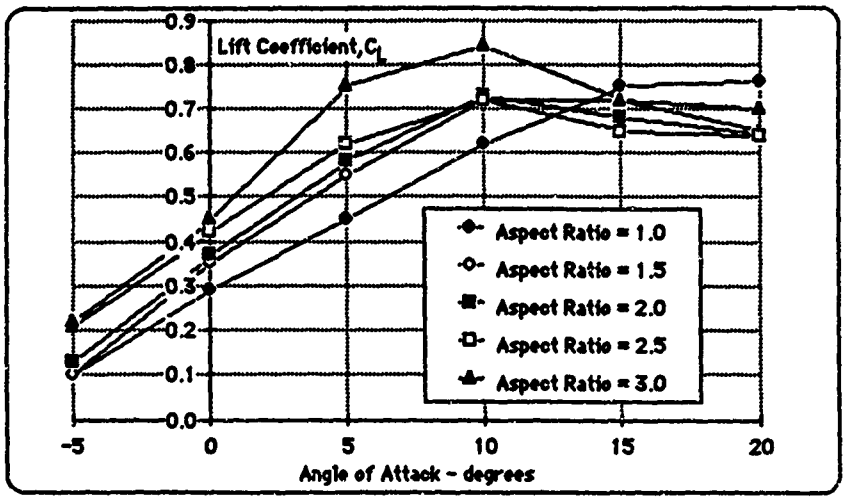

Fig. 2.5 LIFT COEFFICIENT VARIATION WITH ANGLE OF ATTACK FOR RAM-AIR GLIDING PARACHUTES

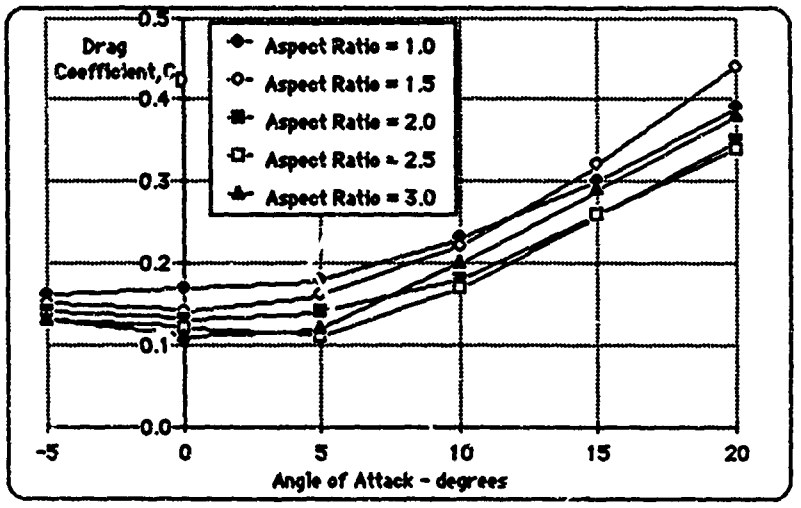

Fig. 2.6 DRAG COEFFICIENT VARIATION WITH ANGLE OF ATTACK FOR RAM-AIR GLIDING PARACHUTES

In Fig. 2.6, the corresponding drag coefficient variation with angle of attack and aspect ratio is shown for ram-air gliding parachutes.

2.2.1.3 What Value of C_T is Required? It will be shown in Section 2.3.3 that for a given canopy size and payload mass the rate of descent of a parachute decreases as the magnitude of the tangential force coefficient C_T increases. In general, as high a value as is practicable is desirable for C_T. At zero angle of attack, C_T is equal to the drag coefficient C_D. Some typical characteristics for the variation of C_D and C_T with angle of attack are shown in Figs.2.6 and 2.7. They are seen to be dependent on the porosity of the parachute canopy, a property which will be discussed in Section 2.4. Whereas in Fig.2.6 characteristics for a typical gliding parachute have been given, in Fig.2.7 they are shown for flat circular parachute canopies, so called because when these canopies are spread out flat on a plane surface they are circular in shape.

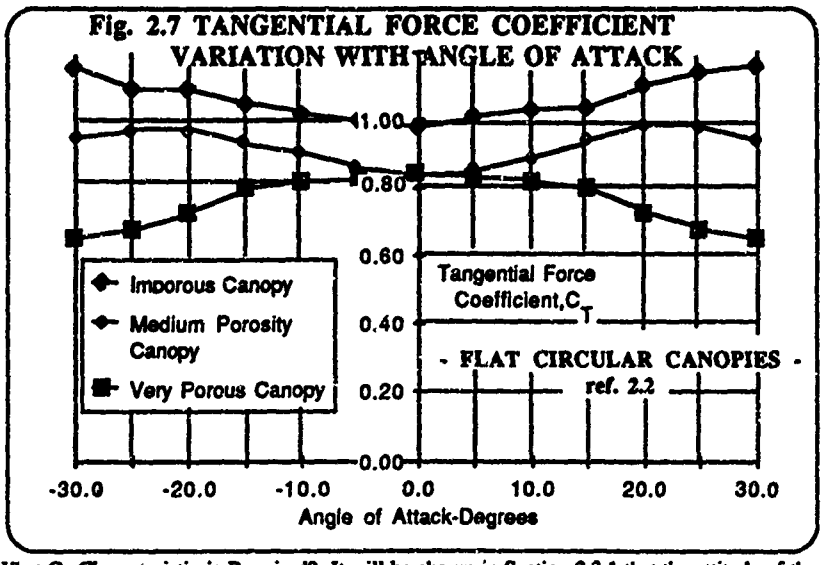

Fig. 2.7 TANGENTIAL FORCE COEFFICIENT VARIATION WITH ANGLE OF ATTACK

2.2.1.4 What C_N Characteristic is Required? It will be shown in Section 2.3.1 that the attitude of the canopy when in equilibrium is determined by the angle of attack at which C_N is equal to zero. Further, the condition for a

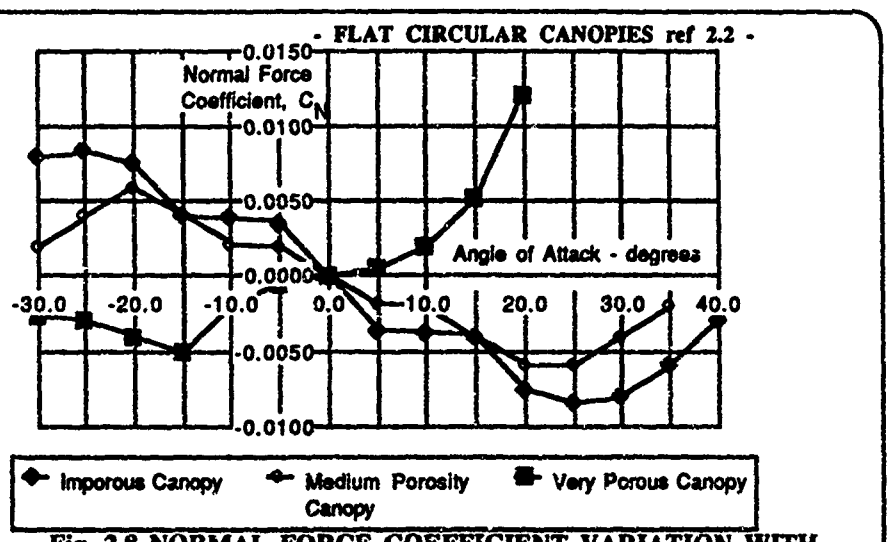

Fig. 2.8 NORMAL FORCE COEFFICIENT VARIATION WITH ANGLE OF ATTACK

parachute to be statically stable in pitch is shown in Section 2.3.2 to be that when in equilibrium, $dC_N/d\alpha$ must be positive. Almost any parachute canopy will descend stably if only it is made sufficiently porous for example, ribbon parachute canopies, being highly porous, characteristically display strong static stability in pitch.

Typical characteristics showing the variation of C_N with angle of attack for flat circular parachute canopies are shown in Fig.2.8. They, too, are strongly porosity dependent. For these and other parachute canopy shapes, as porosity is increased not only does the tangential force coefficient, C_T markedly decrease, resulting for a given canopy shape and size in an increased descent velocity, but as very porous canopies inflate they may exhibit *squidding*, defined by Brown[12] as a tendency for the open canopy to collapse to a form in which the open diameter lies between one-third and one-quarter of the fully-open diameter; the shape of the collapsed parachute canopy then resembling that of a squid. The phenomenon of squidding is further discussed in Section 5.2.

2.2.2. Variation of Aerodynamic Coefficients with Reynolds Number

Published data on the variation of parachute aerodynamic coefficients with Reynolds number are almost entirely concerned with drag coefficient variation. Provided that the Reynolds number, based on parachute canopy nominal diameter, is greater than about 10^5, Figs. 2.9a and 2.9b indicate that little variation in drag coefficient with Reynolds number occurs. By inference, at these Reynolds numbers little variation of other aerodynamic force coefficients with Reynolds number is anticipated. In Fig.2.9a, comparing corresponding data for other bluff bodies, i.e. a sphere and a circular disc normal to the flow, it is evident that at high Reynolds numbers the boundary layers detach and near the leading edge of these bodies flow separation occurs.

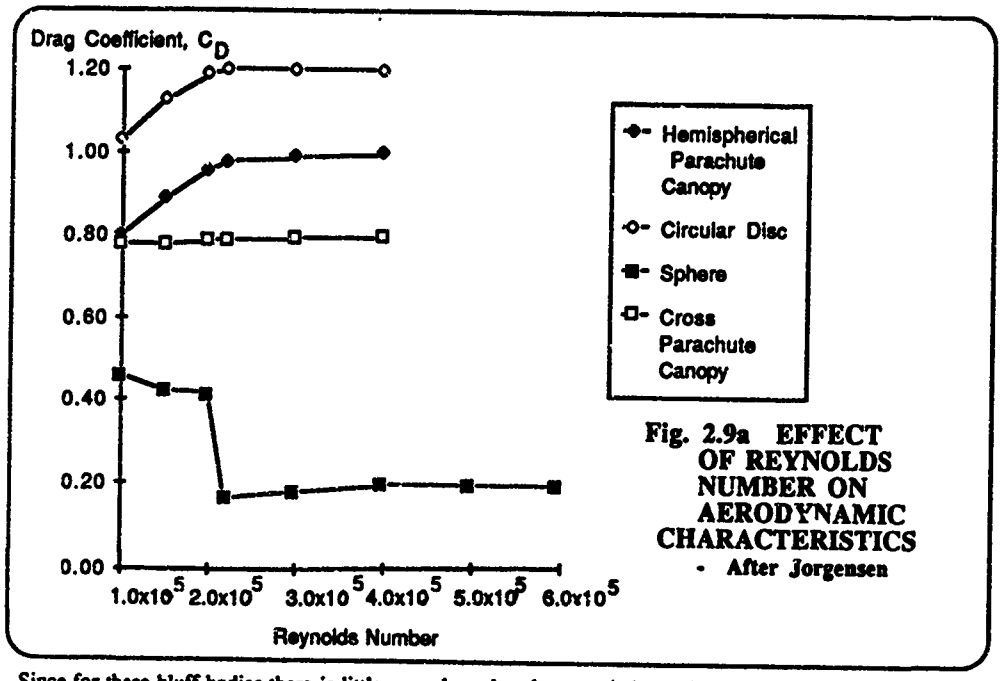

Fig. 2.9a EFFECT OF REYNOLDS NUMBER ON AERODYNAMIC CHARACTERISTICS - After Jorgensen

Since for these bluff bodies there is little or no boundary layer variation with Reynolds number, the resulting variation in aerodynamic coefficients with Reynolds number is also small. In Figs. 2.9a and 2.9b cross parachute canopies canopies are referred to. These are manufactured from two rectangular strips of material joined together to produce a cross or a cruciform shape, appearing as shown in Fig. 2.10.

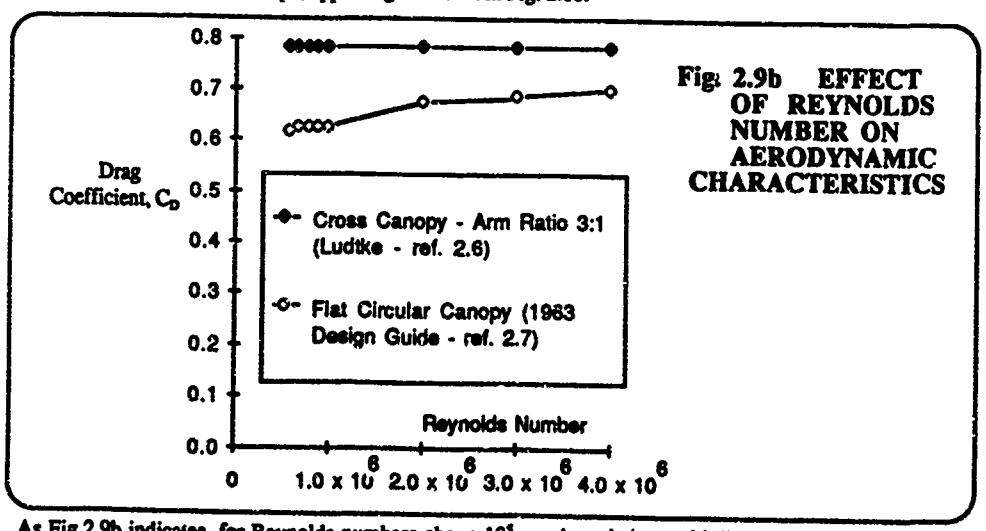

Fig. 2.9b EFFECT OF REYNOLDS NUMBER ON AERODYNAMIC CHARACTERISTICS

As Fig.2.9b indicates, for Reynolds numbers above 10^5, small variations with Reynolds number in the drag coefficient of parachutes can occur, but these variations are of little practical significance. However, from free flight

tests conducted by the U.S. Air Force[2.8] on both models and full scale parachute canopies, different results were obtained. By altering the weight of the payload the rate of descent for a given parachute and its payload was systematically varied from 4.6 m/sec. (15 ft/sec.) up to 9.1 m/sec.(30 ft/sec.). The corresponding Reynolds number variation was from 3.6×10^5 to 7.2×10^5. Fig. 2.9c indicates that as a consequence of its drag coefficient variation with Reynolds number the descent velocity, which is inversely proportional to the square root of the drag coefficient, also varied. This unanticipated drag coefficient variation with Reynolds number may well be an unsteady aerodynamic phenomenon, the parachute dynamic stability in pitch decreasing as its payload is decreased.

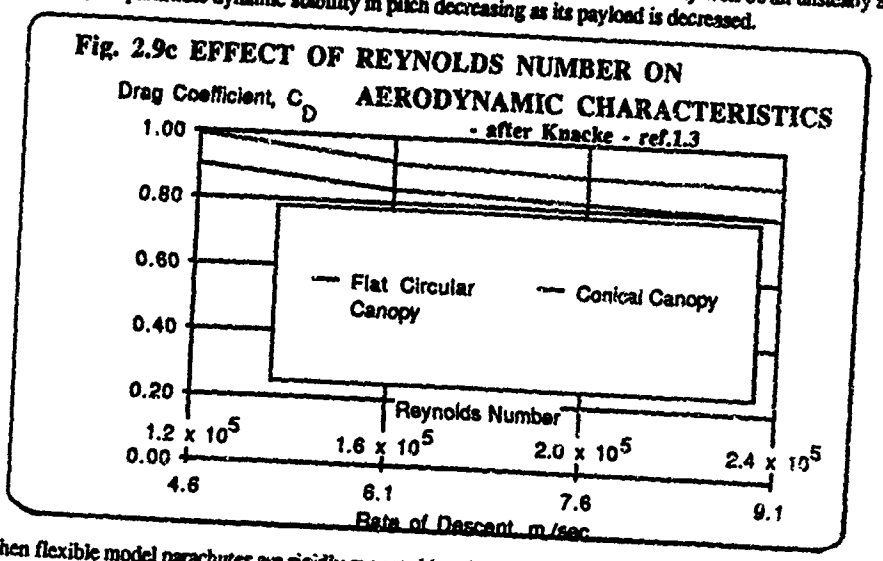

Fig. 2.9c EFFECT OF REYNOLDS NUMBER ON AERODYNAMIC CHARACTERISTICS - after Knacke - ref.1.3

When flexible model parachutes are rigidly mounted in wind tunnels the aerodynamic forces which are measured on them are steady and unless substantial changes in canopy projected area occur with Reynolds number, once the latter exceeds about 10^5 there is little resulting variation in aerodynamic characteristics. In their free descent through the atmosphere the drag coefficients of parachutes which exhibit dynamic stability in pitch at zero angle of attack can also be considered to be effectively independent of Reynolds number. However, this is not the case for unstable parachutes which oscillate substantially during their descent. For these latter, the average drag coefficients measured during descent are functions of the pitching angles through which they oscillate. A distinction must therefore be made between drag measurements made on parachutes which are rigidly constrained in wind tunnels and ones which are free to oscillate as they descend. This point is further developed in Section 2.3.3.

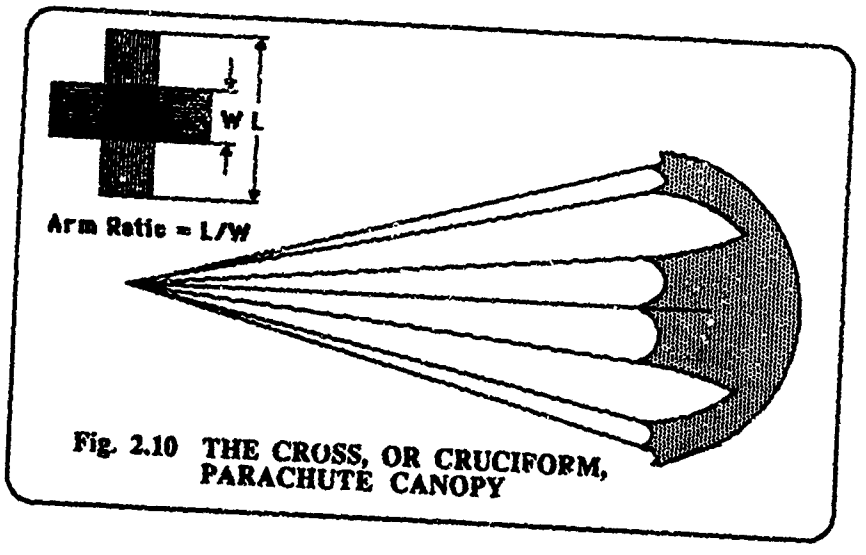

Fig. 2.10 THE CROSS, OR CRUCIFORM, PARACHUTE CANOPY

2.2.3 Variation of Aerodynamic Coefficients with Mach Number

With bluff bodies such as parachute canopies substantial variations in drag coefficients with Mach number are to be anticipated. This variation is strongly dependent on both the canopy shape and the local Reynolds number. Fig. 2.11a is generally illustrative of the substantial drag coefficient dependence on Mach number, a dependence which develops in subsonic flows as Fig. 2.11b, describing the characteristics of a parachute cluster, illustrates. Hyperflo parachute canopies, whose characteristics are shown in Fig. 2.11a, were flexible ribbon concepts which were specifically designed for supersonic operation by the Cook Research Laboratories.

Fig. 2.11a EFFECT OF SUPERSONIC MACH NUMBERS ON PARACHUTE AERODYNAMIC CHARACTERISTICS

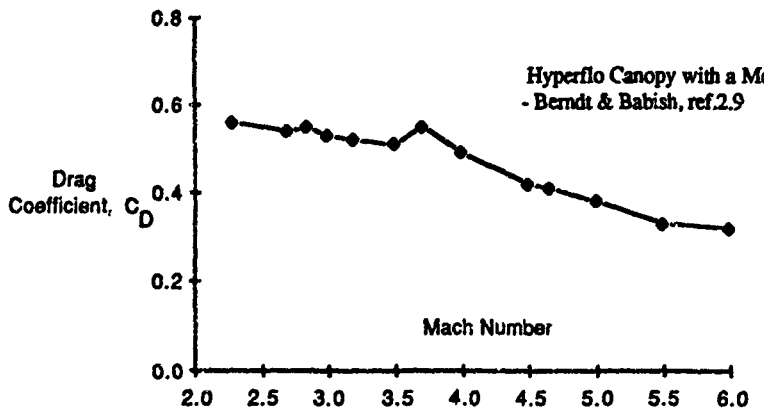

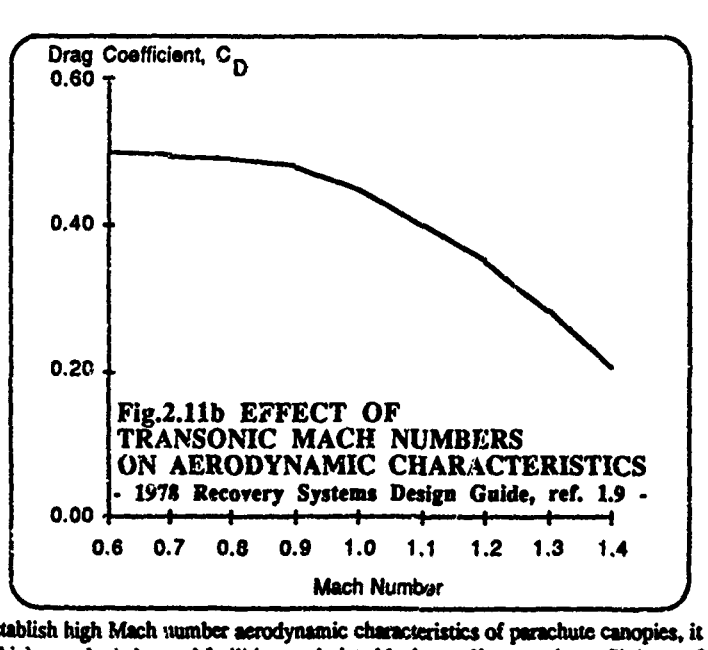

Fig.2.11b EFFECT OF TRANSONIC MACH NUMBERS ON AERODYNAMIC CHARACTERISTICS
- 1978 Recovery Systems Design Guide, ref. 1.9 -

In order to establish high Mach number aerodynamic characteristics of parachute canopies, it is essential to use either very large high-speed wind tunnel facilities to obviate blockage effects or else to flight test full-scale canopies. The blockage constraint of parachute models in wind tunnels is discussed in Section 6.3.

2.3 STEADY-STATE FLIGHT MECHANICS

2.3.1 Equilibrium

2.3.1.1 The Conventional Parachute By resolving and taking the moments of the external forces acting on the conventional parachute shown in Fig.2.12 the conditions for its equilibrium can be established. As the figure shows, the angle θ is the inclination of the parachute axis of symmetry, defined in Section 2.1, with the vertical. Initially, the drag of the payload is considered as negligible compared with that of the canopy.

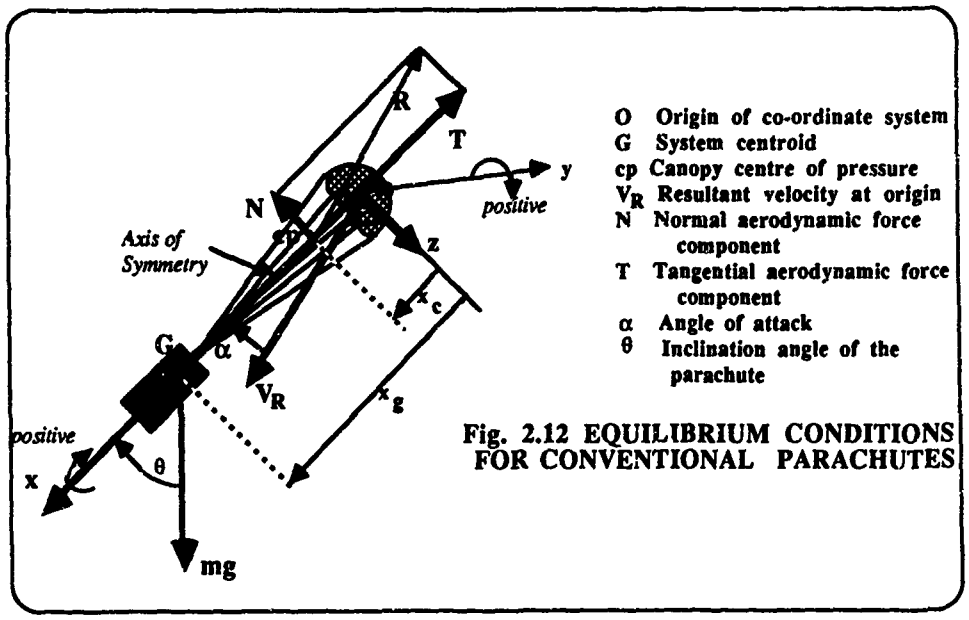

O Origin of co-ordinate system
G System centroid
cp Canopy centre of pressure
V_R Resultant velocity at origin
N Normal aerodynamic force component
T Tangential aerodynamic force component
α Angle of attack
θ Inclination angle of the parachute

Fig. 2.12 EQUILIBRIUM CONDITIONS FOR CONVENTIONAL PARACHUTES

Resolving in the Ox direction:

$$mg \cos\theta - T = 0 \qquad (2.12)$$

Resolving in the Oz direction:

$$mg \sin\theta - N = 0 \qquad (2.13)$$

Taking moments about the system centroid, G:

$$M_G = -N(x_g - x_c) = 0 \ . \qquad (2.14)$$

Then since $(x_g - x_c)$ is non-zero, for equilibrium the normal aerodynamic force component, N must be zero.

Equation 2.13 then shows that since mg is necessarily non-zero, at equilibrium the angle θ must be zero. Under this condition equation 2.12 shows that the tangential force component, T equals mg. Hence, when it is in equilibrium a conventional parachute descends with its axis of symmetry vertical, at such an angle of attack, α that no normal aerodynamic force component is developed on it.

When the drag of the payload is not negligible when compared with that of the canopy, at equilibrium the normal force component is small and positive. Under these conditions, a stable canopy descends at a small positive angle of attack, describing a coning motion with the semi-apex angle of the cone equal to this angle of attack. In order to minimise this coning motion the drag of the payload must be small compared with that of the canopy.

2.3.1.2 The Gliding Parachute For exactly the same reason as for a conventional parachute, if the drag of the payload attached to a gliding parachute is neglected then when this parachute is in equilibrium it descends so that its axis Oz is vertical. This axis is drawn through both the canopy centre of pressure, cp, located on the aerofoil section chord line at about the quarter-chord position and the parachute-payload system centroid, G. From the origin O, selected on the axis Oz, the axis Ox extends at right angles to Oz in the plane of symmetry and in the same sense as that of the parachute's resultant velocity V_R.

Fig. 2.13 has been drawn in the equilibrium position. In this figure the line OP has been drawn through the origin O and perpendicular to the aerofoil chord line. The adjustable *rigging angle* ϕ lies between OP and the axis Oz.

In reference 2.1 the symbol γ is used for the angle of climb of an aircraft. Throughout *The Aerodynamics of Parachutes* the *angle of descent*, γ_d will be adopted instead, where

$$\gamma_d = -\gamma . \qquad (2.15)$$

Using the symbols shown in Fig.2.13 and applying equilibrium conditions corresponding to those adopted for conventional parachutes in equations 2.12 to 2.14, including neglecting the drag of the payload, by resolving forces in the Ox direction:

$$L \sin \gamma_d - D \cos \gamma_d = 0 \qquad (2.16)$$

by resolving forces in the Oz direction:

$$mg - L \cos \gamma_d - D \sin \gamma_d = 0 \qquad (2.17)$$

and by taking moments about the centroid,G:

$$M_G = -(L \sin \gamma_d - D \cos \gamma_d)(z_g - z_c) = 0 . \qquad (2.18)$$

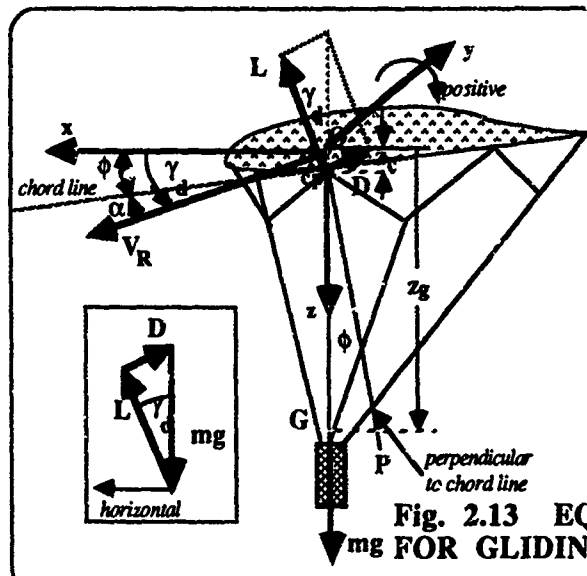

Fig. 2.13 EQUILIBRIUM CONDITIONS FOR GLIDING PARACHUTES

From the inset diagram in Fig. 2.13:

$$\tan \gamma_d = D/L = \frac{1}{L/D} . \qquad (2.19a)$$

and

$$\cos \gamma_d = L/mg . \qquad (2.19b)$$

From the conditions established in Fig. 2.13, at equilibrium the angle of descent γ_d is related to the angle of attack α by:

$$\gamma_d = \alpha + \phi \qquad (2.20)$$

If the drag of the payload is not neglected, then at equilibrium the Oz axis of the gliding parachute is inclined at an angle θ to the vertical, so that:

$$\alpha + \phi = \theta + \gamma_d . \qquad (2.21)$$

By adding the payload drag to the forces shown in Fig. 2.13 it can readily be seen that the condition for equilibrium is that the axis Oz is inclined at a small negative angle θ to the vertical. As this angle is, in general, small equation 2.20 is approximately valid even when it is necessary to take the drag of the payload into consideration. Thus:

$$\gamma_d = \alpha + \phi . \qquad (2.22)$$

Now, through equation 2.19, γ_d is a function of the angle of attack, α. Equation 2.22 demonstrates that the purpose of allowing the rigging angle ϕ to vary is to adjust the angle of attack at which the gliding parachute flies, making possible a range of equilibrium ratios of lift to drag at which the parachute descends.

2.3.2 Static Stability

Whether or not a system is stable is determined by its response to small displacements from its equilibrium position. Static stability is solely concerned with the directions of the moments which are developed on such a displaced system, a statically stable system being one which, as a consequence of a small displacement from equilibrium, develops a moment in a direction which would restore the system to equilibrium. This concept has nothing to say about the equilibrium of forces which act on the system after displacement or about the frequency and attenuation or amplification of any resulting oscillations, nevertheless, it is a very valuable concept in a number of fields including aircraft dynamics and in Section 4.3.2 it is shown to have particular merit when applied to parachute dynamic pitching motion. Since a system which exhibits static stability about one axis need not necessarily do so about any other, it is important to define the axis about which the stability of a system is being considered.

Fig. 2.14 THE STATIC STABILITY CONCEPT

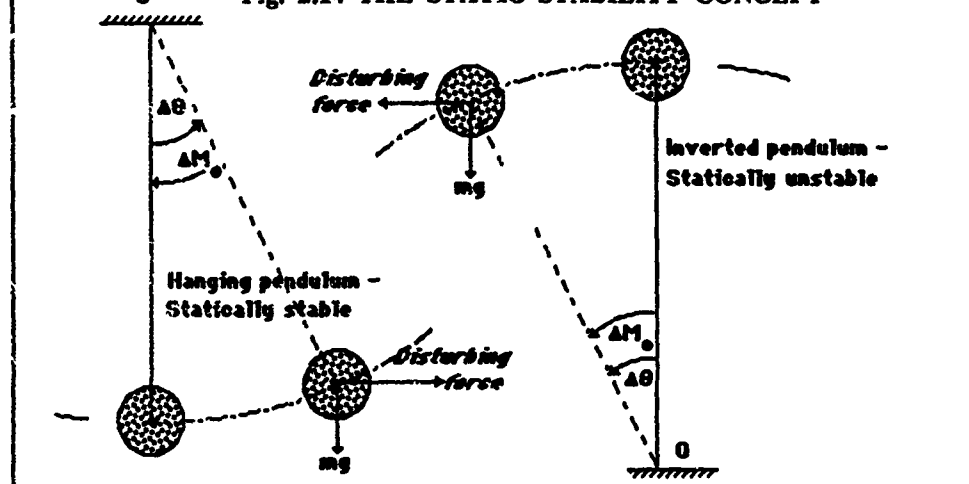

The concepts of static stability and instability are illustrated in Fig.2.14 by reference to a pendulum, hanging on the end of a light, straight rod. When this supporting rod hangs vertically the pendulum's suspended mass is in equilibrium Work must be done to displace it from this equilibrium position and to incline the supporting string through an angle $\Delta\theta$. Having made such a small displacement, the pendulum develops a moment ΔM about the suspension point O. This moment is in the direction to restore the system to the equilibrium state and is opposed to that of the displacement. The static stability of the system is characterised by the relationships that:

(i). in equilibrium, the moment about O:

$$M_o(\theta) = 0 \qquad (2.23)$$

(ii). and after a small displacement:

$$dM_G/d\theta \quad < \quad 0 \ . \qquad (2.24)$$

However, if the pendulum were inverted, with the supporting rod vertical the system is also in equilibrium. But, in allowing the supporting rod to deflect, work is done by the system on the rod. Having deflected through a small angle $\Delta\theta$ the moment then developed about the suspension point O is in the same direction as that of the displacement. Hence, for this inverted pendulum $dM_G/d\theta$ is greater than 0.

In exactly the same way, the criteria required for the equilibrium and the static stability of a parachute in pitch are, from equations 2.12 to 2.14 and 2.16 to 2.18, that

$$M_G(\alpha) \quad = \quad 0 \qquad (2.25)$$

and

$$\partial M_G/\partial\alpha \quad < \quad 0 \ . \qquad (2.26)$$

By specifying moments about the parachute centroid it is ensured that the moment consequent upon a small disturbance from the equilibrium state is wholly aerodynamic. Its magnitude and its sign can then be determined readily, solely from steady-state aerodynamic tests.

For a conventional parachute, the necessary conditions for equilibrium and static stability in pitch are given from equations 2.14 and 2.25 as:

$$M_G(\alpha) \quad = \quad -N(x_g - x_c) \quad = \quad 0 \ . \qquad (2.27)$$

together with

$$\partial M_G/\partial\alpha \quad < \quad 0 \qquad (2.28)$$

or, from equation 2.27:

$$\partial N/\partial\alpha \quad > \quad 0 \qquad (2.29)$$

Whereas, for a gliding parachute, from equations 2.18 and 2.25:

$$M_G \quad = \quad -[L \sin(\alpha + \phi) - D \cos(\alpha + \phi)]z_G \quad = \quad 0 \ . \qquad (2.30)$$

together with

$$\partial M_G/\partial\alpha \quad < \quad 0 \ . \qquad (2.31)$$

Some typical steady-state aerodynamic pitching moment characteristics for conventional parachutes have been taken from the Recovery Systems Design Guide[1.9] and are shown in Fig. 2.15.

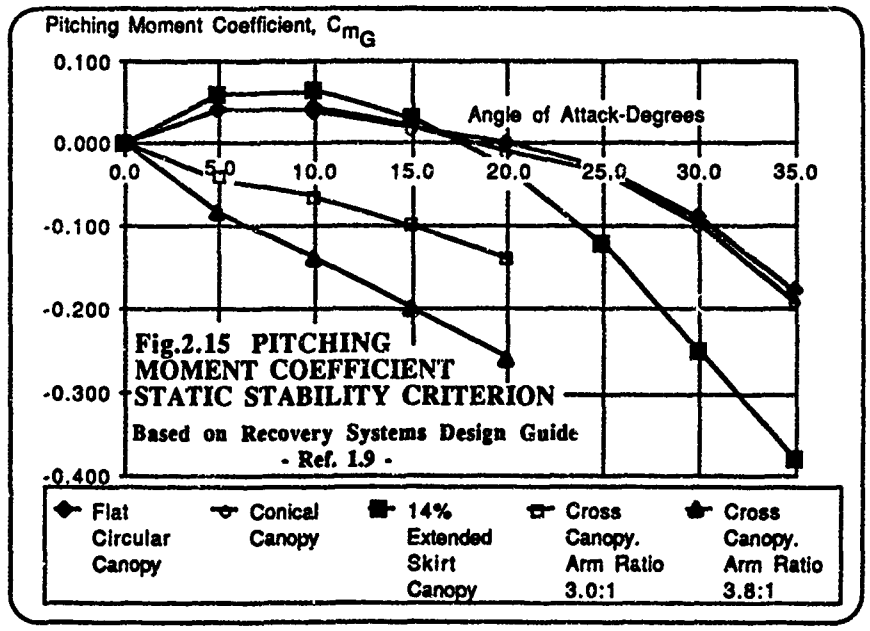

Fig.2.15 PITCHING MOMENT COEFFICIENT STATIC STABILITY CRITERION

Based on Recovery Systems Design Guide - Ref. 1.9 -

The *aerodynamic pitching moment coefficient* C_m is defined in a similar way to the force coefficients in equations 2.1, 2.2, 2.5 and 2.6 by:

$$C_m = \frac{M}{\frac{1}{2}\rho V^2 S_o D_o} \qquad (2.32)$$

the nominal diameter,D_o being defined in equation 2.4.

Since pitching moments are the products of the normal force, N and an appropriate moment arm, when tabulating experimental results it is important to specify precisely the location of the axis about which the pitching moment has been measured . As equation 2.25 indicates, the system centroid, G is often an important location about which pitching moments are required but as this is dependent on the mass of the payload which is suspended from the canopy its location may not be known with precision at the time of performing aerodynamic experiments on the parachute canopy. In much of the established pitching moment coefficient data for parachute canopies the point about which this moment has been measured is unspecified. Often it is the suspension line confluence point which, for all practical purposes, can be considered to be the system centroid. This lack of precision can make these data unreliable. In his experimental data Dohert[2.10] has overcome this problem by specifying the canopy centre of pressure location relative to the canopy hem line at the skirt periphery.

The parachute canopies whose characteristics are shown in Fig.2.15 are all in equilibrium at zero angle of attack. However, of the five canopies illustrated only those that are cross-shaped are statically stable at this angle, the other three canopies illustrated exhibiting simultaneous equilibrium and static stability at certain positive angles of attack. For example, the flat circular canopy is in equilibrium and is statically stable in pitch at an angle of attack of about 20 degrees. These pitching moment characteristics are skew-symmetric about zero angle of attack, thus the flat circular canopy described is also in equilibrium and is statically stable at - 20 degrees angle of attack.

Both of these solutions are within the Oxz plane. The flat circular canopy exhibits the required equilibrium and stability characteristics whenever it flies with its axis of symmetry vertical and the resultant relative airflow lies on the surface of a cone whose axis is the canopy axis of symmetry and whose semi-apex angle is 20 degrees. Since no particular direction is preferred, during descent the parachute oscillates through approximately ± 20 degrees. In the literature such a parachute is referred to as an *unstable parachute* .

On the other hand, the cross (or cruciform) parachute canopy of 3.8:1 arm ratio shown in Fig. 2.10, is referred to as a *stable parachute* . It is in equilibrium and is statically stable in pitch at zero angle of attack, thus any disturbance from this equilibrium state will be attenuated. Since the angles through which stable parachutes oscillate depend on the amplitude of the forces which disturb them from equilibrium, during descent they cannot be stated with any exactitude. However, the oscillatory motion which ensues is often heavily damped, for reasons to be explained in Section 4.3.2. Thus the observed oscillatory motion can be quite minimal and in the literature it is customary, though inaccurate, to specify these small pitching angles through which stable, as well as unstable, parachutes oscillate.

It is clear from Fig.2.15 that the steady-state aerodynamic characteristics of cross parachutes are functions of *arm ratio*, defined in Fig. 2.10 as the constructed length to width ratio of one of the two canopy arms. Normal force coefficient variations with angle of attack for a variety of arm ratios are shown in Fig.2.16. Equations 2.2 and 2.29 indicate that a necessary condition for a conventional parachute to be stable in pitch is that $dC_N/d\alpha$ must be positive at $\alpha = 0°$. For the cross parachute canopies shown in Figs. 2.16, this condition is satisfied by appropriate combinations of arm ratios and fabric porosities, for example the curves drawn in Fig. 2.16a are for imporous canopies, showing that a condition for static stability in pitch is that the arm ratio of imporous cross-shaped canopies should exceed 3.0:1.

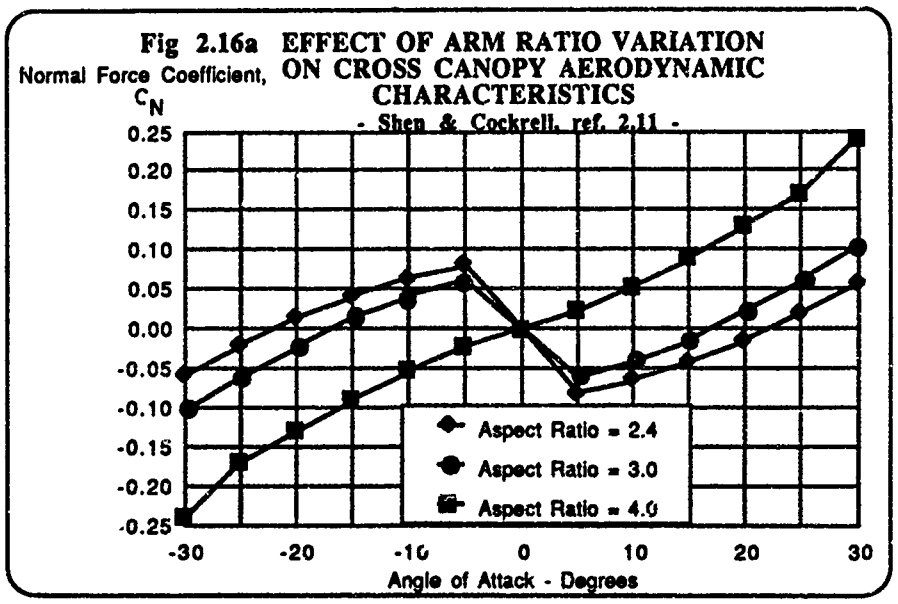

Fig 2.16a EFFECT OF ARM RATIO VARIATION ON CROSS CANOPY AERODYNAMIC CHARACTERISTICS
- Shen & Cockrell, ref. 2.11 -

Reference to Fig. 2.16b shows that cross canopies with an arm ratio of 3.0:1 can exhibit static stability in pitch provided that they are not manufactured from imporous fabric. Figs. 2.4 and 2.5 have already made clear that the porosity of the canopy has a very marked effect on parachute aerodynamic characteristics.

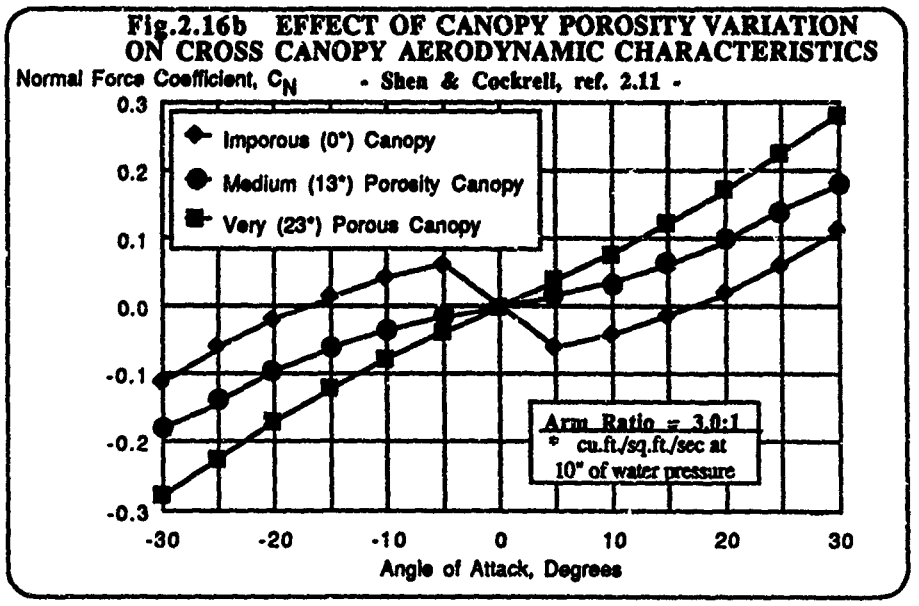

Of course, cross parachutes are not the only canopies which exhibit static stability in pitch. As Figs. 2.3 and 2.15 have already indicated, a tendency to parachute stability is a consequence of canopies increasing in porosity. However, as Fig. 2.5 indicates, this is accompanied by a corresponding reduction in drag coefficient and as explained in Section 2.3.3, leads to deteriorating descent characteristics. A considerable experimental test programme on canopy stability was undertaken in 1962 by Heinrich and Haak[2.3]. A number of its results are given in Chapter 4 of the 1963 Parachute Design Guide[2.7].

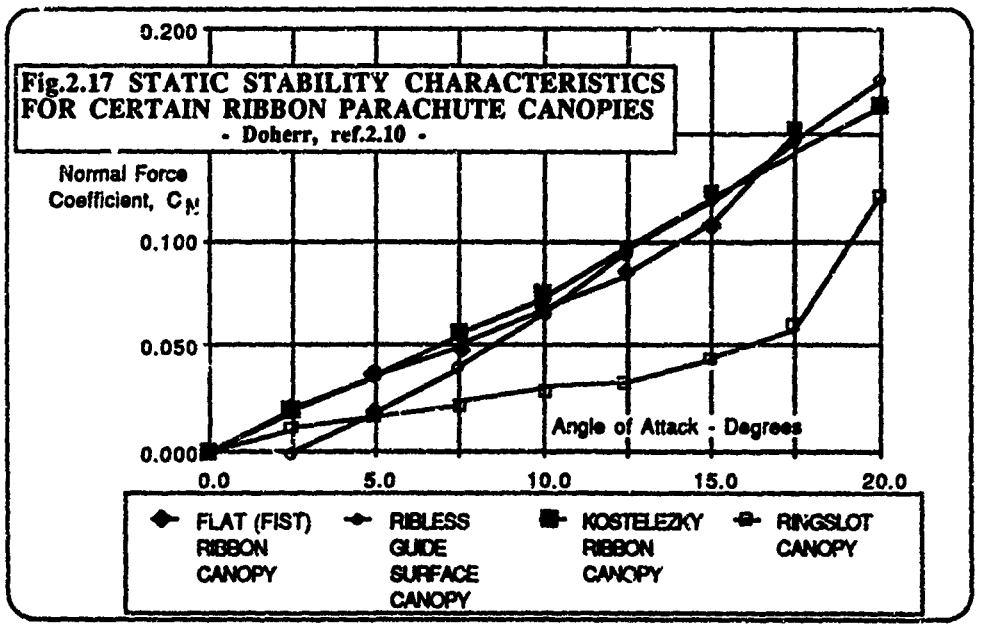

Figure 2.17 is taken from later experimental work performed by Doherr[2.10] in which he demonstrated the static stability in pitch of certain solid textile canopies and that of a number of slotted parachute canopies. In the reference

quoted he indicated that there was some Reynolds number dependency in his results. He also showed that substantial interference to the canopy's aerodynamic characteristics is often caused by the presence of the payload forebody.

Aerodynamic characteristics of unstable conventional parachute canopies can be considerably changed by removal of a panel or a portion of a panel. The consequent loss in axial symmetry results in the parachute acquiring a horizontal component of velocity or 'drive' during descent and thus becoming a gliding parachute. Jorgensen and Cockrell[2.12] have demonstrated that the resultant relative airflow is then at a high and statically-stable angle of attack, thus the parachute acquires a satisfactory descent performance.

2.3.3 Steady Descent

In a steady equilibrium descent it has been shown in Section 2.3.1 that, provided the payload drag is negligible compared with that of the parachute canopy, the attitude of the axis of symmetry Ox for a conventional parachute and of the axis Oz for a gliding parachute is vertical. Under these conditions, for conventional parachutes equation 2.12 reduces to:

$$mg = T \tag{2.33}$$

If the parachute is stable then during descent its angle of attack is zero and from equation 2.7 $C_T = C_D$. Hence, from equation 2.6, for a stable conventional parachute:

$$mg = {}^1/_2\rho V_D^2 S_o C_D \tag{2.34}$$

From this equation it is evident that the *descent velocity* V_D is inversely proportional to the square root of the drag coefficient C_D. It is also proportional to the square root of the parachute and payload weight and as the former is generally negligible compared with the latter the descent velocity can be considered to be a function of the weight of the payload. It decreases as the ground is approached and the air density, ρ increases and it is inversely proportional to the square root of the canopy surface area, S_o. By measuring the descent velocity V_D and knowing the other parameters the *drag area* of the parachute, $C_D S_o$, can thus be calculated.

It is normal practice to apply equation 2.34 to unstable as well as to stable conventional parachutes. This is then an average determination made for a body whose angle of attack during descent will vary. It may therefore differ in magnitude from wind tunnel derivations made at fixed angles of attack. Although with stable parachutes this difference is not marked with unstable canopies it could be significant.

Fig. 2.18 STEADY DESCENT OF A GLIDING PARACHUTE

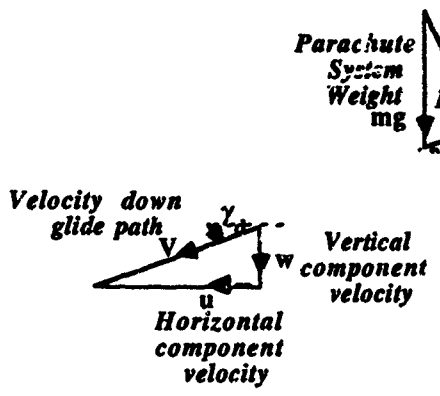

For gliding parachutes, from equation 2.16:

$$mg = L\cos\gamma_d + D\sin\gamma_d \tag{2.35}$$

Thus, from the definitions of C_L and C_D in equations 2.5 and 2.6 and the expression for $\cos\gamma_d$ in equation 2.19b:

$$mg = 1/2\rho V_R^2 S_o [C_L/\cos\gamma_d] \tag{2.36}$$

and thus

$$V_R = \left[\frac{2mg\cos\gamma_d}{\rho S_o C_L}\right]^{1/2} \qquad (2.37)$$

As Fig.2.18 shows, the *horizontal and vertical components of the parachute's resultant velocity*, V_R are given respectively by u and w, where

$$u = V_R \cos\gamma_d \qquad (2.38a)$$

and

$$w = V_R \sin\gamma_d \ . \qquad (2.38b)$$

From equation 2.37, *the velocity down the glide path*, V_R increases with increasing altitude and increasing *wing loading*, mg/S_o. But for a given height loss, the horizontal distance travelled is a function of the angle of descent γ_d which, equation 2.21 shows, is solely a fuction of the gliding parachute's aerodynamic characteristic, C_L/C_D.

2.3.4 Froude Number, F

The *Froude number* F for a parachute is defined as:

$$F = V_D^2 / D_o g \qquad (2.39)$$

Since it relates the descent speed in a given gravitational field to the required size of the parachute canopy, this similarity parameter is a very useful performance number. It is not wholly an aerodynamic characteristic of the parachute, since it is a combination of the system's drag coefficient with its mass ratio, R_m:

$$F \propto 1/(R_m C_D) \qquad (2.40)$$

where the *mass ratio* R_m is a measure of the ratio of air mass enclosed in the fully-inflated parachute canopy to the payload mass m_s, thus:

$$R_m = \rho\forall/m_s \ . \qquad (2.41)$$

In equation 2.41 the symbol $\forall$ denotes the representative displaced volume of an immersed body. For a parachute canopy the representative displaced volume is considered to be that of a hemisphere which has a diameter equal to the canopy nominal diameter D_o. The concept of the representative displaced volume is further discussed in Section 4.2.1.

Fig.2.19 VARIATION OF THE FROUDE NUMBER WITH THE MASS RATIO

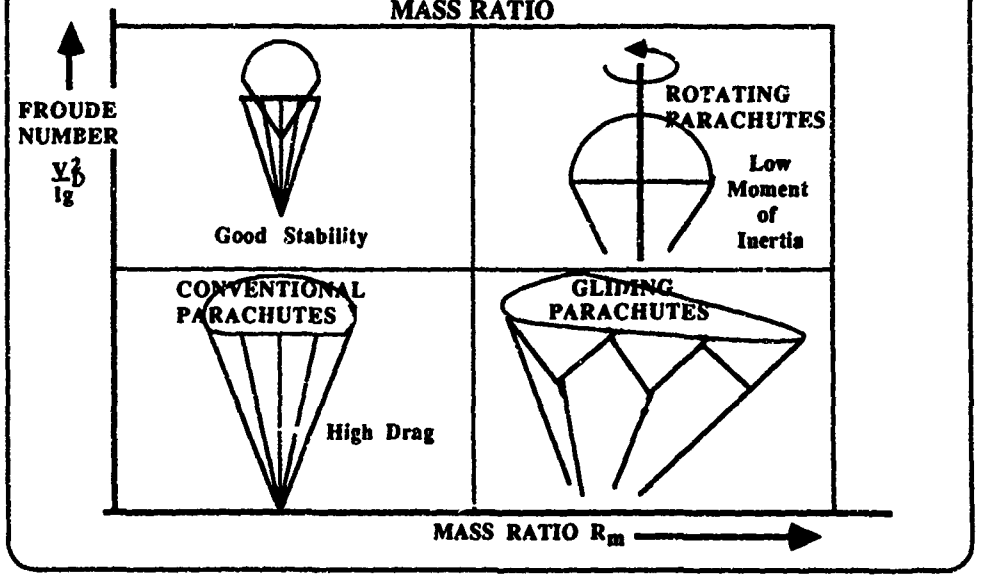

This relationship between the Froude number and the mass ratio for parachutes is illustrated in Fig. 2.19, devised by Doherr as a means of illustrating the descent characteristics for four different parachute classes. It illustrates equation 2.40 which shows that for a given drag coefficient the Froude number F is inversely proportional to the mass

ratio R_m. In the figure, lines of constant drag coefficient would be rectangular hyperbolae, the drag coefficient increasing as the origin is approached.

Conventional parachutes are essentially high drag devices which cause large payload masses to descend slowly. Since the mass ratio R_m is a measure of the mass of air entrained in the canopy to that of the payload carried, while the Froude number F is that of descent speed to payload size, a conventional parachute is characterised by low values of both Froude number and mass ratio.

Both *high stability parachutes* and *gliding parachutes* have smaller drag coefficients. Whereas high stability parachutes descend rapidly and operate at high Froude numbers, gliding parachutes descend more slowly and operate at lower Froude numbers.

One important application for *rotating parachutes* is to decelerate submunitions and then to impart a high rate of spin for a given rate of descent to them . They therefore require high mass ratios. However, their drag coefficients are relatively small and they therefore possess relatively large Froude numbers. Rotating parachutes and their rôle in submunition deceleration are further discussed in Section 9.5.2.

2.4 THE POROSITY OF PARACHUTE CANOPIES

In Section 2.2 it has been shown that the aerodynamic characteristics and consequently the stability of parachutes are strongly influenced by the porosity of the parachute canopy fabric. Canopy porosity also has a significant effect on parachute deployment and inflation. As Brown[1.4] has stated, from the days when canopies were manufactured from silk it has been necessary to specify how permeable is the parachute fabric, hence an appreciation of canopy porosity together with the need and the means for its measurement have extended over at least the last half century. Although aerodynamic characteristics clearly depend on the ratio of the area of openings in the canopy material to the total material area, that is on the canopy *geometric porosity*, the flow through the canopy is a function not only of this grid size but also of the pressure difference across it, as well as the density and the viscosity of the fluid in which the canopy is immersed. Heinrich[2.13] defined the *permeability*, or the *nominal porosity* of the canopy material as the volumetric air flow per unit area of material (e.g cubic ft/sq.ft/sec. is commonly used) and he showed this to be a function of the pressure difference across the canopy. British experiments have indicated that because of material deformation two different materials possessing the same nominal porosity when the pressure difference across them is representative of steady descent conditions display very different nominal porosities when this pressure difference is more representative of canopy inflation. It is standard British practice to measure volumetric air flow through the canopy materials, thereby determining their nominal porosity when the pressure difference across them is 10 inches water gauge, i.e. equal to a 10 inch vertical column of water. This is appropriate to the pressure difference during the deployment phase. In the United States and Europe this volumetric air flow is measured when the pressure difference is only 0.5 inches of water, a pressure difference which is rather more representative of steady descent conditions.

The *effective porosity* of a parachute canopy was defined by Heinrich as the ratio of the average velocity U through the porous surface to the canopy free stream velocity V. He proposed:

$$U/V = f[(\Delta p/(1/2\rho V^2);\ Re;\ Ma] \qquad (2.42)$$

where Δp represents the pressure difference across the canopy; Re and Ma the free stream Reynolds number and Mach number respectively.

For incompressible flow without material deformation Payne[2.14] suggested the largely empirical relationship:

$$\Delta p = k_1 U^2 + k_2 U \qquad (2.43)$$

where the velocity U is here more rigorously defined as the average of the fluid velocities approaching and leaving the porous fabric and k_1 and k_2 are coefficients which when using S.I. units are measured in Ns^2m^{-4} and Nsm^{-3} respectively .

By writing equation 2.43 in the form

$$\Psi = \Delta p/U = k_1 U + k_2 \qquad (2.44)$$

and then plotting Ψ against U graphically, the coefficients k_1 and k_2 can be determined experimentally . Since the average velocity through the fabric U is measured in Great Britain and in the United States at different pressure gradients, if both sets of measurements are available for a given canopy fabric, Payne's expression in equation 2.44 can be used to estimate the volumetric flow rate through the canopy at any required pressure difference.

In a private communication, Lingard has proposed that the effect of canopy porosity on static stability in pitch could be estimated as follows:

An empirical condition that the canopy shall exhibit static stability in pitch is that the total volumetric outflow from the porous canopy should exceed a certain percentage, say 10% of the inflow through the canopy mouth, when

the latter is determined from the product of the mouth area and the rate of canopy descent, V_D. The volumetric outflow can be estimated from the air velocity U discharging through an area which, because of cut outs, is less than the nominal area of the canopy, together with the discharge determined from the product of the descent velocity and the cut-out area. The unknown velocity U at a pressure difference Δp equal to $1/2\rho V_D^2$ can be calculated from equation 2.44, using previously determined values of k_1 and k_2 for the canopy fabric.

2.5 STOKES-FLOW PARACHUTE SYSTEMS

Where the application is one in which very low descent velocities or very high altitude performance is required, the resulting low Reynolds number leads to in a very different parachute concept, that of a *Stokes-flow parachute system,* which Mihora[2.15] has described.

If the Reynolds number is so small that inertia forces are negligible compared with those caused by viscosity the parachute's drag mechanism and therefore its basic shape will be changed. To achieve a low descent velocity the canopy must be of an extremely lightweight construction of open-mesh fabric or else formed from very small diameter widely-spaced filaments. Its nominal drag coefficient, based on its total projected area, could well exceed 1.0. While its overall Reynolds number might exceed 10 000 when based on the canopy diameter, if it were based on the filaments' diameter it could well be less than 0.5, a necessary criterion for Stokes flow. Because of the large voids present in such a canopy it can be packed into a very small container.

Niederer[2.16] describes studies for a Stokes-flow decelerator system, designed to provide subsonic rates of descent at altitudes up to 90 km (56 miles). Experiments were conducted in a high altitude test chamber in which either full scale Reynolds number or full scale Knudsen number could be reproduced but not both at the same time. The *Knudsen number* is the ratio λ/L, where λ is the mean free path for the molecules of the gas in which parachute filaments, having a typical linear dimension L, are immersed. One of Niederer's sample designs is for a Stokes-flow parachute which weighs 0.44 Newtons (0.1 lbf) and which supports a 4.0 Newton (0.9 lbf) payload. At an altitude of 45.8 km (28.5 miles) its rate of descent would be 24.4 m/sec. (80 ft/sec.).

Although suited to high altitude applications because there the kinematic viscosity is high and a low Reynolds number is thus more readily achieved, Stokes-flow parachutes can be used successfully at much lower altitudes. An example in nature of the Stokes-flow parachute, found at sea level, is the dandelion seed.

REFERENCES

2.1 Terms and Symbols for Flight Dynamics - Part 1: Aircraft Motion Relative to the Air. International Standard 1151. *International Organization for Standardization.* Second Edition-1975

2.2 Heinrich,H.G. and Haak,E.L Stability and Drag of Parachutes with Varying Effective Porosity. U.S. Air Force Flight Dynamics Laboratory, Ohio, AFFDL-TR-71-58, February 1971

2.3 Lingard,J.S. The Performance and Design of Ram-Air Gliding Parachutes. U.K. Royal Aircraft Establishment TR 81103, August 1981

2.4 Nicolaides,J.D. Parafoil Wind Tunnel Tests. U.S. Air Force Flight Dynamics Laboratory, Ohio, AFFDL-TR-70-146, 1971

2.5 Jorgensen,D.S. *Cruciform Parachute Aerodynamics.* PhD. Thesis, University of Leicester, 1982

2.6 Ludtke, W.P. Effects of Canopy Geometry on a Cross Parachute, in the Fully Open and Reefed Conditions, for a W:L Ratio of 0.264. U.S. Naval Ordnance Laboratory, NOLTR 71-111, August 1971

2.7 *Performance of and Design Criteria for Deployable Aerodynamic Decelerators.* U.S. Air Force Flight Dynamics Laboratory, Ohio. Technical Report ASD.TR.61.579, December 1963

2.8 Knacke,T.W. and Hegele,A.M. Model Parachutes: Comparison Test of Various Types. U.S. Air Force/Aeronautical Systems Div. Report MCREXE-672-12D, January 1949

2.9 Berndt,R.J. and Babish,C.A. Supersonic Parachute Research. *Proceedings of Retardation and Recovery Symposium*, edited by G.A.Solt, pp.112-157, U.S. Aeronautical Systems Div., Ohio, ASD-TR-63-329, 1963

2.10 Doherr,K.-F. *Theoretisch-experimentelle Untersuchung des dynamischen Verhaltens von Fallschirm-Last-Systemen bei Windkanalversuchen*. Ph.D.Thesis, Technische Universität München, 1981. Published as DFVLR-FB 81-29

2.11 Shen,C.Q and Cockrell,D.J. Aerodynamic Characteristics and Flow Round Cross Parachutes in Steady Motion. AIAA 86-2458-CP. *Proceedings of the 9th Aerodynamic Decelerator and Balloon Technology Conference*, Albuquerque, 1986.

2.12 Jorgensen,D.S. and Cockrell,D.J. Effect of Drive Slots on Parachute Performance. *AIAA Journal of Aircraft*, 18, 6, pp. 501-503, June 1981

2.13 Heinrich,H.G. The Effective Porosity of Parachute Cloth. *Zeitschrift für Flugwissenschaften*, 11, Heft 10,Verlag Friedr.Vieweg & Sohn, Braunschweig, 1963

2.14 Payne,P.R. The Theory of Fabric Porosity as Applied to Parachutes in Incompressible Flow. *Aeronautical Quarterly*, 29, August 1978.

2.15 Mihora, D.J. Engineering Data on Stokes-Flow Drag Devices. Astro Research Corporation,Santa Barbara, U.S.A. March 1973.

2.16 Niederer,P.G. Development of a High Altitude Stokes Flow Decelerator. N68-15425. Astro Research Corporation, Santa Barbara, U.S.A. November 1966.

APPENDIX TO SECTION 2
SOME COMMONLY-ADOPTED SHAPES FOR CONVENTIONAL PARACHUTE CANOPIES
A Summary of Aerodynamic Characteristics, drawn from references 1.7, 1.9 and 2.7.

2A.1 SOLID TEXTILE CANOPIES

Description	Usage	Aerodynamic Characteristics
FLAT CIRCULAR CANOPY CONSTRUCTION SCHEMATIC 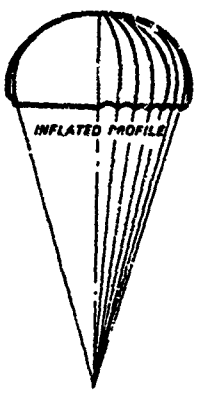 	A low cost, light weight canopy which is suitable for deployment at low dynamic pressures. It is most widely used by personnel and for cargo recovery.	Exhibits instability in pitch, possessing a conic oscillation of some 20-30° semi-apex angle. Clusters of flat circular canopies do not exhibit this characteristic, since each canopy in the cluster is no longer at 0° angle of attack.

Description	Usage	Aerodynamic Characteristics
EXTENDED SKIRT CANOPY CONSTRUCTION SCHEMATIC 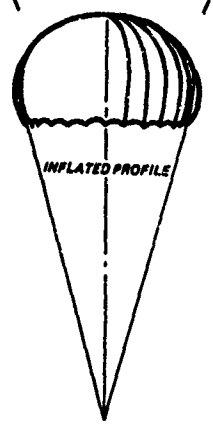	Suitable for the airdrop of material and for the recovery of drones.	This canopy has a higher drag than a flat circular canopy. It also has a longer opening time, but it develops correspondingly lower opening forces.
GUIDE SURFACE CANOPY 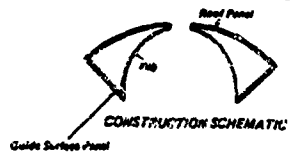 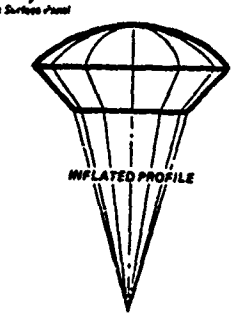	Frequently used as a pilot parachute, for extraction purposes. Has been used with both very low and very high dynamic pressures, the Mach number ranging from 0 to 3.0	Has a high geometric porosity (15% to 30%), which gives it good stability in pitch. It is also very reliable in inflation.

2A.2 SLOTTED TEXTILE CANOPIES

Description	Usage	Aerodynamic Characteristics
CROSS CANOPY 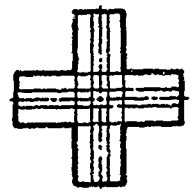 CONSTRUCTION SCHEMATIC  INFLATED PROFILE	An easily-constructed low cost parachute which is frequently used for the deceleration of ground vehicles and aircraft. Its applications also include weapon deceleration and stabilisation.	Good drag characteristics and provided that its arm ratio and porosity are properly selected it has an excellent stability in pitch. However, it displays a tendency to rotate about its axis of symmetry.

Description	Usage	Aerodynamic Characteristics
RIBBON CANOPY CONSTRUCTION SCHEMATIC 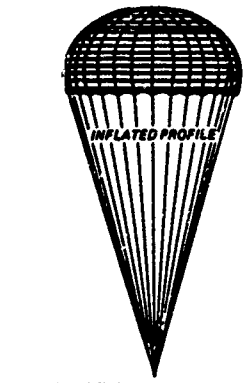	A very strong canopy which is therefore used for aircraft and vehicle deceleration at relatively high dynamic pressures [up to 270 kN/m² (5 700 lbf/ft²)]	Has a lower drag efficiency than a solid textile canopy but it also has an excellent stability in pitch.
RING SLOT CANOPY  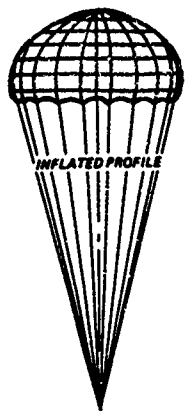	This is like a ribbon canopy but with much wider bands. Since these lead to it being relatively cheap to manufacture it is frequently used for high dynamic pressure cargo delivery and aircraft deceleration.	Its aerodynamic characteristics are comparable with those of the ribbon canopy.

2.3 GLIDING PARACHUTE CANOPIES

The Ram-Air Canopy, drawn from references 1.9, 2.3 and 9.1.

Description	Usage	Aerodynamic Characteristics
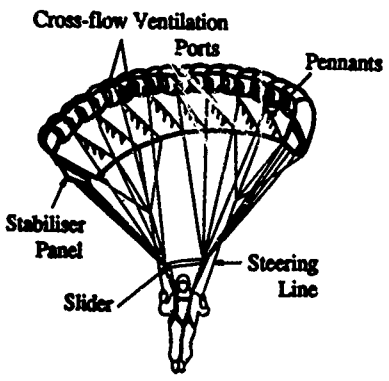 Rear Suspension Lines have not been shown	Used when 'drive' is required. Of the high-glide parachutes described in ref. 1.9 the most common are canopies which are ram-air inflated. They have a variety of commercial names. They are characterised by aerofoil cross-sectional shapes and planforms whose aspect ratios are as large as possible on aerodynamic grounds. However, in order that good control is maintained they are limited to a maximum of about 3:1.	The angle of descent γ_d is inversely proportional to the ratio L/D (equation 2.19a). Typically, $(L/D)_{max}$ is about 3:1, but see Section 9.5.1

3.TRAJECTORY DYNAMICS

The object of Trajectory Dynamics is to predict the flight path for the system which comprises the combination of a parachute and payload. In principle, provided the parachute's significant aerodynamic characteristics, in particular the canopy drag area $C_D S_o$, defined in Section 2.3.3, are known as a function of time, then the appropriate equations of motion for the parachute-payload system can be written and approximate numerical solutions obtained. In the course of the time over which these equations are valid the parachute might be undeployed, undergoing deployment, inflating or be fully inflated.

For all but the simplest models of this system, the equations of motion are not straightforward. Consequently, their solutions, too, are complex.

3.1 THE TRAJECTORY SYSTEM. AXES SYSTEMS. DEGREES OF FREEDOM

The nature of the trajectory system which it is necessary to consider, the axis system to be adopted and the number of degrees of freedom which are required in the consequent analysis depend on both the input data which are available and the complexity of the solution which is required. The number of equations required to describe the motion of the system depend on the number of *degrees of freedom* which the system possesses. A single body which can move freely in a plane possesses three degrees of freedom. It requires three independent variables to define its position relative to fixed axes, two co-ordinates to locate a chosen point in the body and a further co-ordinate to orientate the body. The total number of co-ordinates required to specify the configuration of n unconnected bodies is $3n$, but if these bodies are connected together by various mechanisms then degrees of freedom are lost.

In order to establish the equations of motion it is important to choose carefully the frames of reference which are to be adopted. In Newton's laws, on which rigid-body dynamics is based, all motion is ultimately considered relative to a stationary reference frame. These laws state that the external forces and moments which act on a system, together with the system's inertia forces and moments, are in a state of equilibrium. *Inertia forces and moments* are the reversed rate of change of the system's linear and angular momenta.

For most parachute applications, the earth can be considered to provide an absolute frame of reference and axes which are fixed relative to the earth are termed *earth-fixed axes*. When the frame of reference is fixed relative to a moving body, as could occur in a system consisting of a parachute canopy rigidly connected to its payload, they are termed *body axes*. In general, on both parachute and payload the aerodynamic and the inertial forces and moments which act on the system can be determined relative to these body axes, since they are functions of the body resultant velocity and its attitude. However, not only are the gravitational forces and moments determined relative to earth-fixed axes but the trajectory of the descending system is ultimately required relative to these axes. Thus, in obtaining solutions to trajectory dynamics problems, it is usually necessary to adopt both earth-fixed axes and body axes, together with the geometric transformation relationships between these two axes sets. Since the payload can move relative to the parachute it may be necessary to adopt more than one set of body axes, establishing some idealised relationship to describe the mode of coupling between the parachute and its payload.

There is no universally-agreed method of modelling the parachute-payload system. It is important to model the system's mechanics in no more complex a manner than is appropriate to develop the required solution within the constraints imposed by the available data. The approach adopted here owes much to Purvis[3.1]. Two-degree of freedom equations of motion are first described for the motion in two dimensions of a point mass representative of both the parachute and the payload, subjected to both aerodynamic and gravitational forces. Next, a three-degree of freedom set of equations is developed for two-dimensional motion of a payload which is simply-connected to a parachute of negligible mass. Using these equations, the consequences are considered of including the parachute canopy mass in this trajectory dynamics model. The third case described is a three-degree of freedom model for a parachute canopy assumed to be rigidly-connected to its payload. Finally, reference is made to publications which describe trajectory models with six or more degrees of freedom and to the use of finite-element analysis in order to model parachute canopies during their deployment and inflation phases as if they were a series of elastically-connected mass nodes.

3.2 TWO-DEGREE OF FREEDOM MODEL

Consider the motion of a point mass in the x-z plane, shown in Fig.3.1. As this mass is considered to act at a point, the system which it represents cannot possess any moments of inertia; hence no moments are exerted on it. In the plane Oxz, therefore, the system possesses only two degrees of freedom, translational motion in the direction O-x and translational motion in the direction O-z.

On symmetry grounds, the point mass cannot sustain any component of aerodynamic force normal to the line of flight. Thus, the resultant component forces which act on it in the O-x and O-z directions, F_x and F_z, are respectively given by:

$$F_x = -(D_p+D_s)\cos\gamma_d \qquad (3.1)$$

and $$F_z = mg - (D_p+D_s)\sin\gamma_d \quad (3.2)$$

where m denotes the mass of the system inclusive of any added mass, D_p is the drag developed by the parachute, D_s is the drag developed by the payload and γ_d is the angle of descent. Added mass is discussed in Section 4.

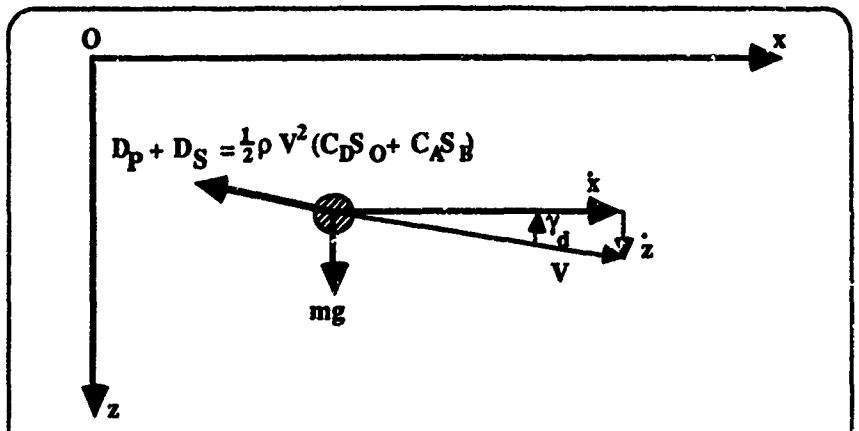

Fig. 3.1 TWO-DEGREE OF FREEDOM TRAJECTORY SYSTEM MODEL

Measuring the displacements x and z relative to the earth-fixed axes O-x and O-z, since

$$\dot{x} = V\cos\gamma_d, \quad (3.3)$$

and $$\dot{z} = V\sin\gamma_d \quad (3.4)$$

then the trajectory equations are:

$$m\ddot{x} = -(1/2)\rho V\dot{x}(C_D S_o + C_A S_B) \quad (3.5)$$

and $$m\ddot{z} = mg - (1/2)\rho V\dot{z}(C_D S_o + C_A S_B) \quad (3.6)$$

where $C_D S_o$ is the parachute canopy drag area, S_B denotes the payload reference area and C_A the payload axial force coefficient.

From known initial conditions of the parachute and payload, equations 3.3 and 3.4 give initial values of $\dot{x}$ and $\dot{z}$. Then, for known values of the payload reference area and axial force coefficient, the system weight mg, the canopy drag area as a function of time, together with the parachute system's initial altitude and velocity, equations 3.5 and 3.6 are soluble. They yield as functions of time the system's horizontal and vertical co-ordinates, its velocity and its flight path.

Initial values of $\ddot{x}$ and $\ddot{z}$ can then be determined from the equations 3.5 and 3.6. These relationships are first-order differential equations in $\dot{x}$ and $\dot{z}$. Over short, finite time increments, Δt their solutions for $\ddot{x}$ and $\ddot{z}$ can be used to update $\dot{x}$ and $\dot{z}$. To achieve this end, a number of appropriate numerical integration schemes exist, of which the following is illustrative:

$$(\dot{x})_2 = (\dot{x})_1 + (\ddot{x})_1\Delta t \quad (3.7)$$

and $$(\dot{z})_2 = (\dot{z})_1 + (\ddot{z})_1\Delta t\ . \quad (3.8)$$

3.3 THREE-DEGREE OF FREEDOM MODEL

When angular as well as linear motion in the Oxz plane is required for the parachute and its payload, then a three-degree of freedom model is adopted. Purvis notes that at this stage the method adopted to represent the parachute and the payload must be considered carefully and lists four different approaches:

(i). a massless parachute is joined by a massless rigid link to its payload, the link being pin-joined at its attachment points;
(ii). the parachute and its payload constitute a single rigid body;
(iii). the parachute and its payload each possess mass and each constitute a single rigid system, the systems being joined by a massless rigid link, and
(iv). the parachute is represented as an elastic system, the payload as a single rigid body.

3.3.1 The Massless Parachute Joined to the Payload

For the point mass system described in Section 3.2 the resultant aerodynamic force must, on symmetry grounds, act along the flight path. But if the parachute is now represented as a solid body, it need not possess axial symmetry and then, in general, aerodynamic force components along and at right angles to the flight path will act on it. However, if m is made equal to zero, Fig 3.2 shows that the parachute is modelled as possessing no mass, then the resultant force T, which it develops on the payload, must be equal and opposite to the parachute drag D_p, acting along the flight path.

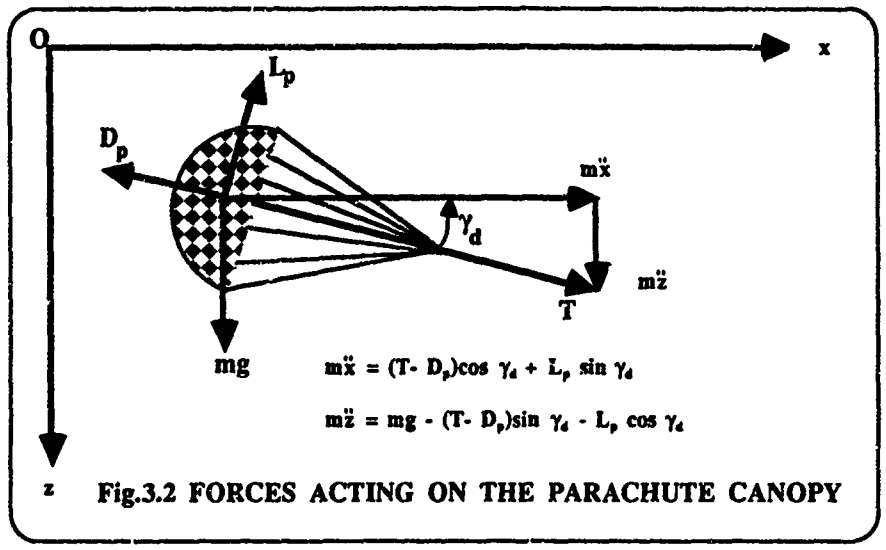

Fig.3.2 FORCES ACTING ON THE PARACHUTE CANOPY

To develop the translational equations of motion, earth-bound axes are used as in Section 3.2, but for the rotational equation, body axes will be adopted.

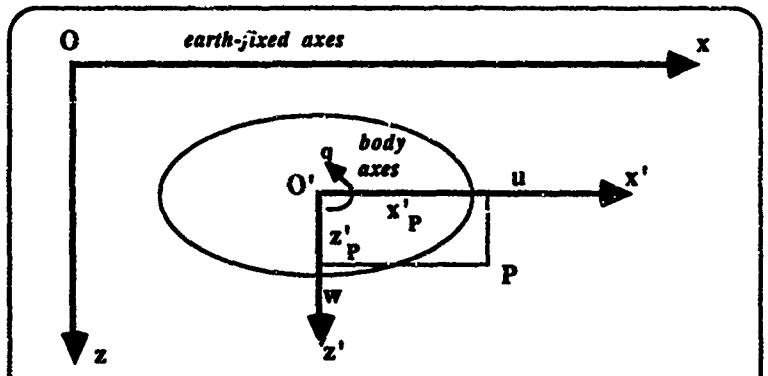

Fig.3.3 ROTATIONAL MOTION, USING BODY AXES

In Fig.3.3 a body rotates with angular velocity q about an origin O'. Relative to the earth-fixed axes Ox and Oz, the velocity components at the origin of the body are u and w respectively. Then, relative to those axes, the velocity components at a general point P within the body are:

$$\dot{x}_p = u + q\,z_p \qquad (3.9)$$

$$\dot{z}_p = w - q\,x_p\,. \qquad (3.10)$$

Relative to these earth-fixed axes, the component rates of change of linear momentum for the body are therefore:

$$\Sigma m_p \dot{x}_p = \Sigma m_p u + q\Sigma m_p z_p = \Sigma m_p u \qquad (3.11)$$

and

$$\Sigma m_p \dot{z}_p = \Sigma m_p w - q\Sigma m_p x_p = \Sigma m_p w\,. \qquad (3.12)$$

Whereas, relative to the body axes origin O', the rate of change of angular momentum in two dimensions can be shown (e.g. Duncan[3.2]) to equal $I_{22}\dot{q}$, where I_{22} is the system moment of inertia about the body axis O'y'.

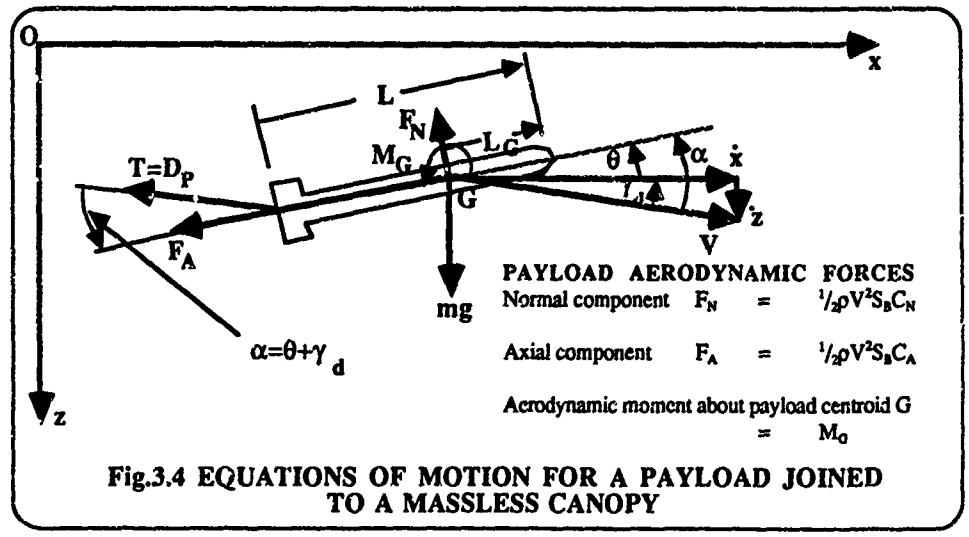

Fig.3.4 EQUATIONS OF MOTION FOR A PAYLOAD JOINED TO A MASSLESS CANOPY

From Fig.3.4, the equations of motion for the payload in three degrees of freedom are therefore:

$$m\ddot{x} = -F_N\sin\theta - F_A\cos\theta - {}^1/_2\rho V\dot{x}C_D S_o \qquad (3.13)$$

$$m\ddot{z} = -F_N\cos\theta - F_A\sin\theta - {}^1/_2\rho V\dot{z}C_D S_o + mg \qquad (3.14)$$

and

$$I_{22}\dot{q} = M_G - {}^1/_2\rho V^2 C_A S_B (L-L_G)\sin\alpha\ . \qquad (3.15)$$

In these equations the drag of the parachute D_p has been expressed as ${}^1/_2\rho V^2 C_D S_o$, while m and I_{22} respectively denote the total mass, inclusive of the added mass and the total moment of inertia, inclusive of the added moment of inertia, for the system under acceleration. Added masses and moments of inertia are explained later, in Chapter 4.

3.3.2 The Parachute and its Payload Modelled as a Single Rigid Body

The classical approach to the derivation of the equations of motion for the trajectory of a rigid body is to use body axes for all the required equations. It is clearly desirable to use body axes for the rotational equations of motion: if they are also used for translational motion the resulting equations can readily be linearised to determine the system response to small disturbances Thus Duncan[3.2] and Etkin[3.3] both use body axes in order to develop the equations of motion for a rigid body such as an aircraft, moving through space.

In developing the dynamical equations of motion for descending parachutes, there are two problems which do not occur with aircraft. The first is the large angles though which parachutes can oscillate during their descent. These might well limit the usefulness of any linearisation techniques which are developed as a part of the solution procedure.

The second problem is the necessity for the introduction of added mass terms in the parachute's equations of motion. The fluid through which the parachute and store descend is real rather than ideal and it will be shown in Section 4 that it is necessary to add experimentally-obtained values of certain added mass components into the equations of motion. These will add to their complexity.

When adopting the more classical approach of using body axes for both the translational and rotational equations of motion the fundamental problem is that, relative to fixed earth-bound axes, the body axes rotate. However, in both establishing the equations of motion and in the presentation of their solution, the motion of the system must be referred to an earth-fixed axes system.

For parachute trajectory analysis Purvis[3.1] has recommended the use of body axes for the associated rotational equations but earth-fixed axes for the translational equations, together with the necessary axis conversion matrix set. The translational motion equations expressed relative to earth-fixed axes, as in equations 3.13 and 3.14, do not include terms which include the product of linear and angular velocities. Equation 3.16 which follows, expresses the parachute's equation of motion relative to the body axis Ox and in so doing it includes the terms $(m+\alpha_{33})(rv-qw)$. The presence of terms of this form adds to the equation's complexity and also, when the parachute's angular velocity components p, q and r are large, to the length of the process for numerical solution of the equation. Using earth-fixed axes rather than body axes for the system's translational motion can therefore simplify both the presentation and solution of these equations, though it will complicate the task of expressing the relationships for the system's attitude angles.

In the presentation of the equations of motion inclusive of added mass terms, in accordance with Section 4.3.2, only the two added mass coefficients k_{11} and k_{33} have been retained and these have been assumed to be known constants, determined experimentally for the parachute system under consideration.

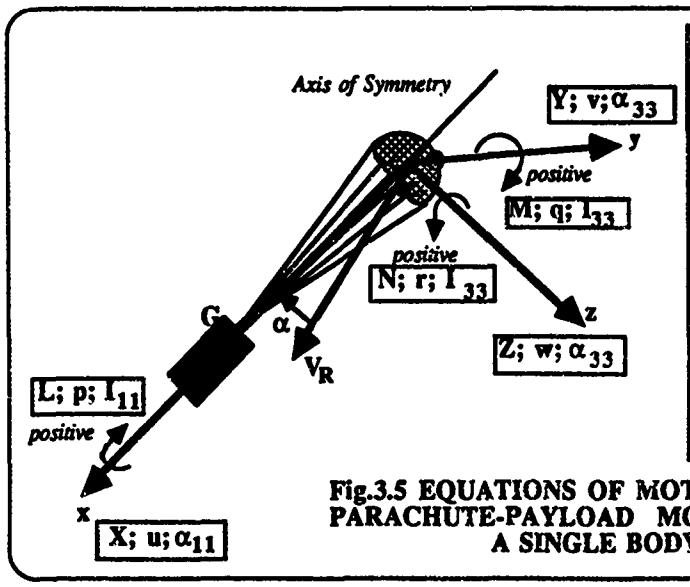

Fig.3.5 EQUATIONS OF MOTION FOR A PARACHUTE-PAYLOAD MODELLED AS A SINGLE BODY

For a conventional parachute subjected to external aerodynamic and gravitational force components X,Y and Z and external aerodynamic and gravitational moment components L, M and N, as shown in Fig.3.5, relative to the body axes Ox, Oy and Oz the appropriate equations of motion have been shown by Cockrell and Doherr[3.4] to be:

$$X = (m + \alpha_{11})\dot{u} - (m + \alpha_{33})(rv - qw) - mx_g(q^2 + r^2) \quad (3.16)$$

$$Y = (m + \alpha_{33})(\dot{v} - pw) + (m + \alpha_{11})ru + mx_g(\dot{r} + pq) \quad (3.17)$$

$$Z = (m + \alpha_{33})(\dot{w} + pv) - (m + \alpha_{11})qu - mx_g(\dot{q} - pr) \quad (3.18)$$

$$L = I_{11}\dot{p} \quad (3.19)$$

$$M = I_{33}\dot{q} - mx_g(\dot{w} - qu + pv) + (I_{11} - I_{33})pr \quad (3.20)$$

$$N = I_{33}\dot{r} + mx_g(\dot{v} + ru - pw) - (I_{11} - I_{33})pq \quad . \qquad (3.21)$$

In this family of equations the origin O has been located at the canopy centroid and the store, at a distance x_g from O, has been assumed to be rigidly connected to the canopy. The symbols I_{11} and I_{33} have been used to denote moments of inertia of the entire system about the axes Ox and Oy (or Oz) respectively and α_{11} and α_{33} to denote the added mass components of the canopy in the directions of the axes Ox and Oy (or Oz) respectively.

In accordance with equation 4.3, the added mass components α_{11} and α_{33} are given by:

$$\alpha_{11} = \rho_f \forall k_{11} \qquad (3.22)$$

and

$$\alpha_{33} = \rho_f \forall k_{33} \, . \qquad (3.23)$$

The symbols ρ_f and $\forall$ respectively denote the density of the fluid in which the parachute is immersed and the representative displaced volume of the parachute canopy. In comparison with other terms, the added masses and added moments of inertia of the store have been neglected. The symbols u,v and w, also the symbols p,q and r refer to linear and angular velocity components respectively, along and about the axes 0x, 0y and 0z, as shown in Fig.3.5.

In this presentation, the reasoning of Sedov[3.5] and others has been followed and the steady translational inertial moments, such as $(\alpha_{11} - \alpha_{33})uw$, have been neglected.

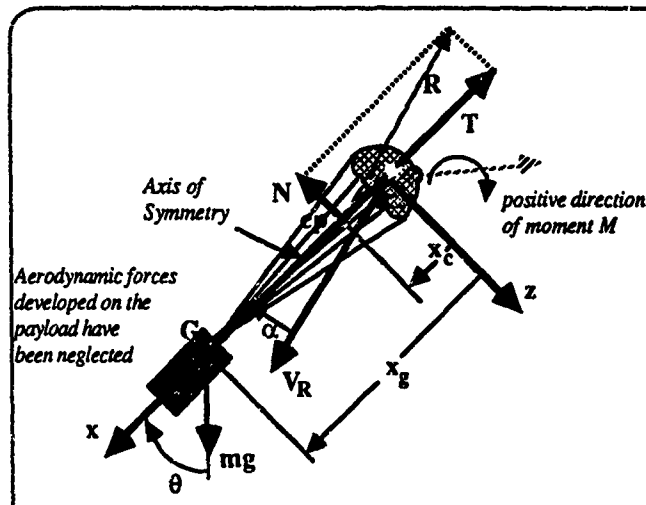

O	Origin of co-ordinate system
G	Parachute system centroid
cp	System centre of pressure
V_R	Resultant velocity at origin
α	Angle of attack
θ	Inclination angle of parachute system
R	Resultant aerodynamic force
N	Normal aerodynamic force component
T	Tangential aerodynamic force component

Fig.3.6 AERODYNAMIC AND GRAVITATIONAL FORCES AND MOMENTS

Neglecting any aerodynamic forces developed on the payload, for a parachute which is oscillating in the Oxz plane, Fig.3.6 gives for the external forces and moment about O acting on it:

$$X = mg \cos\theta - T \qquad (3.24)$$

$$Z = mg \sin\theta - N \qquad (3.25)$$

$$M = N x_c + (mg \sin\theta) x_g \qquad (3.24)$$

and expressions like these, or the corresponding ones in three dimensions which are given by both Duncan[3.2] and Etkin[3.3], should be inserted into equations 3.16 to 3.21, the equations of motion.

When solutions are required in all three planes, Euler angle transformations appropriate both to the gravitational forces and moments acting on the system and also to the trajectory solution which is being sought, are used to relate the body axes to the earth-fixed set of axis.

The equations of motion given in equations 3.16 to 3.21 were developed from a model, originally published by Tory and Ayres[3.6], of a parachute which was rigidly-connected to its payload. A somewhat similar five-degree of

freedom model for this system, but with rather different assumptions about the magnitudes of the unsteady aerodynamic forces and moments, has been developed and published by White and Wolf[3.7].

3.3.3 The Parachute and its Payload Modelled as Two Rigid and Linked Systems

If the mass of the parachute canopy cannot be considered to be negligible, so that the parachute and its payload comprise two separate but linked rigid systems, then appropriate modifications to equations 3.13 to 3.15 for the payload can be written and solved in conjunction with the equations given in Fig.3.2 for the parachute.

For a six-degree of freedom coupled payload and parachute model, Cutchins, Purvis and Bunton[3.10] have developed the concept discussed in Section 3.3.1 of using earth-fixed axes for the translational equations of motion and body axes for the rotational equations of motion.

Traditionally however, this problem has been tackled by the method developed in Section 3.3.2, using body axes for both the rotational and translational motions. For example, using two different sets of body axes, Schatzle and Curry[3.8] have developed a nine-degree of freedom model consisting of a system of equations for a forebody (or payload) coupled to a parachute. They considered the aerodynamic forces and moments developed on each body, together with the weight of the forebody. Similarly, allowing for the weight of the parachute as well as that of the forebody, Doherr[2.10] developed a body axis model and among others, Wolf[3.9] has published a model for a coupled payload and parachute. All these models start from the same premises but differ slightly in the way that they treat the unsteady aerodynamic forces, in the presentation of their equations of motion and in the subsequent linearisation techniques which they propose.

3.3.4 The Parachute as an Elastic System, Linked to a Rigid Body Payload

Sundberg[3.11] has explained the application to trajectory dynamics of finite-element methods, which enable both the canopy and its suspension lines to be modelled as flexible, distributed mass structures, coupled to a rigid payload. This is a particularly appropriate model for the deployment and inflation phases of the parachute. An extension of this earlier work has been made by Purvis[3.12].

REFERENCES

3.1 Purvis,J.W. Trajectory and *Loads. Proceedings, University of Minnesota Decelerator Systems Engineering Short Course*, Albuquerque, New Mexico, July 1985.

3.2 Duncan,W.J. *The Principles of the Control and Stability of Aircraft.* Cambridge University Press, 1959.

3.3 Etkin,B. *Dynamics of Flight.* J.Wiley & Sons,New York, 1959.

3.4 Cockrell,D.J. and Doherr,K.-F. Preliminary Consideration of Parameter Identification Analysis from Parachute Aerodynamic Flight Test Data. AIAA-81-1940. *Proceedings of the 7th Aerodynamic Decelerator and Balloon Technology Conference*, San Diego, 1981.

3.5 Sedov,L.T. *Two-Dimensional Problems in Hydrodynamics and Aerodynamics.* J.Wiley & Sons,New York, 1965.

3.6 Tory,A.C. and Ayres,R.M. Computer model of a fully- deployed parachute. AIAA Journal of Aircraft, 14, 675-679, July 1977.

3.7 White,F.M. and Wolf,D.F. A Theory of Three-Dimensional Parachute Stability. AIAA Journal of Aircraft, 5, 1, 86-92, Jan.-Feb. 1968.

3.8 Schatzle,P.R. and Curry,W.H. Flight Simulation with a Two-Stage Parachute System. AIAA-79-0448. *Proceedings of the 6th Aerodynamic Decelerator and Balloon Technology Conference*, Houston, 1979.

3.9 Wolf,D. Dynamic Stability of a Nonrigid Parachute and Payload System. AIAA Journal of Aircraft, 8, 8, 603-609, Aug. 1971.

3.10 Cutchins,M.A., Purvis,J.W. and Bunton,R.W. Aeroservo-elasticity in the Time Domain. AIAA Journal of Aircraft, 20, 9, Sept.1983.

3.11 Sundberg,W.D. Finite-Element Modeling of Parachute Deployment and Inflation. AIAA-75-1380. *Proceedings of the 5th Aerodynamic Deceleration Systems Conference*, Albuquerque, 1975.

3.12 Purvis,J.W. Numerical Simulation of Decelerator Deployment. *Proceedings, University of Minnesota Decelerator Systems Engineering Short Course*, Albuquerque, New Mexico, July 1985.

4. UNSTEADY AERODYNAMICS

During the deployment and inflation stages and even during descent, much of a parachute's motion is unsteady. Whether the axis system which is adopted is earth-bound or is fixed within the canopy-store system, linear and angular components of acceleration, along and about these axes, will occur. In this chapter the aerodynamic consequences of this unsteady motion are discussed.

4.1 INTRODUCTION TO THE UNSTEADY FLOW PROBLEM

In describing the unsteady motion of a body immersed in a fluid care must be taken in defining the constituent parts of the system under consideration.

First, consider it to consist of a sphere of mass m immersed in a fluid. Suppose this sphere to be driven through the fluid by a thrust T so that at time t the sphere is moving with an instantaneous linear velocity V(t) and an instantaneous linear acceleration $\dot{V}(t)$. On the sphere an aerodynamic force D'(t) is developed. This force is larger than the drag force D, which would be developed if it were to move steadily through the fluid at velocity V. The difference, D'-D, certainly depends the instantaneous acceleration, $\dot{V}(t)$. As is discussed in Section 4.2.2, it may also depend on the nature of the accelerated motion, though this may not be an important dependency.

The reason for this increased drag is that the fluid which surrounds the moving sphere will also acquire momentum. Thus, as the sphere accelerates, not only is there a rate of change in the momentum of the sphere, $m\dot{V}$, but in that of the surrounding fluid. If this fluid were *ideal*, that is if it were incompressible and irrotational, then the rate of change of fluid momentum, $\dot{M}_f$, is determinable by methods to be explained in Section 7. It can be expressed by:

$$\dot{M}_f = D'-D = \alpha\dot{V} \qquad (4.1)$$

where α is described as an *added mass component* for the system. For a sphere whose volume is denoted by $\forall$, linearly accelerating through an ideal fluid of density ρ_f, the added mass component α_i can be shown to be equal to $0.5\rho_f\forall$.

If the sphere were to accelerate through a *real fluid* as distinct from one which is ideal, a similar added mass component, α_r, but of a different numerical value from α_i, would be developed. A real fluid is one whose viscosity is the cause for it to possess vorticity, hence to be rotational. Writing the rate of change of momentum for the body immersed in the real fluid as $\dot{M}_b$ and assuming α_r to be independent of time gives:

$$\dot{M}_b = T-D'$$

where from equation 4.1, since $D'-D = \alpha\dot{V}$;

then $$\dot{M}_b = T - D - \alpha\dot{V}$$

and thus $$(m + \alpha_r)\dot{V} = T - D . \qquad (4.2)$$

where D is the drag force which the sphere develops in steady motion. Unlike equation 4.1, equation 4.2 treats the immersed body of mass m together with the fluid in which it is immersed as two constituent parts of a single dynamical system. The approach has a 120-year long history, extending from both Thomson and Tait[4.1] and Kirchhoff[4.2]. Lamb[4.3] remarked that, "it avoids the troublesome calculation of the effect of fluid pressures on the surfaces of solids", which would be a necessary procedure if the aerodynamic force D' were to be determined directly for the unsteady motion of a sphere through an ideal fluid. Both the importance and the method of determining added mass components relevant to the motion of a parachute canopy through ideal fluids remains to be discussed in Section 7.1. No analytical methods exist by which aerodynamic forces can be determined for unsteadily-moving bodies immersed in real fluids: the ideal fluid concept gives an approximate model which, for a bluff body like a conventional parachute, is of uncertain value.

In exactly the same way as that outlined in equation 4.1, when any immersed body moves unsteadily in any direction through a fluid the aerodynamic forces and moments are developed on it differ in magnitude from their steady state values. In a given problem, whether or not this difference is of any engineering significance depends on the relative magnitudes of the rate of change of momentum for the immersed body, $\dot{M}_b$, to that of the fluid in which it is immersed, $\dot{M}_f$. This ratio is a function of:

(i). the immersed body density compared with that of the fluid which it displaces;
(ii). the immersed body shape inclusive of its porosity, if any; and
(iii). the direction in which these rates of change of momenta occur.

For parachutes, the ratio is certainly of engineering significance when considering parachute inflation and also when modelling the oscillatory motion of parachute canopies in their descent through the air.

4.2 THE ADDED MASS CONCEPT IN PARACHUTE UNSTEADY MOTION

4.2.1 General Considerations

There are two important applications of the added mass concept to unsteady parachute motion. The first is to canopy inflation. Knacke[1.3] states that Scheubel[4.4], reported in 1946, was the first to investigate added mass effects on parachute opening processes and these will be discussed here in Sections 4.3.2 and 5.3. The second application is to the parachute's dynamic stability characteristics in pitch during its fully-inflated descent motion. Whereas static stability has been shown in Section 2.3.2 to be concerned with the direction of the moments developed on a parachute system after it has been disturbed from the equilibrium state, dynamic stability characteristics are related to the frequency and to the damping of the oscillatory unsteady motions which then ensue. To analyse these motions satisfactorily it is necessary to write and to solve systems of equations similar in form to those expressed in Section 3.3. For the adequate analysis of both the canopy inflation phase and the oscillatory motion of the parachute system when the canopy is fully inflated, it is first necessary to determine the added mass components appropriate to a given canopy shape. If analytical methods are to be adopted, it is necessary to assume that the fluid field in which the parachute canopy is immersed is ideal.

With the application to parachute canopies in mind and following Lamb and Milne-Thomson[4.5] among other authors, Ibrahim[4.6] in 1965 evaluated some of the added mass components for cup-shaped parachute canopies in ideal fluid flow. Later, Klimas[4.7] demonstrated that these analytical values are strongly dependent on the porosity of the canopy. By methods such as they adopted it can be shown that the canopy added mass component α is a function of its shape and attitude. It is also proportional to the body size and the fluid density, ρ_f thus:

$$\alpha_{ij} = k_{ij}\rho_f \forall, \qquad (4.3)$$

where, in ideal fluid flow, *the added mass coefficient* k_{ij} is a constant for a given immersed body shape and attitude. The symbol $\forall$ is used for the *representative displaced volume*. Where a straightforward definition is possible, e.g. for an immersed sphere, the representative displaced volume is the actual displaced volume. For a parachute canopy it is conventionally considered to be that of a *hemisphere* (though some authorities define the added mass coefficients for a canopy in terms of a sphere rather than a hemisphere) having a diameter D_o equal to the nominal diameter of the canopy, i.e

$$\forall = \pi D_o^3/12 . \qquad (4.4)$$

SHAPE		k_{11} along axis Ox	k_{22} along axis Oy	k_{33} along axis Oz	k_{44} about axis Ox	k_{55} about axis Oy	k_{66} about axis Oz
2-dimensional Circular Cylinder. a=b as Fig (i)		Varies with cylinder length	1.0	1.0	0	-	-
Circular Disc as Fig (i)		0	0.64	0.64	0	0.39[1]	0.39
Elliptical Cylinder a/b as Fig (i)	0.25	Varies with cylinder length	4.00	0.25	1.65[2]	-	-
	0.50		2.00	0.50	0.45	-	-
	2.00		0.50	2.00	0.45	-	-
	4.00		0.25	4.00	1.65	-	-
Sphere		0.50	0.50	0.50	0	0	0
Ellipsoidal Axisymmetric Bodies Length/Dia as Fig (ii)	2.00	0.21	0.70	0.70	0	0.24[3]	0.24
	4.00	0.08	0.86	0.86	0	0.61	0.61
	8.00	0.03	0.94	0.94	0	0.84	0.84

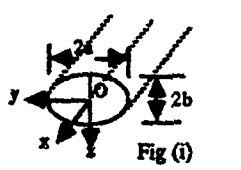

Fig (i)

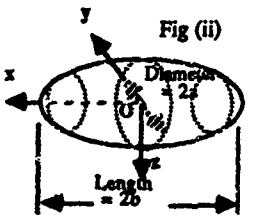

Fig (ii)

Notes
1. For the circular disc $I_f = \rho_f \forall \frac{2}{\pi}$
2. For the elliptical cylinder $I_f = \rho_f \forall \frac{(a^2+b^2)}{4}$
3. For ellipsoidal bodies $I_f = \rho_f \forall \frac{(a^2+b^2)}{5}$ where $\forall = \frac{4}{3}\pi a^2 b$

Table 4.1 ADDED MASS COEFFICIENTS DETERMINED ANALYTICALLY FOR BLUFF BODIES IMMERSED IN IDEAL FLUIDS
(after Robertson[4.8])

Some appropriate analytical values of added mass coefficients are given in Table 4.1. In this Table the added moment of inertia coefficient k_{55}, measured about an axis at right angles to the plane containing k_{11} and k_{33}, is defined in terms of the added moment of inertia component α_{55} as

$$k_{55} = \alpha_{55}/I_f \qquad (4.5)$$

where I_f is the moment of inertia of the fluid in the representative volume. For a parachute canopy:

$$I_f = (\rho_f D_o^2 \forall)/16 \ , \qquad (4.6)$$

the density of the fluid in which the canopy is immersed being denoted by ρ_f.

A number of experiments have been performed to determine the added mass components for bluff bodies moving unsteadily through fluids since at least as long ago as 1826, when Bessel[4.9] tested the periodic motion of a spherical pendulum, both in air and under water. As shown in Table 4.2, many of these results have proved to be inconclusive. Often the added mass components which have been evaluated differed only marginally from those obtained analytically for unsteady motion through an ideal fluid. However, other tests have shown some marked differences.

SHAPE	INVESTIGATOR	k_{11} (Axial)	REYNOLDS NUMBER	NATURE OF EXPERIMENT
Sphere	Bessel - 1826	Air 0.9 Water 0.6	- -	Oscillating Spherical Pendulum
	Lunnon - 1928	Air & 0.5 to Water 2.0	10^4 to 10^5	Unidirectional
	McEwan-1911	Water 0.5	-	Oscillating Torsional Pendulum
	Relf & Jones - 1918	Water 0.8	-	Oscillating Torsional Pendulum
	Cock - 1920	Water 0.5	10^5	Free Fall
	Frazer & Simmons-1919	Water 1.0 to 2.0	10^4	Unidirectional
Flat Plate	Gracey- 1947	Air- 0.94 & 0.96		Oscillating Pendulum
Disc	Yee-Tak Yu - 1942	Various - 0.81		Oscillating Torsional Pendulum
	Ibrahim-1965	Water 0.8	10^3	Oscillating Torsional Pendulum

References

Bessel 4.9; Lunnon 4.10 ; McEwan 4.11 ; Relf & Jones 4.12 ; Cook 4.13 ; Frazer & Simmons 4.14 ; Gracey 4.15 ; Yee-Tak Yu 4.16 ; Ibrahim 4.17

Table 4.2 ADDED MASS COEFFICIENTS DETERMINED EXPERIMENTALLY FOR BLUFF BODIES IN REAL FLUIDS

4.2.2 Determining the Added Mass Components

In their determination of the added mass components from suitably-designed experiments most workers adopted methods similar to those which Iversen and Balent[4.18] described in 1951. From equation 4.2;

$$(m + \alpha_r)\dot{V} = T - D$$

and writing the steady-state drag D as equal to $\frac{1}{2}\rho V_R^2 S_o C_D$, they considered the appropriate component of aerodynamic force, F(t) to consist of two parts: one which could be expressed in terms of the instantaneous velocity, V(t) and the other which could be expressed in terms of the instantaneous acceleration, $\dot{V}(t)$. Thus in unsteady flow the total aerodynamic force F(t) at time t was written in terms of coefficients a and b as:

$$F(t) = aV^2(t) + b\dot{V}(t) \ . \qquad (4.7)$$

It remains to devise an appropriate experimental programme from which to determine a and b.

One way of doing this is would be to measure the aerodynamic force, F_s at a steady velocity V first, so obtaining the component a. The component b would then be given from the difference in magnitude between the aerodynamic forces developed on the immersed body in corresponding unsteady and steady motion, $F(t)-F_s$. Using equation 4.3, the appropriate added mass coefficient could then be calculated from the component b. This method assumes that the velocity-dependent component of aerodynamic force in unsteady motion is unchanged from its corresponding value in steady motion, an assumption which is difficult to justify on physical grounds.

In a method applicable to periodic motion, which owes much to both Sarpkaya & Isaacson[4.19] and also to Bearman et al[4.20], average values of the components a and b are calculated by first multiplying equation 4.7 either by V(t) or by $\dot{V}(t)$, then taking mean values of the resulting relationship over a period T , so that:

$$\frac{1}{T}\int_0^T F(t)V(t)\,dt = \frac{1}{T}\int_0^T aV^2(t)\,dt + \frac{1}{T}\int_0^T b\dot{V}(t)V(t)\,dt \qquad (4.8)$$

and

$$\frac{1}{T}\int_0^T F(t)\dot{V}(t)\,dt = \frac{1}{T}\int_0^T aV^2(t)\dot{V}(t)\,dt + \frac{1}{T}\int_0^T b\dot{V}^2(t)\,dt\ . \qquad (4.9)$$

Average values of a and b can then be determined, since

$$\int_0^T \dot{V}(t)V(t)\,dt = \int_0^T V^2(t)\dot{V}(t)\,dt = 0\ . \qquad (4.10)$$

A simpler procedure would be to apply the method described in Section 2.4 by first writing equation 4.7 in the form:

$$\{F(t)/V^2(t)\} = a + b\{\dot{V}(t)/V^2(t)\}\ . \qquad (4.11)$$

This is a linear relationship between the two variables $\{F(t)/V^2(t)\}$ and $\{\dot{V}(t)/V^2(t)\}$. Having plotted experimental data in this form, regression analysis can be used to yield values for the two components a and b.

An advantage of this latter technique over the one described previously is that it is immediately possible to see from the graph of equation 4.11 if the two components a and b are sensibly constant over an entire period, or if they vary. For example, they could possess different values when the acceleration of the system is positive from those when it is negative. An illustration by Harwood[4.21], in the course of his determination of Table 4.3, is shown in Fig.

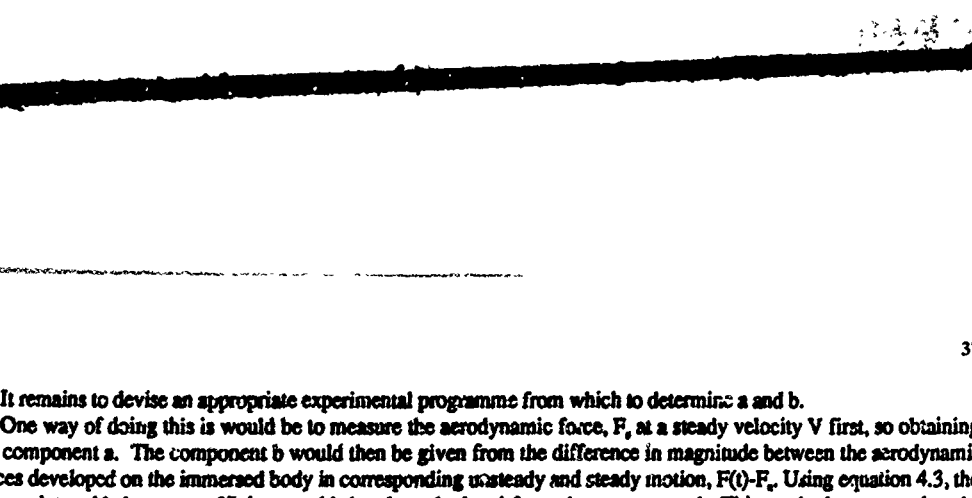

4.1. This graph indicates that although equation 4.7 is an approximation it can serve as an acceptable engineering relationship for the unsteady aerodynamic force F(t) developed on parachute canopies.

Experimental conditions under which the various tests reported in Table 4.2 were performed varied greatly. In some, the unsteady motion was unidirectional. In others it was either wholly oscillatory or a combination of these two modes. Methods of determination of the added mass coefficient varied too; in some experiments average values of aerodynamic force were determined, in others instantaneous values were obtained. In most of these tests, the experimental uncertainty with which the added mass coefficients were obtained was high.

Among others, Hamilton and Lindell[4.22] have suggested that the manner in which unsteady motion is imparted to an immersed body is significant and there is a significant weight of experimental evidence to support their view. They suggested that only if there are long periods of constant velocity or constant acceleration can the instantaneous

aerodynamic force F(t) be well expressed solely in terms of the instantaneous velocity, V(t) and the instantaneous acceleration, $\dot{V}(t)$, in the manner proposed in equation 4.7. Hamilton and Lindell stated that 'the practice of expressing fluid force as a function of the instantaneous velocity and the acceleration of the body (or the fluid) has carried over to engineering problems in which convective accelerations, flow separation and wakes are important (nonlinear) cases. The force is determined experimentally and its relationship to velocity, acceleration and other parameters is expressed in a variety of ways. The equations may, or may not, include an added mass term and, if they do, it may be a constant or a function of various parameters. The choice depends on the kind of motion and, to some extent, on the view of the author'. Instead they proposed that a more general form of equation 4.7 should be written:

$$F(t) = aV^2(t) + b\dot{V}(t) + \text{flow history term} \qquad (4.11a)$$

the form of the latter term depending on the manner in which the unsteady motion is imparted to the immersed body.

4.3 SIGNIFICANCE OF ADDED MASS COEFFICIENTS TO PARACHUTE UNSTEADY MOTION PREDICTION

4.3.1 Their Historical Importance

For fluid dynamical problems concerning parachute canopies, whose drag-producing capabilities are among their most significant aerodynamic characteristics, to base analysis on the assumption that the fluid through which the canopy descends is ideal would appear to be unrealistic, for in such a fluid no separated wake could be developed and steady motion descent would necessarily be drag free. It is thus clear that results obtained from such a mathematical model must be validated through appeal to appropriate experimental programmes.

Considering the canopy deployment and inflation application and based on flow visualisation studies for inflating parachute canopies, Lingard[4.23] and others have suggested that since canopy deployment is a very rapid process it may well be realistic to consider the surrounding flow field as though it were irrotational and thus, if it were also effectively incompressible, as ideal. O'Hara[4.24], for example, assumed that the added mass coefficient for an inflating parachute canopy was equal to that for a flat disc immersed in an ideal fluid, with a diameter equal to that of the canopy and thus during inflation its added mass would increase as the cube of its diameter.

In his 1944 paper on parachute descent behaviour, Henn[4.25] discussed the significance of added mass components on parachute dynamic stability. He called these components 'co-accelerated air masses' and stated that they were of the order of size of the combined mass of the canopy and its load. For their determination in two degrees of freedom he introduced an ellipsoid having the same major diameter, volume and location as the parachute canopy, using the analytical values for this ellipsoid of the axial, transverse and rotational added mass coefficients which Lamb[4.3] had previously determined and which have been given in Table 4.1. He concluded that added masses have a significant effect on the determination of parachute dynamic stability. Later, Lester[4.26] reformulated Henn's equations. Both Henn and he had shown that added mass coefficients were of importance in determining parachute dynamic stability characteristics. Lester commented on the unsatisfactory procedure of using analytical values, derived from the behaviour of ideal fluids around bluff parachute canopies, for these coefficients.

White and Wolf's[3.7] 1968 paper on parachute dynamic stability and Wolf's[3.9] later 1971 contribution, while recognising that the added mass coefficients were tensors, nevertheless over-simplified the problem of representing parachute unsteady motion. More recently Eaton[4.27] has reformulated the analytical problem, discussing the relative significance of the analytical values for the added mass coefficients which various authors have obtained. However, he presented its solution without recourse to experimentally-determined added mass coefficients.

In 1965 Ibrahim[4.17] published a paper describing an experimental method of determining added moments of inertia for parachute canopies. Apart from this earlier work, systematic experiments to determine added mass coefficients for parachute canopies were not reported until Yavuz[4.28] first published his work in 1982.

4.3.2 Their Contemporary Importance

During canopy inflation there is no doubt that the effects of added mass are of significance. If they were neglected and instead a series of steady flow solutions were obtained for canopies with increasing degrees of inflation in potential flow, it is highly unlikely that good approximations would be obtained for pressure distributions within the inflating canopies. In the continuity relationship given as equation 5.10 in Section 5.3.2 Heinrich introduced the added mass of the inflating canopy. However, as the aerodynamics of canopy inflation is still very much in its infancy, even very approximate estimates for the pressure distribution round the inflating canopy would be of real value. Insufficient material has been published to warrant any further discussion here of canopy added masses during the inflation process, in consequence only the dynamic stability pitching characteristics of fully-inflated canopies will be considered.

For a body which moves unsteadily through a fluid the added mass coefficients form a second-order tensor with twenty-one independent components, comprising six in which both the force and the acceleration components are translatory, six in which both moments and angular accceleration components are rotary and nine which describe mixed

translatory and rotary behaviour. Following the form of the equations derived in Section 3.4 for a parachute system with six degrees of freedom and after making a number of simplifying assumptions, Cockrell and Doherr[3,4] argued that for a conventional parachute canopy considered to be rigidly connected to its payload and for which, as shown in Fig.2.1, Ox is the axis of symmetry with planes of symmetry Oxy and Oxz, only four independent and significant added mass coefficients need be considered. In the tensor nomenclature which they adopted the first subscript denoted the direction in which the unsteady force was measured and the second that of the acceleration causing the added mass component under consideration. The numbers 1,2 and 3 implied linear motion in the directions of the axes Ox, Oy and Oz respectively while 4,5 and 6 described angular motion respectively about the axes Ox, Oy and Oz. Thus k_{11} is the added mass coefficient (referred to as the axial added mass coefficient) which is determined when an x-directed force is measured on a canopy undergoing an x-directed linear acceleration, i.e along the axis of symmetry.

These four significant added mass coefficients are:

(i). $$k_{11} = \alpha / \rho\forall \; ; \qquad (4.12)$$

(ii). $$k_{22} = k_{33} \; ; \qquad (4.13)$$

These latter are, respectively, the added mass coefficients determined when a y-directed force is measured on a canopy undergoing a y-directed linear acceleration and when a z-directed force is measured on a canopy undergoing a z-directed linear acceleration. They are non-dimensionalised from their appropriate added mass components α_{22} and α_{33} in exactly the same way as was k_{11} in equation 4.3;

(iii). $$k_{55} = k_{66}. \qquad (4.14)$$

These are the added moment of inertia coefficients determined when a moment about the y-axis is measured on a canopy undergoing an angular acceleration about the y-axis and when a moment about the z-axis is measured on a canopy undergoing an angular acceleration about the z-axis, respectively. As has been shown in equations 4.4, 4.5 and 4.6, they are non-dimensionalised from their respective added moment of inertia components, α_{55} and α_{66} thus:

$$k_{55} = \alpha_{55}/(\pi\rho_t D_o^5/192) \qquad (4.15)$$

and $$k_{66} = \alpha_{66}/(\pi\rho_t D_o^5/192) \; . \qquad (4.16)$$

(iv). The remaining significant added mass coefficient is:

$$k_{26} = k_{35}, \qquad (4.17)$$

non-dimensionalised from $\alpha_{26} = \alpha_{35}$. This is the added mass coefficient which is determined when a y-directed force is measured on a canopy undergoing an angular acceleration about the O-z axis, or when a z-directed force is measured on a canopy undergoing an angular acceleration about the O-y axis. Yavuz[4.28] has shown that if the origin of the co-ordinate system is located close to the canopy centre of pressure then this latter coefficient is of negligible magnitude.

Hence the problem of determining added mass coefficients has become one of determining experimentally only three added mass coefficients, k_{11}, $k_{22} = k_{33}$ and $k_{55} = k_{66}$. These three can be further reduced to two coefficients. If the origin of the co-ordinate system is located close to the canopy centre of pressure then the apparent moment of inertias of the canopy, α_{55} about the axis O-y and α_{66} about the axis O-z will be totally dominated by the moments of inertia of the payload and hence they can be neglected.

The two remaining added mass coefficients are k_{11} and $k_{22} = k_{33}$. In the determination of parachute dynamic stability characteristics these can be shown to be significant.

In tests performed on parachute canopies which moved steadily under water while they were forced to oscillate in either their axial or transverse direction, Cockrell, Shen, Harwood and Baxter[4.29] obtained the average values for the added mass coeficients k_{11} and k_{33} which are given in columns 5 and 6 of Table 4.3. From these experiments it is evident that the real fluid flow values obtained for these added mass coefficients substantially exceed the potential flow evaluations which Lamb, Ibrahim and others earlier determined.

Using Table 4.1 and idealising a parachute canopy into an ellipsoid having a length/diameter ratio of 0.5, analytical values for the added mass coefficients $k_{11} = 0.70$ and $k_{33} = 0.21$ can be obtained. These are based on the ellipsoid's displaced volume, which is equal in magnitude to that of a hemisphere whose diameter is equal to length of the ellipsoid's major axis. Hence, for this model for the parachute canopy, analytical values based on the canopy projected diameter are also 0.70 and 0.21 respectively. Assuming the projected diameter to equal 0.7 of the nominal

projected diameter are also 0.70 and 0.21 respectively. Assuming the projected diameter to equal 0.7 of the nominal diameter the analytical values, in terms of the representative displaced volume based on nominal canopy diameter D_o, would equal:

$$k_{11}(\text{analytical}) = 0.24; \quad k_{33}(\text{analytical}) = 0.07. \qquad (4.18)$$

Corresponding values which Doherr and Saliaris[4.30] used, written in terms of the nominal canopy diameter D_o and the present axis convention were:

$$k_{11}(\text{analytical}) = 0.34; \quad k_{33}(\text{analytical}) = 0.17. \qquad (4.19)$$

CANOPY TYPE	C_T Steady State	C_T Un-steady Motion	$[dC_N/d\alpha]_s$ $\alpha=0^o$ Steady State /radian	$[dC_N/d\alpha]_u$ $\alpha=0^o$ Unsteady Motion /radian	Added Mass Coefficients	
					k_{11} Axial	k_{33} Transverse
Round Canopies:						
Without Drive Slots	0.63	0.64	- 0.40	-	1.1	0.2
With Drive Slots	0.61	0.57	- 0.26	-	1.0	-
Cross Canopies:						
3:1 Arm Ratio						
Imporous	0.64	0.68	- 0.19	- 0.13	2.4	0.3
Very Porous,λ=23*	0.66	0.67	+0.46	+0.41	0.8	0.1
4:1 Arm Ratio						
Imporous	0.77	0.76	+0.52	+0.43	1.6	0.1

cubic ft./sq.ft./sec. measured at 10 inches of water pressure

Table 4.3 EXPERIMENTAL CHARACTERISTICS FOR PARACHUTE CANOPIES IN STEADY AND IN UNSTEADY MOTION

(after Cockrell, Shen, Harwood and Baxter[4.29] and later revised by Harwood[4.21])

Ibrahim[4.6], modelling the canopy as if it were a spherical cup, obtained a value of k_{11} (based on projected diameter) of about 2.6. In terms of nominal diameter D_o this becomes a value of about three times that in equation 4.19; of the order of the experimental values shown in Table 4.3. They vary with the volume of air enclosed by the canopies and they decrease appropriately with increasing canopy porosity. The uncertainties in the measurements of the transverse added mass coefficients k_{33} are high but they are seen to be of the order of one fifth to one tenth the corresponding values of k_{11}.

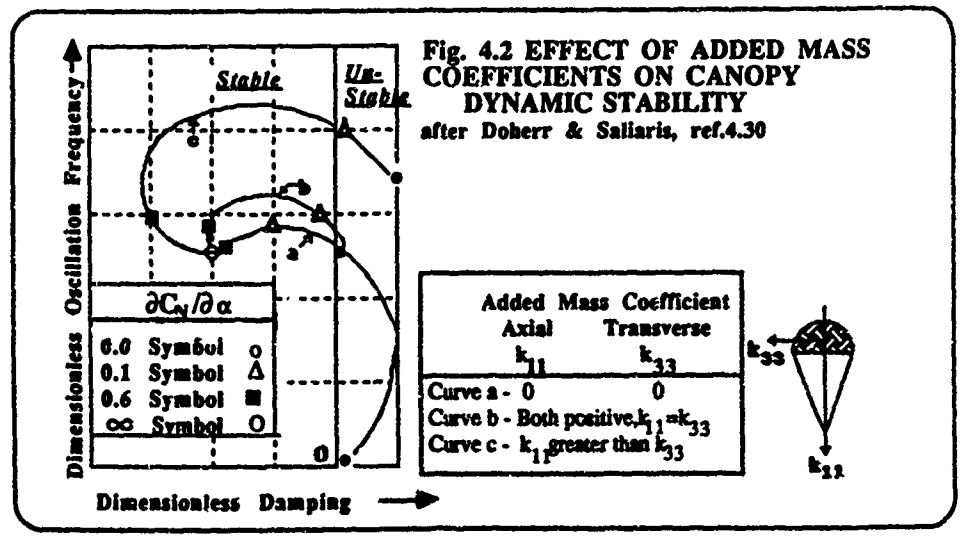

Fig. 4.2 EFFECT OF ADDED MASS COEFFICIENTS ON CANOPY DYNAMIC STABILITY
after Doherr & Saliaris, ref.4.30

The velocity-dependent tangential force coefficients measured in these tests and presented in column 2 of Table 4.3 are approximately equal the corresponding tangential force coefficients in steady motion given in column 1. Values of $[dC_N/d\alpha]_{\alpha=0}$ determined in unsteady motion and presented in column 4 of the table do not differ appreciably from

their steady-state equivalent values, $[dC_N/d\alpha]_{\alpha=0}$, presented in column 3. These similarities imply that because fully-inflated parachute canopies oscillate relatively slowly during their descent, the descent motion of parachute canopies can be considered to be quasi-steady. In the appropriate unsteady flow equations of motion, the axial added mass coefficients appear to be of considerable significance and cannot be ignored.

By appropriately linearising the equations of motion shown in Section 3.2.2 and thereby analysing dynamic stability in pitch, Doherr and Saliaris[4.30] have shown that the single most important aerodynamic characteristic a parachute canopy should possess in order for it to exhibit dynamic stability in pitch is that at an equilibrium angle of attack the rate of change of normal force coefficient with angle of attack, $dC_N/d\alpha$, must be large and positive. This, as shown in Section 2.3.2, is the same condition as that for static stability in pitch.

Where k_{11} is greater than k_{33} which Cockrell, Shen, Harwood and Baxter[4.29] have indicated to be the case for conventional parachute canopies, the effect of the added mass coefficients in the parachute equations of motion is to increase the frequency of pitching oscillations over what they would be in their absence, with little corresponding effect on the oscillation damping rate. A typical roots-locus diagram from reference 4.29 is shown in Fig.4.2.

In the curve a shown in this figure both the axial and the transverse added mass coefficients have been neglected. By considering the added mass coefficients k_{11} and k_{33} to have equal values the curve b has been obtained. With this characteristic there is a greater frequency of oscillation for a given value of $\partial C_N/\partial\alpha$ than is shown in curve a. The curve c represents the condition that $k_{11} = 2 \times k_{33}$. Here the frequency of pitching oscillations has considerably increased and there is also a mildly destabilising tendency.

In summary, unsteady aerodynamic effects on parachute dynamic stability in pitch are only of real consequence if $[dC_N/d\alpha]_{\alpha=0}$ is small. But if this is the case, in unsteady flow the axial added mass coefficient k_{11} has a destabilising tendency. Since added masses are volume dependent whereas aerodynamic forces are area dependent, this destabilising tendency will increase as the size of the paracnute canopy increases.

REFERENCES

4.1 Thomson,W. and Tait,P.G. *Treatise on Natural Philosophy*. Oxford University Press, 1867.

4.2 Kirchhoff,G.R. *Über die Bewegung eines rotations Körpers in einer Flussigkeit* (On the motion of a body of revolution in a fluid). Journal für Reine und Angew. Math., 71,237-62, 1870.

4.3 Lamb,H. *Hydrodynamics*. Cambridge University Press,1932.

4.4 Scheubel,F.N. *Notes on the Opening Shock of a Parachute*. Progress Report IRE-65, Foreign Exploitation Section,Intelligence (T-2), April 1946.

4.5 Milne-Thomson,L.M. *Theoretical Hydrodynamics*. MacMillan, 4th edition, 1962.

4.6 Ibrahim,S.K. *Apparent added mass and moment of inertia of cup-shaped bodies in unsteady incompressible flow*. Ph.D. thesis, University of Minnesota,Minneapolis,May 1965.

4.7 Klimas,P.C. Fluid Mass Associated with a Parachute Canopy. AIAA Journal of Aircraft, 14, 6, 577-580, June 1977.

4.8 Robertson,J.M. *Hydrodynamics in Theory and Applications*. Prentice-Hall, 1965.

4.9 Bessel,F.W. *On the Incorrectness of the Reduction to a Vacuum Formerly Used in Pendulum Experiments*. Berlin Academy,1826.

4.10 Lunnon,R.G. Fluid Resistance to Moving Spheres. Proc.Royal Society A, 118, 1928, 680-694.

4.11 McEwan,G.F. The Measurement of the Frictional Force Exerted on a Sphere by a Viscous Fluid, when the Centre of the Sphere Performs Small Periodic Oscillations along a Straight Line. Phys.Rev. 33, 1911, 429-511.

4.12 Relf,E.F.and Jones,R. Measurement of the Effect of Accelerations on the Longitudinal and Lateral Motions of an Airship Model. U.K.Aeronautical Research Council R.& M.613, 1918.

4.13 Cook,G. An Experimental Determination of the Inertia of a Sphere Moving in a Fluid. Phil.Mag. 6, 39, 1920, 350-352.

4.14 Frazer,R.A. and Simmons,L.F.G. The Dependence of the Resistance of Bodies upon Acceleration, as Determined by Chronograph Analysis. U.K. Aeronautical Research Council R.&M. 590, 1919.

4.15 Gracey,W. Additional Mass Effects of Plates as Determined by Experiments. NACA Report 707,1947.

4.16 Yee-Tak Yu. Virtual Masses and Moments of Inertia of Discs and Cylinders in Various Liquids. Journal of Applied Physics, 13, 1942, 66-69.

4.17 Ibrahim,S.K. Experimental Determination of the Apparent Moment of Inertia of Parachutes. U.S. Wright-Patterson AFB, FDL-TDR-64-153, 1965.

4.18 Iversen,H.W. and Balent,R. A Correlating Modulus for Fluid Resistance in Accelerated Motion. Journal of Applied Physics, 22, 3, March 1951, 324-328.

4.19 Sarpkaya,T. and Isaacson,M. *Mechanics of Wave Forces on Offshore Structures.* Van Nostrand Reinhold Co., 1981.

4.20 Bearman,P.W.,Chaplin,J.R., Graham,J.M.R., Kostense,J.K., Hall,P.F. and Klopman,G. *The Loading of a Cylinder in Post-Critical Flow Beneath Periodic and RandomWaves.* Behaviour of Offshore Structures, Elsevier Science B.V., Amsterdam, 1985.

4.21 Harwood, R.J. *Private communication.*

4.22 Hamilton,W.S. and Lindell,J.E. Fluid Force Analysis and Accelerating Sphere Tests. Proc. A.S.C.E. HY 6, June 1971, 805-817.

4.23 Lingard,J.S. A Semi-Empirical Theory to Predict the Load-Time History of an Inflating Parachute. U.K. Royal Aircraft Establishment TR 79141, November 1979.

4.24 O'Hara,F. Notes on the Opening Behaviour and the Opening Forces of Parachutes. Journal R.Ae.S. 53, Nov.1949,1053-1062.

4.25 Henn,H. Die Absinkeigenschaften von Fallschirmen *(Descent Characteristics of Parachutes)* . Deutsche Luftfahrtforschung, ZWB-U&M 6202, 1944. U.K. Royal Aircraft Establishment Translation 233,1948.

4.26 Lester,W.G.S. A Note on the Theory of Parachute Stability. U.K. Aeronautical Research Council R. & M. 3352, 1964.

4.27 Eaton,J.A. Added Fluid Mass and the Equations of Motion of a Parachute. Aeronautical Quarterly, 34, 226-242, August 1983.

4.28 Yavuz,T. *Aerodynamics of Parachutes and Like Bodies in Unsteady Motion.* Ph.D. Thesis, University of Leicester, 1982.

4.29 Cockrell,D.J.,Shen,C.Q.,Harwood,R.J. and Baxter,A.C. Aerodynamic Forces Acting on Parachutes in Unsteady Motion and the Consequential Dynamic Stability Characteristics.AIAA-86-2470CP. *Proceedings of the 9th Aerodynamic Decelerator and Balloon Technology Conference,* Albuquerque, 1986.

4.30 Doherr,K.-F. and Saliaris,C. On the Influence of Stochastic and Acceleration Dependent Aerodynamic Forces on the Dynamic Stability of Parachutes. AIAA-81-1941. *Proceedings of the 7th Aerodynamic Decelerator and Balloon Technology Conference,* San Diego, 1981.

5.PARACHUTE DEPLOYMENT AND INFLATION

Since parachutes must be designed to be sufficiently strong to withstand the opening loads which occur as part of the inflation process, when considering parachute aerodynamics an appreciation of the parameters which influence these loads and the manner in which they relate to these independent parameters is of fundamental concern. Because inflation is an unsteady aerodynamic phenomenon in which there are necessary changes in the canopy shape during the process, it is no simple matter to develop an adequate inflation model. Aerodynamic models which are available range from readily-usable empirical methods to models which by comparison are so complex as to be almost useless to the parachute designer.

5.1 INTERACTION FORCE BETWEEN CANOPY AND PAYLOAD

During the canopy deployment phase, the time-varying interactive force developed between the canopy and its payload significantly exceeds its steady-state value and it is therefore of importance. This interactive force can be measured and interpreted either when the parachute-payload system is in free flight or when it is in a wind tunnel. However, it is very difficult to establish a mathematical model which contains all the relationships necessary for it to be adequate for design purposes. From such a model the maximum loading during deployment and inflation is certainly required. Some information is desirable so that the trajectory of the parachute and payload during the inflation process can also be predicted. From more sophisticated models it might be possible to predict with confidence the stress distribution over the canopy. It certainly would be desirable if, during the inflation process, the model were capable of predicting the canopy shape and size.

Methods of analysis have been developed in three different directions:

(i). the determination of physically-based relationships the closure of which depends on the development of appropriate empirical expressions;

(ii). the reproduction of dynamic similitude in either full-scale or model test situations through the establishment of appropriate functional relationships for the required unknown parameters; and

(iii). the construction of complex mathematical models which depend on knowledge of the pressure distribution around the inflating canopy in order to establish the force required to drive the inflation process.

5.1.1 Expression for the Interactive Forces, F_I

In order to develop expressions for the time-varying force which is developed between the canopy and its payload, consider in the direction of the flight path the separate equations of motion for the parachute canopy and the payload, as

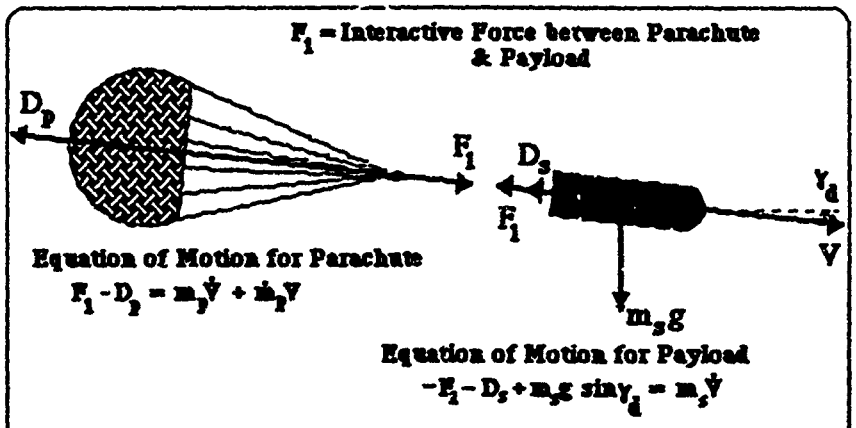

Fig.5.1 EQUATIONS FOR THE INTERACTIVE FORCE, F_I

are shown in Fig 5.1.

For the parachute canopy, neglecting its component of weight down the flight path in comparison with the canopy drag D_p and the interactive force F_I:

$$F_I = D_p + m_p\dot{V} + \dot{m}_p V \qquad (5.1)$$

As Lingard[22] has indicated, the total interactive force F_I depends on both the aerodynamic force D_p and the inertial force $-(m_p\dot{V} + \dot{m}_p V)$. When establishing the inertial force during the deployment and inflation phases,

developing an expression for the canopy mass, inclusive of its added mass (the latter defined in Section 4.1) as a function of time presents real difficulties. The aerodynamic force could be measured directly in an appropriate wind tunnel test, as could the inertial force, e.g. Lingard[5.1], but if the canopy is rigidly mounted in the wind tunnel the measured interactive force would not include the inertial term in equation 5.1.

In figure 5.2a conditions in such a wind tunnel test are shown. Under these circumstances, not only is the inertia force excluded but as the canopy inflates the velocity of air relative to it does not decrease but will remain of constant magnitude. The measurement of the interactive force is described as having been made under an *infinite mass* condition, since if the canopy mass were infinite then under the action of a finite force there could be no deceleration of

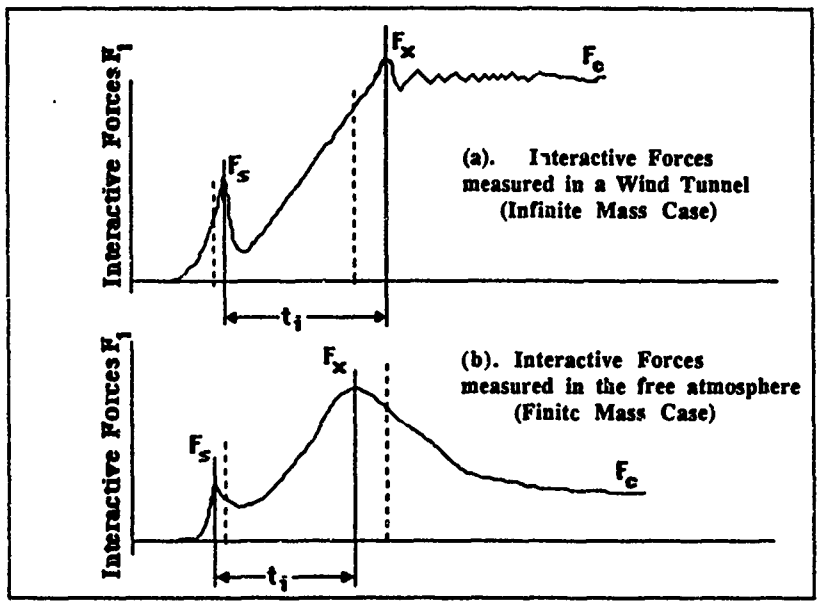

F_s Snatch Force F_x Peak Opening Force F_c Steady-State Force
t_i Inflation Time

Fig 5.2 Forces Developed Between the Canopy and the Payload During Inflation
(after Knacke[1.3])

the relative airflow.

By contrast, in figure 5.2b canopy inflation is shown as taking place under free flight conditions. Under such circumstances deceleration of the relative airflow occurs and there is a consequential reduction in the interactive forces. Appropriate measurements are now described as having been made under *finite mass* conditions, when the peak opening force F_x occurs considerably earlier than at the instant when the canopy becomes fully inflated.

The processes of canopy deployment and inflation can be divided into a number of distinct stages. The first of these is before deployment, when no aerodynamic force is developed on the canopy. The trajectory of the canopy and the payload system is then solely determined by the system's initial conditions and by the payload's aerodynamics and weight. Next follows the initial deployment stage, which ends when the canopy rigging lines are fully stretched. As this occurs the interactive force peaks to a local maximum, called the *lines-taut snatch force*. Then follows the inflation stage: this is from the instant at which the parachute canopy begins to open until it first reaches its normal fully-inflated projected area. At the commencement of this third stage the canopy skirt forms a mouth which begins to open and inhale the air. Within the canopy this inhaled air forms a ball which moves down the length of the partly-inflated canopy to the vent, with which it impacts. Once this impact has occurred the canopy begins to inflate radially and during this process the interactive force achieves a *peak opening load* As figure 5.2 indicates, this peak opening load is the maximum interactive force which the system experiences.

In this figure the interactive forces are shown as functions of time, the *inflation time* t_i being that between the peak of the lines-taut snatch force and the peak value of the inflation force or, more strictly, between the peak values of their respective coefficients. Though the inflation time is shorter than the *filling time* t_f, defined as the time taken

production of the snatch force to the instant at which the canopy first reaches its steady-state diameter and is thus considered to be fully inflated, in an experimental situation the inflation time is more clearly defined than is the filling time.

5.2 CRITICAL OPENING AND CLOSING SPEEDS. SQUIDDING

Consider an uninflated canopy in a wind tunnel. If the relative velocity of the airflow is increased a speed will be reached at which the canopy will just inflate. The practical applications of parachutes ensure their usage at much higher relative air speeds than this minimum inflation speed so this latter is not considered to be one of the canopy's critical speeds.

If in the wind tunnel the canopy were now fully inflated at a relative airflow which is above this minimum inflation speed and if this relative velocity were now gradually increased, conditions would eventually occur at which the canopy collapses to a form in which its maximum diameter was only between one-quarter and one-third of its fully-inflated diameter. Since the shape of the canopy then resembles that of a sqid, this phenomenon of canopy partial closure, occurring at a *critical closing speed* , is termed *squidding*. The occurrence of this squid configuration is a consequence of premature equilibrium between the radial pressure load and structural tension, thus the critical closing speed varies from one canopy shape to another and is a function of the canopy porosity. Still further increases in the relative air speed do not cause the squidding parachute shape to alter greatly. When the relative air speed is reduced below this critical closing speed the crown of the squidding parachute begins to inflate and at some considerably lower relative air speed, called the *critical opening speed*, the canopy suddenly opens fully.

Since it is the maximum speed at which the canopy fully inflates the critical opening speed is of importance and the velocity at which a canopy is required to deploy must be less than the critical opening speed. Once the canopy has fully inflated, the air speed relative to it seldom increases any more and thus the critical closing speed is of much less practical significance.

5.3 CANOPY INFLATION THEORIES

In his 1927 examination of canopy inflation physics, Müller[5.2] applied the principle of conservation of mass to the control volume defined by the physical boundary of the parachute canopy. In so doing, he stated that the rate of increase of the canopy volume was equal to the product of the canopy mouth area and the canopy speed. In *filling time* models which developed from this work empirical expressions were established for the variation of the canopy mouth area with time during inflation. Through his proposal that "the distance necessary for the complete inflation of a given canopy is a constant and is proportional to the linear dimensions of the parachute", Scheubel[4.4] idealised the inflation process into one in which the assumed shape of the canopy remains effectively constant as its size increases. His *filling distance* inflation theory which resulted was extended by O'Hara[4.23], who adopted a rather more sophisticated shape for the inflating canopy than Scheubel had proposed. It was then further developed by others who established relatively simple and effective inflation theories. Since Scheubel's hypothesis is generally valid and since the empirical relationships upon which these inflation theories depend must fit the circumstances for which they have been formulated, these empirical inflation theories are reliable and have been very widely adopted. However, Roberts and Reddy[5.3] have commented that their essential weakness rests in their acceptance as a necessary input of the shape which the inflating canopy adopts, rather than this time-dependent canopy shape being determined instant-by-instant as a significant output from the inflation calculation.

5.3.1 Semi-empirical Inflation Models Based on the Filling Distance Concept

In a wind tunnel test at a constant relative wind speed V, i.e. under infinite mass conditions, consider the instantaneous peak opening force F_x to be measured on the inflating canopy compared with the corresponding steady-state force F_c, measured on the fully-inflated canopy. The ratio of the peak to steady force is called the *opening force coefficient* C_x, thus

$$F_x = {}^1/_2\rho V^2 (C_DS)_p \qquad (5.2)$$

$$= F_c.C_x = {}^1/_2\rho V^2 (C_DS)_o.C_x \qquad (5.3)$$

where $(C_DS)_p$ is the canopy's instantaneous drag area and $(C_DS)_o$ is the drag area of the fully inflated canopy. Thus

$$C_x = (C_DS)_p / (C_DS)_o . \qquad (5.4)$$

Figure 5.2 shows that during canopy inflation in free flight,i.e. under finite mass conditions the peak opening force is considerably reduced from its infinite mass value. The ratio of its magnitudes, under infinite mass conditions to finite mass conditions, is called the *opening force reduction factor* and this is denoted by the symbol X_1.

Thus in free flight the peak opening force is written as

$$F_x = F_c.C_x = {}^1/_2\rho V_s^2 (C_DS)_o.C_xX_1 \qquad (5.5)$$

where V_s is the *snatch velocity*, i.e. the velocity of the parachute system at the instant when the snatch force is developed. Very approximately, this is the velocity at which the canopy deploys.

To use equation 5.5 it is first necessary to determine both C_x and X_1. Knacke[1.3; 1.9; 5.4] argues that for a given canopy shape the opening force reduction factor X_1 is a function of the *canopy loading* $W/(C_D S_o)$, where W denotes the payload weight. Since the canopy loading has dimensions, its units must be specified.

Typical values quoted by Knacke for X_1 are 1.0 for an aircraft decelerator parachute with a canopy loading of 14 kPa; 0.33 for a parachute retarder of ordnance supplies with a canopy loading of some 200 Pa and as little as 0.03 for a personnel parachute with a canopy loading of only 25 Pa.

5.3.1.1 The Mass Ratio Method In the mass ratio method, the coefficients C_x and X_1 are combined to form an *instantaneous shock factor*, x_i thus:

$$x_i = C_x X_1 = \{V^2 (C_D S)_p\} / \{V_s^2 (C_D S)_o\}. \qquad (5.6)$$

The factor x_i is the ratio of the peak interactive force developed during inflation to the interactive force when the canopy is fully inflated. In Section 5.3.3 the *load factor* X will be further described. Unlike x_i, the load factor is defined as the instantaneous value of the ratio of the aerodynamic force developed on the inflating canopy to the force in the steady state. The load factor is thus a function of time and at its maximum value it is equal in magnitude to the opening force factor x_i.

Following Schilling[5.5] the opening force factor is considered to be an empirical function of the *mass ratio* R_m. The mass ratio is a measure of the air mass included in the fully-inflated parachute canopy to the store mass m, where $m = W/g$.

Hence $$R_m = [\rho (C_D S_o)^{1.5}]/m \, . \qquad (5.7)$$

and $$C_x = \text{function } (R_m) \, . \qquad (5.8)$$

5.3.1.2 The Canopy Loading Method In the canopy loading method, the values for X_1 are given as functions of canopy loading in the manner explained in Section 5.3.1. Then, following Knacke, the opening force coefficient C_x can be considered to be a function of the canopy shape only, hence for different canopy shapes C_x can be tabulated. For example, for flat circular canopies Knacke quotes C_x as equal to 0.7.

5.3.1.3 The Pflanz Method Following Pflanz[5.6], in the manner outlined above the opening force coefficient C_x is considered to be a function of canopy shape. Then, once the increasing drag area of the inflating canopy has been modelled as a function of time by one of a number of simple, definable relationships, for a specific canopy shape the opening force reduction factor X_1 is given as an empirical function of a relationship whose magnitude can be determined.

In any of these semi-empirical inflation methods, once the peak opening force has been determined the filling time can be estimated. Using Scheubel's concept that the filling distance s_f is expressed in terms of the canopy's nominal diameter D_o by:

$$s_f = n D_o \qquad (5.9)$$

where the *fill constant* n can be determined experimentally for a given type of parachute, the filling time t_f is then expressed in terms of the velocity at deployment V_s as:

$$t_f = s_f / V_s = (n D_o)/V_s \, . \qquad (5.10)$$

5.3.2 More Sophisticated Filling Time Models

By using the two equations quoted in figure 5.1, a first order linear differential equation can be written for the motion along the flight path of the parachute and payload system.

Since the interaction force F_1 is there expressed through:

$$F_1 - D_p = m_p \dot{V} + \dot{m}_p V$$

and $$-F_1 - D_s = m_s g \sin \gamma_d + m_s \dot{V} \, ,$$

by neglecting both the payload drag compared with that of the canopy and the component along the flight path of the store weight, then:

$$-D_p = (m_o + m_p)\dot{V} + \dot{m}_p V. \qquad (5.11)$$

During the inflation process, the drag of the canopy D_p could be estimated as a function of time by adopting steady values of drag coefficient corresponding to simulated canopy shapes. In this equation the mass of the canopy is inclusive of its time-varying added mass. In order to obtain its time rate of change, some estimation must be made for the rate of change of canopy volume during the inflation process. Heinrich[5.7] and others have suggested that this be done through the application of the continuity principle:

$$\dot{\forall} = v_{in}\pi R_m^2 - v_{out}\,{}^1/_2\pi D_p^2 \qquad (5.12)$$

where $\dot{\forall}$ represents the rate of change of fluid within the canopy control volume;
$v_{in}\pi R_m^2$ represents the inflow to the canopy, with velocity v_{in} through the canopy mouth, radius R_m;
and $v_{out}\,{}^1/_2\pi D_p^2$ represents the outflow from the canopy, with velocity v_{out} through a porous hemispherical canopy of projected diameter D_p.

There remains the problem of estimating the inlet flow velocity v_{in}. Heinrich, utilising the filling time concept, assumed this to be an empirical function of the filling time t_f, determining this function from the results of appropriate wind tunnel tests.

Wolf[5.8] has argued that by using such a continuity expression, requiring empirical inputs, the prediction of canopy inflation has become unnecessarily restricted. What such filling time models have neglected is the prospect of a dynamic relationship in which the shape of the inflating canopy would be determined instant-by-instant through knowledge of the radial component of fluid momentum driving force, which depends on the pressure difference across the inflating canopy. In 1951 Weinig[5.9] had introduced such ideas and these were later developed both by Toni[5.10] and by Roberts[5.11].

5.3.3 Ludtke's Parachute Opening Force Analysis

In reference 5.12, by introducing the dimensionless ballistic mass ratio M, Ludtke throws some fresh light on the interrelationship between velocities and aerodynamic forces during the inflation process. Neglecting the mass of the parachute compared with that of the payload, in equation 5.1:

$$F_1 = D_p \qquad (5.13)$$

Then, from equations 5.2 and 5.13, together with the equation of motion for the payload in Fig. 5.1, assuming that both the payload drag and the angle of descent γ_d are negligible:

$$-D_p = -{}^1/_2\rho V^2 (SC_D)_p = m_s\dot{V} \; . \qquad (5.14)$$

Integrating equation 5.14 with respect to time from t = 0, at the peak value of the lines-taut snatch force and the velocity is the snatch velocity V_s, to t = t, when the canopy is fully-inflated and its velocity is V:

$$\int_0^t (SC_D)_p\, dt = (2m_s/\rho) \int_0^t (-\dot{V} / V^2)\, dt \qquad (5.15)$$

and since $\dot{V}\, dt = dV$:

$$= (2m_s/\rho) \int_{V_s}^{V} (-\, dV / V^2) \; . \qquad (5.16)$$

Dividing equation 5.16 through by $(C_DS)_s\, t_0 V_s$, where t_0 is the inflation time, and by writing:

$$M = \{2m_s/\rho\ (C_DS)_s\, t_0 V_s\} \qquad (5.17)$$

where M is called the *dimensionless ballistic mass ratio*. Equation 5.16 can then be solved in terms of M to give:

$$V/Vs = \frac{1}{\{1 + (1/Mt_0)\int_0^t [(SC_D)_p/(SC_D)_0]\, dt\}} \; . \qquad (5.18)$$

During inflation the expression $\int_0^t [(SC_D)_p/(SC_D)_0]\, dt\}$ is a known constant for a given type of canopy so, once a value has been ascribed to the ballistic mass ratio, the ratio V/V_s can be determined. Then, having calculated V/V_s, other characteristics of the inflation phase, such as the instantaneous shock factor x_t, can be evaluated. Ludtke argued that the dimensionless ballistic mass ratio is the most appropriate scaling parameter with which to consider the aerodynamic characteristics of parachutes during the inflation process.

5.3.4 A Dynamic Similitude Model for Parachute Canopy Inflation

Using dimensional analysis, for a given parachute system Lingard[4.22,5.13] developed a semi-empirical method of predicting over the entire operational envelope, from a limited number of field trials, the relationship between the total interactive force F_i, or the inflation load, and the time which elapses.

Assuming that the drag D_p of the parachute canopy at an instant in time is a function of:

canopy shape and size;
its instantaneous velocity V and acceleration $\dot{V}$;
the density ρ and viscosity μ of the fluid in which it is inflating;

then, by further assuming that the acceleration $\dot{V}$ is a function of:

the snatch velocity V_o;
the time t, measured from the instant when the snatch force is developed;
the canopy drag D_p;
the gravitational acceleration g;
the masses of the payload m_s and the canopy m_p;
the canopy rate of change of mass $\dot{m}_p$; and
the instantaneous angle of the parachute trajectory relative to the vertical, or the deployment angle θ;

then:

$$D_p = \text{function}\{\text{shape};\ D_o\ ;\ V_o\ ;\ t\ ;\ \rho\ ;\ \mu\ ;\ g\ ;\ m_s\ ;\ m_p\ ;\ \theta\}\ . \quad (5.19)$$

For a canopy of a given shape, by neglecting the effects of μ, m_p and $\dot{m}$, Lingard showed that for geometrically similar parachute systems with similar porosity constants:

$$C_F^* = D_p/\rho D_o^2 V^2 = \text{function}\{M_r\ ;\ F;\ \tau\ ;\ \theta\} \quad (5.20)$$

and

$$X = D_p/m_s g = \text{function}\{M_r\ ;\ F;\ \tau\ ;\ \theta\} \quad (5.21)$$

where C_F^* is the dimensionless aerodynamic force developed on the canopy;

X is the load factor, defined as the ratio of the instantaneous to the steady aerodynamic force developed on the parachute canopy;

M_r is the mass ratio, here defined as the ratio of payload mass m_s to a mass representative of that included within the canopy, ρD_o^3;

F is the Froude number V_o/gD_o defined in Section 2.3.4;

τ is the dimensionless time, $V_o t/D_o$;

θ is the deployment angle, i.e. the instantaneous angle of the parachute trajectory, relative to the vertical.

Since he was primarily concerned with personnel parachutes, in his analysis Lingard did not consider the Mach number to be a significant independent parameter.

Unsteady inflation force data obtained from experiments conducted on a variety of canopies tested over a range of mass ratios and descent parameters correlated well when plotted in the form:

$$C_F^* = \text{function}\ (\tau) \quad (5.22)$$

Lingard[5.13] therefore concluded that each canopy shape has a unique dimensionless inflation force/time signature, which can be extracted from a limited number of trials of a given system. By employing this information, together with the application of Newton's laws of motion, as shown in Chapter 3, to the system it is possible to predict the performance of the parachute and the payload system over its entire operational envelope.

5.3.5 Kinetic Models for Parachute Canopy Inflation

The inflation method, introduced in 1971 by Roberts, represented the parachute canopy by a continuous elastic system. The pressure distribution required to determine the force which causes the necessary rate of change of fluid momentum was calculated by assuming potential flow about an expanding and decelerating parabolic shell, representative of the canopy. Because of its geometrical and mathematical sophistication such an advanced model is difficult to apply and thus receives only partial acceptance within the parachute industry.

Provided that some overall data for canopies during their inflation phase have been obtained by conducting appropriate experiments, e.g. the peak opening force coefficient and the dimensionless filling time, together with their payload and canopy mass ratios, Wolf's[5.8] 1973 single degree of freedom canopy model solves the necessary momentum equations and satisfactorily predicts some observed phenomena, such as the effects of altitude on parachute inflation time. The mass ratios are defined here as the respective payload or canopy mass, divided by the mass of air displaced by a fully-inflated representative spherical canopy.

Different methods were adopted by Roberts[5.11], by Klimas[5.14; 5.15] and by others in order to identify the pressure distribution in the flow field associated with the inflating canopy. These are discussed in greater detail in Section 7.1. In 1981 Purvis[5.16] developed an analytical model based on a simplifcation of the changing canopy shape during the inflation process. This model needs no experimental inputs at all. It could be used to predict the trajectory of an inflating canopy.

In his model the canopy is modelled as a right circular cylinder whose radius is free to increase with time. For the inflation of this cylinder immersed in an inviscid and incompressible fluid an expression for the time rate of change of axial momentum over the surface of the expanding cylinder is first established and then solved. First-order effects only are considered. In reference 5.16 Purvis made comparisons for both imporous and porous canopies between the results obtained with this model and experimentally-obtained data, inflating under both infinite mass and finite mass conditions.

The real significance of analytical inflation models, such as this one developed by Purvis, is that they reveal which are the gross parameters governing the inflation process, indicating what may be the consequences of their independent variation.

REFERENCES

5.1 Lingard,J.S. *The Aerodynamics of Parachutes During the Inflation Process.* Ph.D.Thesis, University of Bristol, 1978.

5.2 Müller,W. Parachutes for Aircraft. NACA TM 450, October 1927.

5.3 Roberts,B.W. and Reddy,K.R. A Discussion of Parachute Inflation Theories. AIAA 75-1351. *Proceedings of 5th Aerodynamic Deceleration Systems Conference,* Albuquerque, 1975.

5.4 Knacke,T.W. Decelerator Systems Engineering. *Proceedings, University of Minnesota Decelerator Systems Engineering Short Course,* Albuquerque, New Mexico, July 1985.

5.5 Schilling,D.L. A Method for Determining Parachute Opening Shock Forces. Lockheed Aircraft Corporation Report 12543, August 1957.

5.6 Pflanz,E. Determination of the Decelerating Forces During the Opening of Cargo Parachutes. ATI 26111, July 1942. USAF translation of German Report FGZ 231.

5.7 Heinrich,H.G. Opening Time of Parachutes under Infinite-Mass Conditions. *AIAA Journal of Aircraft* ,6, 3, 268-272, May-June 1972.

5.8 Wolf,D. A Simplified Model of Parachute Inflation. AIAA-73-450. *Proceedings of 4th Aerodynamic Deceleration Systems Conference,* Palm Springs, 1973.

5.9 Weinig,F.S. On the Dynamics of the Opening Shock of a Parachute. TR-6, USAF Office of Aeronautical Research, Wright Air Development Center, Ohio, Feb.1951.

5.10 Toni,K.A. Theory on the Dynamics of a Parachute System Undergoing its Inflation Process. AIAA-70-1170. *Proceedings of Aerodynamic Deceleration Systems Conference,* Dayton, 1970

5.11 Roberts,B.W. Aerodynamic Inflation of Shell Type Parachute Structures. AIAA *Journal of Aircraft,* 11, 390, July 1974.

5.12 Ludtke,W.P. Notes on a Generic Parachute Opening Force Analysis. AIAA-86-2440. *Proceedings of the 9th Aerodynamic Decelerator and Balloon Technology Conference,* Albuquerque, 1986.

5.13 Lingard,J.S. A Semi-Empirical Theory to Predict the Load-Time History of an Inflating Parachute. AIAA-84-0813. *Proceedings of the 8th Aerodynamic Decelerator and Balloon Technology Conference,* Hyannis, 1984.

5.14 Klimas,P.C. Internal Parachute Flows. AIAA *Journal of Aircraft,* 9, 313-314, April 1972.

5.15 Klimas,P.C. Inflating Parachute Canopy Differential Pressures. AIAA *Journal of Aircraft,* 16, 861,Dec.1979.

5.16 Purvis,J.W. Theoretical Analysis of Parachute Inflation Including Fluid Kinetics. AIAA *Journal of Aircraft*, 19, 4,290-296, April 1982.

6. EXPERIMENTS TO DETERMINE PARACHUTE AERODYNAMIC CHARACTERISTICS

At first sight, the proper manner in which to conduct experiments in order to establish the aerodynamic characteristics of parachutes would appear to be through the use of full-scale protoypes deploying, inflating and descending through their natural environment. Indeed, some experiments are conducted in this way. Many others are performed in wind tunnels or similar environments, both because these can readily be controlled and because under these circumstances it is often much easier to obtain the required data by instrumenting the support required for the model parachute than it is to determine them from flight tests. Wind tunnels are most often used for both static and dynamic tests on model parachutes, as a means of enabling the flow around the parachutes to be visualised and for measuring as a fuction of canopy attitude the aerodynamic forces which are developed. Other facilities which have been used for special-purpose tests include water tunnels, in which air is replaced with water as the test medium in which the parachute is immersed.

6.1 EXPERIMENTS CONDUCTED ON FULL-SCALE PARACHUTES IN AIR

As described in Section 2.3.3, the drag area $C_D S_o$ of a descending parachute can be determined from a knowledge of the weight of the parachute system, the density of the air through which it descends and the descent velocity V_D. The latter can be crudely estimated by observation. James[6.1], for example, hung a 61-m long axial cord below the payload and observed the time which elapsed between the two ends of this cord striking the ground. However, Drake[6.2], by analysing kinétheodolite data over a 500ft descent, used a more sophisticated technique with which to estimate the descent velocity.

The drag area so obtained over the time of descent would be an average value. Since the canopy nominal surface area S_o is known, the average drag coefficient for the system is determined. For stable parachutes this measurement accords well with wind tunnel evaluations, but as the angle of attack of an unstable parachute varies continuously during its descent, for such a parachute there may well be a substantial discrepancy between the average value of C_D obtained during its free descent through the air and the corresponding wind tunnel evaluation of C_D at zero angle of attack.

Depending on their application, parachutes being tested may be allowed to inflate freely, having been dropped from tethered balloons, they may be ejected from aircraft, using specially-designed test vehicles such as those which have been described by Key and Barker[6.3] or they could be launched from ground-based test vehicles such as the British compressed-air launcher, recently being used at the Royal Aircraft Establishment. Such facilities can be instrumented to telemeter appropriate data from the parachute system to the ground. A test vehicle described by Barker and Nosworthy[6.4] was designed to be dropped from tethered balloons which fly at altitudes up to 1 000 m. This test vehicle fell freely and as it did so, after pre-set time intervals the test parachutes were deployed from it. Lingard used this test vehicle to obtain required the canopy inflation dimensionless time signature described in Section 5.3.4.

6.2 EXPERIMENTS IN A CONTROLLED ENVIRONMENT

Although when the weights of both canopy and payload are known the drag coefficients for stable parachute canopies can be determined by measuring their rate of descent through the atmosphere, to acquire more sophisticated aerodynamic data the instantaneous angle of attack of the canopy will also be required. To deduce this angle both the magnitude and the direction of the relative airflow must be obtained. The most satisfactory way of determining these data is to fly the canopy in a controlled environment in which the relative velocity of the fluid will be known. Thus the main reason for conducting measurements on scale models of parachutes in wind tunnels is in order to provide such a controlled environment. It is highly desirable to use wind tunnels rather than flight tests when obtaining drag data for unstable parachute canopies and when determining canopy static stability characteristics. For such measurements static tests can be performed on rigidly-mounted canopies. Similarly, some form of controlled environment is preferable when canopy inflation behaviour or dynamic stability characteristics are sought, but for these purposes dynamic testing is necessary, on models which can move through the controlled environment with a limited amount of freedom.

6.3 REQUIREMENTS FOR MODEL TESTS CONDUCTED IN A CONTROLLED ENVIRONMENT

To model the airflow round a descending parachute faithfully when it is flying in a controlled environment such as that in a wind tunnel two important requirements must be satisfied:

(i). the shape of the model, including the means of fixing it to any force-measuring apparatus and to the walls of the controlled environment, together with the canopy porosity and its flexibility, must be truly representative of the prototype full-scale parachute. The scaling of canopy flexibility, as Lee[6.5] has indicated, is particularly difficult to achieve and this can lead to problems in data interpretation, particularly for inflation loads. This shape requirement also includes ensuring that any blockage constraint which is caused by the presence of the controlled environment walls is minimal;

(ii). the Reynolds number of the test programme and also its Mach number, where it is applicable, must also be representative of the full-scale parachute. As discussed in Sections 2.2.2 and 2.2.3 these parameters need not necessarily be equal to those in full-scale flight but in the model tests any differences in their magnitudes must be considered carefully.

Inevitably, when conducting model tests the shape requirement will, to some extent, be compromised. Early experiments were often performed on rigid rather than flexible models of canopies and in some cases the tests conducted on these canopies were not performed at sufficiently high Reynolds numbers to avoid laminar boundary layer separation. Often in static tests models are mounted on axial stings which can both limit the movement of the model canopies and may develop drag forces on their own account. Because parachute canopies are bluff rather than streamlined bodies any effects on aerodynamic characteristics caused by blockage constraint can be of considerable significance.

6.4 WIND TUNNEL TESTS ON MODEL PARACHUTES

The scale effect and blockage problems referred to above were mentioned as long ago as 1946, in Block's[6.6] brief report. Early German wind tunnel tests which Manson[6.7] described are principally concerned with the establishment of the proper dimensionless parameters influencing the aerodynamic forces developed on parachute canopies, also with determining both static stability requirements and the opening-shock forces. Heinrich's wind tunnel tests, originally conducted in Germany and later in the United States, have been described in a variety of reports, such as references 1.8, 2.2, 6.8 and 6.9.

Later German research has been considered by both Doherr, in references 6.10 and 2.10, and by Saliaris[6.11]. In this experimental work the techniques which were adopted for static tests can be considered as a development of those which Heinrich had earlier implemented in the United States. Experimental methods to determine parachute dynamic stability characteristics were also developed in Germany.

Although much of the more recent British parachute testing has been performed in the free air, in reference 1.5 Dennis refers to some wind tunnel testing in the United Kingdom. Other recent British experimental work has been described by Shen and Cockrell in reference 2.11.

6.4.1 Flow Visualisation Around Model Parachutes

Wool tufts fixed to detect the onset of flow separation from model parachute canopies and smoke employed as a flow tracer are the most commonly-used wind tunnel techniques for flow visualisation around parachute canopies, though because of the rapid dissipation of the smoke the latter is not a very appropriate technique at Reynolds numbers which approach full scale.

Techniques for using neutrally-buoyant helium-filled soap bubbles as flow tracers around model parachute canopies have been described by Pounder[6.12], Klimas & Rogers[6.13], Lingard[5.1] and by Shen & Cockrell[2.11].

One of the major advantages of testing parachutes under water rather than in air is that this makes possible the use as flow tracers of either small, near neutrally-buoyant, polystyrene beads and this technique has been described by Lingard[5.1],or of hydrogen bubbles generated by local electrolysis at fine wire cathodes immersed in the water. This latter technique has been outlined by Cockrell, Huntley and Ayres[6.14].

When testing model parachute canopies under water scaling problems can arise. In particular, as Cockrell, Harwood and Shen[6.15] have discussed, the nominal porosity λ of a parachute tested under water can differ appreciably from its value when determined in air.

6.4.2 Measurement of Steady Aerodynamic Forces and Moments

In order to measure steady aerodynamic forces and moments developed on model parachutes, generally the models are rigidly fixed in their test media. By using strain gauges or other appropriate transducers the required aerodynamic reactions on the supporting structure can be determined. Such a measuring technique has been well described both by Heinrich & Haak[2.2] and by Dohen[2.10].

6.4.3 Unsteady Aerodynamic Measurements

Unsteady aerodynamic measurements have been made on model parachute canopies in order to determine both the opening loads during inflation and the added masses which are developed on unsteadily-moving fully-inflated canopies.

6.4.3.1 Wind Tunnel Measurements of Interactive Forces During Inflation under Finite Mass Conditions If model parachute canopies which are rigidly fixed in wind tunnels are inflated, this process will occur at a constant wind velocity relative to the model. In Section 5.1.1 it is explained that infinite-mass measurements made under these conditions of the interactive force F_i developed between the parachute canopy and the payload are unrepresentative of full-scale canopy inflation. However, both Heinrich & Noreen[6.16] and Lingard[5.1] have shown that by mounting the canopy in the wind tunnel so that as it inflates it is free to move, then during its inflation the surrounding air flow will decelerate relative to the canopy and the finite-mass inflation process can be modelled.

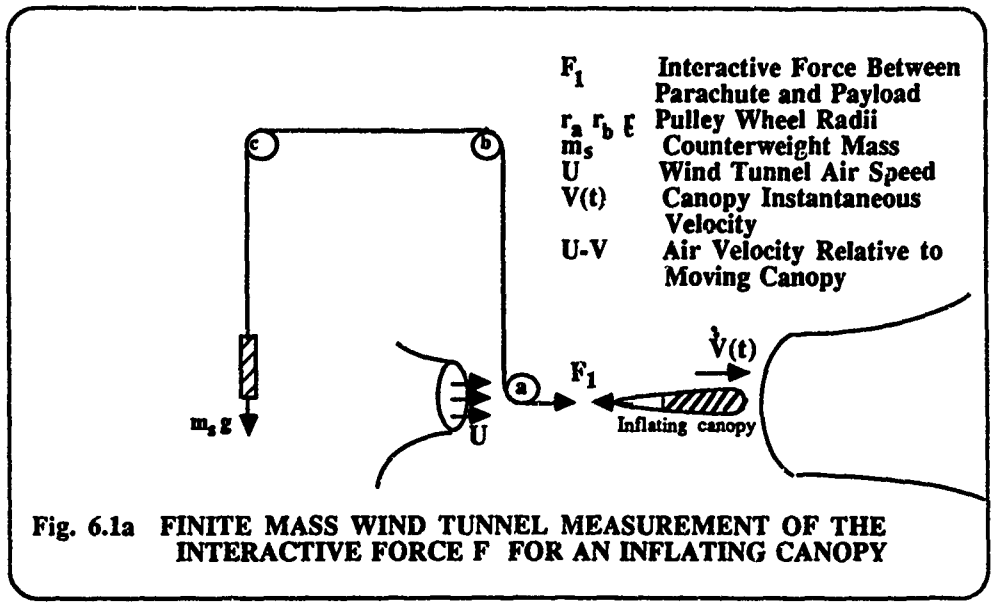

Fig. 6.1a FINITE MASS WIND TUNNEL MEASUREMENT OF THE INTERACTIVE FORCE F FOR AN INFLATING CANOPY

By appropriately modelling the system shown in Fig. 6.1a, its ensuing behaviour can be designed to be representative of that around a vertically-descending payload in the free air, decelerating under the influence of a parachute undergoing a finite mass inflation.

For the purposes of analysis Fig. 6.1b shows the same system broken into a number of separate free-body diagrams.

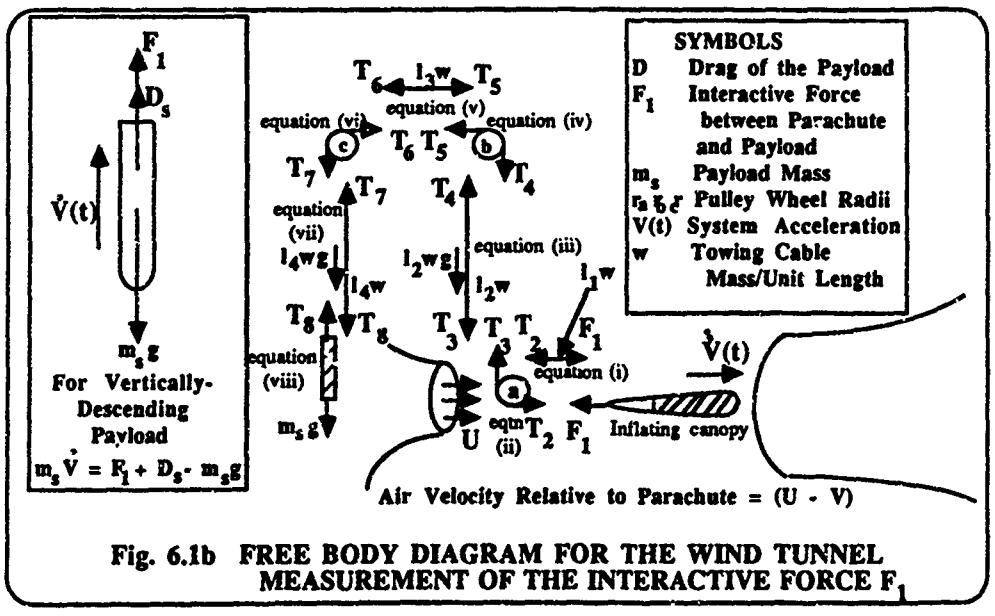

Fig. 6.1b FREE BODY DIAGRAM FOR THE WIND TUNNEL MEASUREMENT OF THE INTERACTIVE FORCE F_1

The equations of motion for each of these sub-systems are then as follows:

$$F_1 - T_2 = l_1 w\dot{V} \quad \text{equation (i);}$$
$$(T_2 - T_3)r_a = Ia\dot{V}/r \quad \text{equation (ii);}$$
$$T_3 + l_2 wg - T_4 = l_2 w\dot{V} \quad \text{equation (iii);}$$
$$(T_4 - T_5)r_b = I_b\dot{V}/r_b \quad \text{equation (iv);}$$
$$T_5 - T_6 = l_3 w\dot{V} \quad \text{equation (v);}$$
$$(T_6 - T_7)r_c = I_c\dot{V}/r_c \quad \text{equation (vi);}$$
$$T_7 - l_4 wg - T_8 = l_4 w\dot{V} \quad \text{equation (vii);}$$
$$T_8 - m_s g = m_s\dot{V} \quad \text{equation (viii).}$$

The solution to this set of equations is:

$$\dot{V}[w(l_1+l_2+l_3+l_4) + I_a/r_a^2+I_b/r_b^2+I_c/r_c^2 + m_s] = F_1 - g[(l_4-l_2) + m_s \qquad (6.1)$$

This equation is of the same form as that for the vertically-descending payload shown in Fig. 6.1b where in both equations F_1 represents the required interactive force between the payload and the parachute.

Thus, with an appropriate choice of the constants for the wind tunnel system equation 6.1 can be made to represent:

$$\dot{V}m_s = F_1 + D_s - m_s g \qquad (6.2)$$

and so the interactive force can be determined.

6.4.3.2 Experiments to Determine the Added Masses for Unsteadily-Moving Fully-Inflated Parachute Canopies In order to determine these added mass coefficients experimentally, Cockrell, Shen, Harwood and Baxter[4.28] measured the aerodynamic forces which were developed on fully-inflated model parachute canopies when the latter were subjected to a known periodic motion. The aerodynamic forces were calculated from output signals transmitted from strain gauges which were attached to the models' support sting.

6.5 AERODYNAMIC MEASUREMENTS MADE ON PARACHUTES IN OTHER FACILITIES THAN IN WIND TUNNELS

From time to time aerodynamic measurements on parachute canopies have been made in other facilities than wind tunnels. For example, at some time prior to 1967 measurements which Colbourne[6.17] has described were made of the drag developed by a 4.6 m. (15 ft.) flat circular parachute when it was caused to descend freely inside the 107 m. (350 ft.) high cooling tower of an electricity power station. This tower had a base diameter of 100 m. (325 ft.), a diameter at the apex of 66 m. (218 ft.) and a throat diameter of 62 m. (205 ft.). Its varying diameter was a source of some difficulty in that it caused a corresponding variation in descent velocity. This facility was only available over a very limited period for experimental purposes and, probably in consequence, Colbourne's report on the measurements which he made is somewhat inconclusive.

As described in reference 6.15, in order to minimise the ratio of the inertia forces developed on the canopy supports to the added masses developed on parachute canopies when they move unsteadily, measurements of the aerodynamic characteristics for fully-inflated parachute canopies have been made under water rather than in the air. Water is a suitable medium because the aerodynamic forces are proportional to the fluid density and that of water is some 800 times the density of air, whereas the inertia forces, being proportional to the density of the canopy supports, are of the same order of magnitude whichever medium is adopted. In the experiments described the canopy models were towed through a 61.0 m. long ship tank, having been suspended from the ship-towing carriage.

6.6 BLOCKAGE CAUSED BY MODEL PARACHUTE CANOPIES

The flow past any body immersed in a stream of fluid is subjected to blockage constraint, caused by restraint of the fluid's free lateral displacement. This stream of fluid might be constrained either by the test environment's solid walls, as it is when the body is held in the closed working section of a wind tunnel or in a less confined situation such as would occur if the model were immersed in an open jet of fluid. In the former state the boundary condition imposed on the flow is that at the solid boundary there can be no transverse velocity component: in the latter state the corresponding boundary condition is that the pressure along the boundary must be approximately constant and equal to the ambient pressure. In these two states, the corrections which are to be applied to measured pressures, aerodynamic forces and moments are of opposite sign. Maskell[6.18] shows that the dominant effect of blockage constraint is a simple increase in the fluid's free-stream velocity, in part related to the volume distribution of the body itself, termed *solid blockage*, and in part related to the displacement effect of the wake, termed *wake blockage*.

Conventional parachute canopies are *bluff bodies*, that is bodies for which the surrounding flow is dominated by large regions of flow separation. Unless the *blockage area ratio*, defined as the ratio of the cross-sectional area of the

body S to the cross-sectional area of the fluid stream at the body location A, is small (say under 15%), the variation in the flow pattern around the body and its downstream wake which is caused by blockage, is extreme. In the published literature, e.g. *Blockage Corrections for Bluff Bodies in Confined Flows*, reference 6.19, the emphasis is on correction of drag measurements for blockage constraint and because bluff bodies are inefficient generators of lift, little has been written about the correction of aerodynamic force components developed on them which are normal to the direction of the relative flow. An estimate from reference 6.19 for this bluff body across-flow force coefficient blockage correction ΔC_c is:

$$(\Delta C_C)/C_C \quad \approx \quad -0.2\,{}^{S}/_{A} \qquad (6.3)$$

and for a parachute canopy presenting as large a blockage ratio in a wind tunnel (or similar facility) as 15%, this gives a negligible - 3% across-flow force coefficient blockage correction .

Reference 6.19 states that for bluff bodies such as parachute canopies blockage areas of 5% and under are to be preferred; blockage areas in excess of 10% are not to be recommended. For blockage ratios under 10% corrections to the drag of conventional parachutes can readily be made by one of four methods, the choice of which depends on the location of flow separation from the canopy and the amount of experimental data which are available. This reference also contains data on blockage corrections for both mean pressure measurements and for fluctuating quantities, such as for Strouhal numbers.

Estimates of blockage constraint for gliding parachutes should be based on the more extensive literature available concerning blockage corrections for model wings in wind tunnel tests, e.g. *Lift-interference and Blockage Corrections for Two-dimensional Subsonic Flow in Ventilated and Closed Wind Tunnels*, reference 6.20.

6.6.1 Maskell's Bluff-body Blockage Constraint Method

For a conventional parachute canopy, from which the flow separates at or ahead of its maximum cross-sectional area, the estimated correction to drag, ΔC_D, consequentional on wind tunnel blockage which was obtained by Maskell[6.18] can be expressed as:

$$\Delta C_D/C_D \quad = \quad -2.77\ C_D\,{}^{S}/_{A}\ . \qquad (6.4)$$

Thus, for a model parachute canopy subjected to a 5% blockage area ratio in a wind tunnel, if the measured drag coefficient were 0.80 the corrected drag coefficient would be 0.71.

6.6.2 Cowdrey's Alternative Expression for Bluff-body Blockage Constraint

When values of drag coefficient are not readily available Cowdrey's[6.21] alternative expression for blockage constraint can be used:

$$\Delta C_D/C_D \quad = \quad -3.15\,{}^{S}/_{A}\ . \qquad (6.5)$$

Since in this relationship Cowdrey was primarily concerned with very large bluff bodies such as buildings, equation 6.5 tends to overestimate the blockage correction necessary for parachute canopies. When the blockage area ratio is only 5% the drag coefficient for the wind tunnel model must be as high as 1.3 in order to acheive the same drag correction from equation 6.5 as is given by equation 6.4. If the measured drag coefficient were 0.80, then by using equation 6.5 the corrected drag coefficient would be 0.67, instead of 0.71 which is given in the paragraph above.

6.6.3 The Quasi-Streamlined Flow Method for Bluff-body Blockage Constraint

If separation were to occur downstream of the canopy's maximum cross-sectional area, a relationship originally developed by Garner, Rogers, Acum and Maskell[6.22] gives for the blockage constraint of a conventional parachute canopy mounted centrally in a wind tunnel which has a rectangular working section of aspect ratio A:

$$\Delta C_D/C_D \quad = -0.54\ \lambda\ ({}^{S}/_{A})^{3/2} - 0.50\ C_D\,{}^{S}/_{A}. \qquad (6.6)$$

where

$$\lambda \quad = \quad 0.72(1+A)/A\ . \qquad (6.7)$$

For a measured drag coefficient of 0.80 on a conventional parachute canopy with a 5% blockage area ratio in a 1.4:1 aspect ratio wind tunnel working section, the corrected drag coefficient determined by using equations 6.6 and 6.7 is 0.77.

6.6.4 Bluff-body Blockage Constraint Determined from the Working Section Wall Pressure Distribution

If the static pressure can be measured on the wind tunnel wall at the sections at which the blockage is a maximum and at a second section downstream of the first a further method, described in reference 6.19 and originally developed by Garner et al[6.22] can be used to estimate the blockage correction.

6.6.5 Estimation of Blockage Constraint in Wind Tunnel Tests on Parachute Canopies

In order to minimise blockage effects, aerodynamic tests on model parachutes must be performed in large wind tunnels. For much of the published experimental data, not only is it not known if any blockage corrections were made by the originators, but as wind tunnel blockage area ratios may not now be readily available, making contemporary corrections is often not possible. Values of drag coefficient obtained from different wind tunnel tests can vary substantially from one another and although in published data the sign of $dC_D/d\alpha$ may be reliable, its numerical value is much less certain.

In determining the aerodynamic characteristics of parachute clusters Braun and Walcott[6.23], using the 3.7 m. (12 ft.) diameter vertical wind tunnel at the Wright-Patterson Air Force Base, Ohio found that their blockage factors approached 19%. Earlier Auterson[6.24], using the 7.3 m. (24 ft.) diameter low-speed wind tunnel at the Royal Aircraft Establishment, Farnborough, U.K., performed tests on clusters of from one to five parachute canopies with only a 4% maximum blockage area ratio. Heinrich and Noreen[6.16] tested clusters of from one to four solid flat circular and ring slot parachute canopies in the 1.5 m. x 1.5 m. (5 ft. x 5 ft.) open working section wind tunnel at the University of Minnesota at Minneapolis, experiencing blockage factors of up to 22%. Using the 2.1 m. x 3.0 m. (7 ft. x 10 ft.) working section of the Vought Corporation wind tunnel, clusters of between one and eight 0.4 m. (16 in.) nominal diameter flat circular canopies were tested by Baca[6.25]. In these latter tests the blockage factor varied from 1.8% to 14%. In his determination of the canopy drag coefficient for the free stream dynamic pressure Baca estimated the effect of this blockage factor by determining the dynamic pressure variation along the wind tunnel ceiling outside of the parachutes' boundary layer and using the value which was obtained in the plane closest to that containg the canopy skirt hem. His method is an approximation to that outlined in Section 6.6.4 above.

Shen and Cockrell[2.11] measured the drag of cross-shaped parachute canopies both in a wind tunnel with a working section of 1.14 m x 0.84 m and in a water tank which had a cross-sectional area of 3.66 m x 1.83 m. The blockage area ratios, based on the projected areas of the canopies, were between 7% and 8% in the wind tunnel and of the order of a negligible 1% in the ship tank. Corresponding drag coefficient characteristics have been drawn in Fig. 6.2. The upper curve shows the values of drag coefficient which were obtained in the wind tunnel. The corrected wind tunnel results which are shown by the open symbols in Fig. 6.2 were obtained by using equation 6.4 for the correction to drag, ΔC_{D_o}. These compare very well with the drag coefficient measurements independently obtained in the ship tank with the much larger cross-sectional area using the same model parachute canopies.

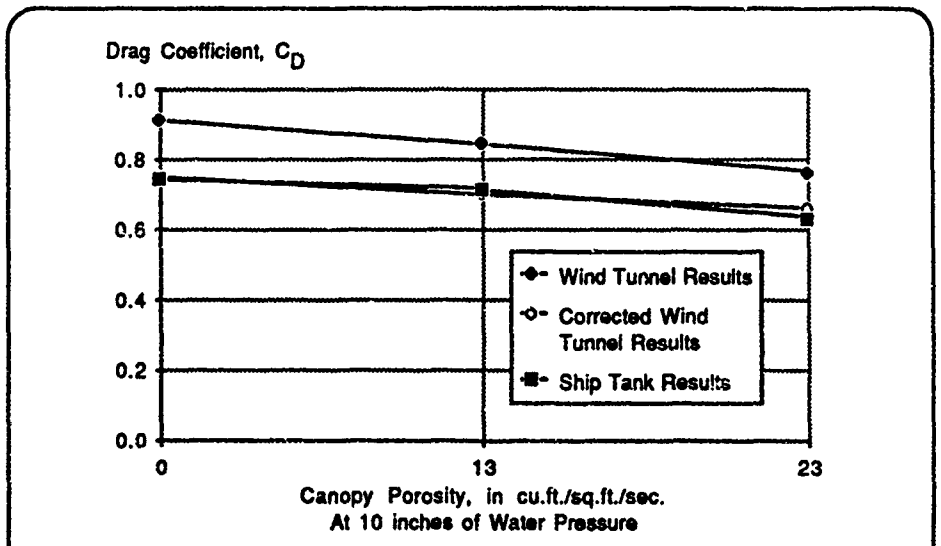

Fig. 6.2 BLOCKAGE CORRECTIONS APPLIED TO CROSS-SHAPED PARACHUTE CANOPIES - after Shen and Cockrell, ref. 2.11

REFERENCES

6.1 James,K. The Effects of Axial Cords on the Characteristics of Parachutes. U.K. R.A.E. Technical Report 72198, January 1973.

6.2 Drake,V.N. A Method of Presenting a Record of Parachute Swing. U.K. A&AEE Memo.No.302 1970 (approx.)

6.3 Key,E.J. and Barker,D.H. Development and Flight Trials of an Air-Launched Vehicle for Testing Emergency Escape Parachutes. U.K. R.A.E. Technical Report 79042, April 1979.

6.4 Barker,D.H. and Nosworthy,D.J. A Simple Test Vehicle for Preliminary Testing of Parachutes. U.K. R.A.E. Technical Report 82114, December 1982.

6.5 Lee,C.K. Experimental Investigation of Full-Scale and Model Parachute Opening. AIAA-84-0820. *Proceedings of the AIAA 8th Aerodynamic Decelerator anmd Balloon Technology Conference*, Hyannis, April 1984.

6.6 Block,W.E. Problems of Wind Tunnel Investigation of Parachute Stability. U.S. Army Air Forces Air Command Memorandum TSEA C14-45816-2-1, June 1946.

6.7 Manson,F.G. German Wind Tunnel Parachute Research. U.S. Air Materiel Command Report F-SU-2136-ND, May 1947.

6.8 Heinrich,H.G. Performance of and Design Criteria for Deployable Aerodynamic Decelerators. U.S. ASD-TR-61-579, December 1963.

6.9 Heinrich,H.G. Drag and Stability of Parachutes. *Aeronautical Engineering Review*, June 1956, pp.73-79.

6.10 Doherr,K.-F. Dreikomponentenmessungen an Fallshirmmodellen zur Ermtllung der ststischen Stabilität. DFVLR report FB 68-50, March 1968.

6.11 Sa'iaris,C. Subsonic Parachute Design, Performance and Similarity Laws (Scale Effects). Testing Capabilities Workshop, U.S. Air Force Flight Dynamics Laboratory, October 1980.

5.12 Pounder,E. Parachute Inflation Process Wind Tunnel Study. Wright Air Development Center, TR 56-391, Wright-Patterson Air Force Base, September 1956.

6.13 Klimas,P.C. and Rogers,D.F. Helium Bubble Survey of a Parachute Opening Flowfield Using Computer Graphics Techniques. AIAA 75-1368. *Proceedings of the 5th Aerodynamic Deceleration Systems Conference*, Albuquerque, November 1975.

6.14 Cockrell,D.J., Huntley,I.D. and Ayres,R.M. Aerodynamic and Inertial Forces on Model Parachute Canopies. AIAA 75-1371. *Proceedings of the 5th Aerodynamic Deceleration Systems Conference*, Albuquerque, November 1975.

6.15 Cockrell,D.J.,Harwood,R.J. and Shen,C.Q. Measurements of Aerodynamic Forces on Unsteadily Moving Bluff Parachute Canopies. *Proceedings of the 59th Meeting of the AGARD Fluid Dynamics Panel Symposium*, Monterey, October 1986.

6.16 Heinrich,H.G. and Noreen,R.A. Analysis of Parachute Opening Dynamics with Supporting Wind-Tunnel Experiments. *AIAA Journal of Aircraft*, 7 ,4, pp. 341-347, July-August 1970.

6.17 Colbourne,P.J. Use of a Cooling Tower as a Vertical Wind Tunnel. U.K. Royal Aircraft Establishment TR 67312, December 1967.

6.18 Maskell, E.C. A Theory of the Blockage Effects on Bluff Bodies and Stalled Wings in a Closed Wind Tunnel. ARC R & M 3120, Aeronautical Research Council, U.K. Nov.1965.

6.19 Blockage Corrections for Bluff Bodies in Confined Flows. Item No.80024, Engineering Sciences Data Unit, London, 1980.

5.20 Lift-interference and Blockage Corrections for Two-Dimensional Subsonic Flow in Ventilated and Closed Wind Tunnels Item No.76028, Engineering Sciences Data Unit, London, 1976.

6.21 Cowdrey,C.F. The Application of Maskell's Theory of Wind Tunnel Blockage to Very Large Solid Models. NPL Aero.Rep. 1268, National Physical Laboratory, Teddington, U.K. 1968.

6.22 Garner,H.C., Rogers,E.W.E.,Acum,W.E.A. and Maskell,E.C. Subsonic Wind Tunnel Wall Corrections. AGAKDograph 109, Advisory Group for Aerospace Research & Development, NATO, Paris, October 1966.

6.23 Braun,J.F. and Walcott,W.B. Wind Tunnel Study of Parachute Clustering. Technical Report ASD-TDR-63-159, Aeronautical Systems Division, Wright-Patterson Air Force Base,Ohio,1963.

6.24 Auterson,E.I. Wind Tunnel Tests on Clusters of Parachutes. ARC R & M 2322, Aeronautical Research Council, U.K. March 1945.

6.25 Baca,K. An Experimental Study of the Performance of Clustered Parachutes in a Low-Speed Wind Tunnel. Sandia Report SAND 85-0813, National Technical Information Service, Springfield VA, Dec.1985.

7. METHODS OF ANALYSIS FOR FLOW AROUND PARACHUTE CANOPIES

For a variety of reasons analytic solutions are required to a number of parachute aerodynamic problems. Because of the interactive relationship between the canopy shape and the aerodynamic forces developed on it, even when it is possible to make experimental measurements they may well be insufficient for predictive purposes. Often the unsteady nature of the flow around bluff parachute canopies causes difficulties in both the planning and the execution of experimental programmes and even where many aerodynamic characteristics have been described in Section 2 as steady, they are in fact the average values of time-varying quantities which fluctuate with the unsteady wake pattern downstream. For these and other reasons reliable experimental solutions for parachute aerodynamic characteristics can be difficult to obtain and analytical solutions are sought, not only for predictive purposes but also in order to obtain a better understanding of the fluid flow processes involved.

A thorough analysis of the whole flow field around the parachute is possible only by solution of the Navier-Stokes equations. Though certain low Reynolds number flow problems do respond to the computer solution of these equations the flow round a parachute canopy and payload is at a high Reynolds number, implying that convection in the flow field is of more significance than diffusion and that viscosity is a relatively unimportant fluid property. In the immediate future parachute aerodynamic characteristics are most unlikely to be obtained from full solutions to the Navier-Stokes equations and other methods must be sought instead. However, because the three-dimensional flow field around a bluff body such as a parachute canopy contains large-scale structures which arise from free-shear layers brought about by flow separation, its solution is far from staightforward..

Currently there are two possible lines of attack, in both of which a largely irrotational flow field is assumed. In the first of these approaches, in spite of some evident disadvantages in this assumption, the entire flow field outside of any near-surface singularities is considered to be irrotational. This is the method that Ibrahim, Klimas and Roberts all adopted, described below in Section 7.2. In the second, described in Section 7.3, an identifiable region of vorticity is used to model the characteristics of the wake which is shed by the parachute.

Irrotational flow is an essential ingredient of any analytical model which is developed in order to determine the characteristics of the flow around an arbitrarily-shaped body, for it is only if the flow is irrotational that it possesses a velocity potential and hence can be termed *potential flow*. Potential flows can be steady or unsteady. In steady potential flows streamlines can be drawn orthogonal to the equipotential lines. Vorticity is a measure of fluid element rotation thus, in a region in which a fluid is considered to be *irrotational*, there can be no vorticity. Since vorticity is necessarily present in fluid regions in which there are shear stresses, within boundary layers and wakes the flow is not potential. Thus, it is an idealisation to conceive of the whole flow field in which a given body is immersed as being potential. To contrast this idealisation with the actual flow field, in which vorticity is present in certain high shear regions, the potential flow field is also referred to as *ideal fluid flow*, or sometimes as *perfect fluid flow*. It is customary, though not essential, to consider that a characteristic property of an ideal fluid is its incompressibility.

Certain features of unsteady flows around bluff bodies such as parachute canopies can be predicted with remarkable accuracy by using steady flow models but with such methods a cautious approach is necessary. In reference 7.1 it is stated that "they may amount to little more than the creation of a highly idealised flows, some of whose features coincide with the corresponding features of the real flow. The extent of the approximations inherent in such models might only be revealed by the comparison with experiment of other features of the flow, such as the pressure distribution over the downstream surface of the bluff body. It is at this point that we are handicapped by the fact that experimental techniques are, at this moment, lagging behind the advance of theory".

7.1 RELEVANCE OF POTENTIAL FLUID FLOW SOLUTIONS TO PARACHUTE AERODYNAMICS

In steady potential fluid flow all or a part of the immersed body's impervious boundary is considered to be one of a family of streamlines which represent the flow. Since these streamlines and their associated equipotential lines form an orthogonal net, in a fluid which is wholly irrotational the flow pattern which is developed around a symmetrically-shaped body is itself symmetrical. This leads to a symmetrical pressure distribution and in consequence in steady flows, to zero normal pressure drag, or *form drag*, developing on the immersed body. By considering the momentum of the entire flow field surrounding the immersed body it can readily be shown that, provided that the body's dimensions are finite and it is considered to be immersed in a steady, frictionless incompressible fluid which is entirely free of vorticity, then regardless of its shape no net aerodynamic force can be developed on that immersed body. This is a statement of the *D'Alembert Paradox*.

In view of this paradox and considering the aerodynamic characteristics which are required from an analytical model of a parachute, the apparent lack of relevance of potential flow solutions to parachute aerodynamic problems must certainly be considered. In spite of what D'Alembert declared to be a paradox, lift is certainly developed on some bodies which are immersed in potential flows and similarly, trailing-vortex drag component forces can be generated on models which have a finite span. However, the major part of the drag developed on parachute canopies is form drag

and if they are immersed in steady potential fluid flows which are wholly irrotational, it is not possible to determine this form drag from solutions to potential flow problems. This is the evident disadvantage of the first approach.

Through free-streamline theory, originating with Helmholtz[7.2] and Kirchhoff[7.3], which postulated that the pressure is constant on streamlines which extend to infinity from the bluff body and which bound the wake region, a non-zero drag force on such an immersed bluff body can be established. Following Fage and Johansen's[7.4] assumption that the fluid pressure varies along these boundary streamlines, a plausible value for the bluff body drag can be obtained. Although in free-streamline theory the assumption is made that flows are steady, this approach serves as a useful introduction to the vortex-sheet methods of analysing unsteady flows around bluff bodies, described below in Section 7.3.

7.2 THE IRROTATIONAL FLOW FIELD APPROACH

7.2.1 Ibrahim's Solution for the Added Mass of Fully-Inflated Parachute Canopies

By idealising their shapes into thin-walled, rigid cup shapes and applying conformal transformation techniques Ibrahim[4.6], in his 1965 doctoral thesis, developed a potential solution for flow around fully-inflated parachute canopies. His reason for making this analysis was in order to determine the added mass coefficients associated with the unsteady oscillatory motion of the parachute during its descent. Lester[4.25], whose work was broadly contemporary with that of Ibrahim, noted that "the theoretical concept of added mass with regard to motion of bodies in an ideal fluid is not necessarily representative of the physical phenomena which occur in a real fluid". Later experimental measurements tend to justify this earlier opinion.

7.2.2 Klimas' Parachute Canopy Method

Only certain representative shapes of immersed bodies respond well to the methods of conformal transformation and a more flexible technique is required with which to represent axi-symmetrical canopies with arbitrary cross-sectional shapes. Milne-Thomson[4.5] modelled two-dimensional thin aerofoil sections, representing them by a line vortex sheet and in 1972 Klimas[5.13] followed his example, modelling an axi-symmetric parachute by a system of vortex rings which covered the canopy. The modelling of axi-symmetric shapes by vortex rings is discussed in reference 7.1. This representation enabled Klimas to include the effects of canopy porosity in his model.

Klimas' initial objective was that of determining the pressure field round an inflating canopy. In seeking to meet this aim he needed good experimental data with which to validate his model and this was not easy to find. In 1977, like Ibrahim, Klimas[4.7] used a development of his earlier model as the basis for determining the added mass coefficients in unsteady motion, remarking that "no obstacle exists to extension of the approach to include the non-steady canopy geometries (of the inflation process)". In a third paper published in 1979 Klimas[5.14] adopted his earlier vortex sheet canopy model as the means by which he determined the pressure field round an inflating parachute canopy. The shapes adopted by the inflating canopy were assumed and the process of inflation was permitted to continue until the axial aerodynamic force, evaluated by integration of the pressure distribution, was equal to a value which had been indepently determined or had been assumed.

An objection, ascribed to Roberts and Reddy[5.3] in Section 5.3, to this technique which Klimas adopted is the necessity for the inflating canopy shape to be an input to the determination of the pressure field, rather than the canopy shape developing as a significant output to the analytical procedure which is adopted.

7.2.3 Roberts' Inflating Canopy Method

In order to determine inflation times and inflation loads for parachutes, Roberts[5.11] determined the unsteady pressure distribution over an axisymmetric, impervious, inflating shell. In order that its potential flow pressure distribution could be developed by conformal transformation techniques from that in a right-angled corner a paraboloid was chosen as the general shape of this shell. At any instant in time the dynamics of the canopy inflation process could be determined from the payload mass and knowledge of the drag force developed on the canopy, the latter being given immediately from the known pressure distribution which developed over it.

Its aerodynamic analysis is developed by considering the existence of a starting vortex ring which forms and grows in a location adjacent to the skirt of the shell. It is through the existence of this vortex ring that the Kutta-Joukowski condition is satisfied at the shell skirt. From observations of parachute characteristics it is evident that, as the shell becomes nearly fully inflated, the vortex ring at the shell skirt become unstable, drifting downstream from the shell and forming the axisymmetric wake in the canopy. In his model Roberts showed how the position of this vortex ring could be determined.

In Roberts' method, unlike the one which Klimas adopted, the particular shape of the inflating canopy followed from the determination of the pressure field which developed around it. Essentially, it is a vortex sheet method of calculation applied to a canopy shape which varies with time.

7.3 VORTEX SHEET METHODS OF REPRESENTING THE WAKES SHED BY PARACHUTES

The representation within an otherwise irrotational fluid flow of an identifiable region of vorticity has a long history. This is the method which Prandtl[7.5] adopted to model the boundary layer. Lanchester[7.6] similarly

modelled the vortex system which forms behind an aircraft wing and von Kármán[7.7] used vortex sheet methods to model the wake established behind a bluff body .

The first representation by discrete vortices of a two-dimensional continuous vortex sheet was made by Rosenhead[7.8]. He showed that this vortex sheet was unstable, rolling up smoothly into concentrated clusters of vortices. An extensive review of more recent two-dimensional vortex sheet representations has been made by Clements and Maull[7.9].

The simulation by vortex rings of the wakes shed by axi-symmetrical bodies poses an additional problem to the two-dimensional representation; that of the self-induced velocity field induced by the curvature of the vortices. In order to model the asymmetry of the real fluid flow around a symmetrical parachute canopy, Shirayama and Kuwahara[7.10;7.11] have simulated the wake by using segmented vortex rings, thereby forming a series of vortex sticks. In a recent review paper Strickland[7.12] has described a number of contemporary applications of vortex-sheet analysis methods for parachute canopies.

By using vortex-sheet methods it is possible to determine the pressure distribution over an immersed bluff body under any known instantaneous velocity and acceleration. This can then be integrated to obtain the component aerodynamic forces and moments developed in any required direction. Work by Rehbach[7.13] has shown that by such a method normal force coefficients developed on inclined flat plates can be determined.

Canopy porosity can be simulated in any panel of the bound vortex rings. Although compressibility effects have been included in steady flow vortex methods Strickland remarked that at this instant of time their inclusion into the unsteady method necessary to simulate the a bluff body wake appeared to be premature.

7.3.1 Vortex Sheet Methods Applied to Bodies of Various Geometries by Meyer and Purvis

Preliminary results from a model capable of predicting unsteady, viscous, incompressible flows about parachute canopies have been published by Meyer and Purvis[7.14]. At the time at which they made this presentation the results from their model were limited to the two-dimensional pressure distribution around a circular cylinder, which they compared with experimental results. Ultimately, they plan to extend their technique so that it can be applied to predictions of the pressure distribution associated with an inflating axi-symmetric parachute canopy.

7.3.2 Flow Around Discs by de Bernardinis, Graham and Parker

Assuming potential fluid flow around a disc and representing that disc by an appropriate distribution of bound vortex rings while the vortex sheets that it sheds are simulated by discrete vortex rings, de Bernardinis, Graham and Parke[7.15] obtained a solution to flow behaviour in the neighbourhood of a sinusoidally-oscillating disc. The method which they adopted is essentially similar to that used by Roberts in reference 5.11. The Kutta-Joukowski condition was applied at the region of flow separation from the disc. From this region a free vortex sheet, represented by a number of vortex rings, was convected with the local fluid velocity.

The flow was determined at a number of different Keulegan-Carpenter numbers, $K = V_{max}T/R$, where V_{max} is the amplitude of velocity oscillation for the disc, R is the disc radius and T the period of oscillation. These calculations were found to be in reasonably good agreement with results from flow visualisation experiments. The unsteady pressure field acting on the disc was also determined. It was concluded that the vortex-sheet method which they adopted accurately predicted the dominant features of the flow around the oscillating disc.

7.3.3 McCoy and Werme's Axisymmetric Vortex Lattice Method Applied to Parachute Shapes

Applications to axisymmetric parachute canopy shapes are shown in the paper describing McCoy and Werme's[7.16] vortex lattice method, still in its early stages of development. By assuming that the velocity-dependent drag coefficient was equal to its steady-state value in a decelerating flow and considering the remaining part of the total aerodynamic force to be acceleration-dependent, the instantaneous added mass coefficients described in Section 4.2 were calculated. McCoy and Werme found that although the initial value of these coefficients compared well with an inviscid flow calculation made in the absence of vortex sheets, over a period of time the added mass coefficients rapidly decreased in value, eventually becoming negative.

7.4 SUMMARY OF REQUIREMENTS FOR THE DETERMINATION OF PARACHUTE AERODYNAMIC CHARACTERISTICS BY VORTEX SHEET METHODS

Currently, analytical methods are required by which the aerodynamic characteristics of parachute canopies can be determined under the following flow conditions:

(i). in steady flows.

The current state of the art is that parachute drag coefficients appear to be calculable by vortex-sheet methods and it is probable that by similar techniques both normal and axial aerodynamic force coefficients could be calculated. Although determinations have been made by Rehbach[7.13] on rectangular plates, no publications are known in which this has been shown for axisymmetric bodies like parachute canopies, set at known angles of attack in steady flows.

(ii). in unsteady flows, for fully-inflated parachute canopies.
The problem here is to determine the added mass coefficients analytically. Ibrahim[4,5] and others have achieved this for wholly irrotational flows, although Lester[4,15] has questioned the engineering significance of the results which they obtained. As McCoy and Werme[7,16] have indicated such determinations can be made by vortex-sheet methods but as yet it is still too early for much published data to be available.

(iii). in unsteady flows, for inflating parachute canopies.
Here, reliable methods are still required with which to couple the aerodynamic forces obtained by vortex-sheet methods to a structural analysis technique. Roberts[5,11] has indicated that such a coupling is possible: Meyer and Purvis[7,14] are attempting its solution, but, as yet, there are no indications that a solution has been obtained to this problem.

REFERENCES

7.1 Thwaites, B. (Editor). *Incompressible Aerodynamics*. Clarendon Press, Oxford. 1960

7.2 Helmholtz, H.von. Über Discontinuierliche Flüssigkeitsbewegungen. *'Mber' K. Akad. Wiss.*, Berlin, 23, 215, 1868.

7.3 Kirchhoff, G. Zur Theorie Freier Flüssigkeitsstrahlen. *J. Reine Angew. Math.* 70, 289, 1869.

7.4 Fage, A. and Johansen, F.C. On the Flow of Air Behind an Inclined Flat Plate of Infinite Span. U.K. Aeronautical Research Council R. & M. 2127, 1927

7.5 Prandtl, L. Über Flüssigkeitsbewegung bei sehr kleiner Reibung. *Verh. 3. int. Math.-Kongr.*, Heidelburg 484, 1904.

7.6 Lanchester,F.W. *Aerodonetics*. Constable, London. 1908.

7.7 Kármán, T.von Flüssigkeits- und Luftwiderstand. *Phys.Z.* 13, 49, 1911.

7.8 Rosenhead,L. Formation of vortices from a surface of discontinuity. *Proceedings of the Royal Society, A*, 134, pp.170-192, 1931.

7.9 Clements, R.R. and Maull, D.J. The Representation of Sheets of Vorticity by Discrete Vortices. *Progress of Aerospace Science*, 16, 2, pp.129-146, Pergamon Press, 1975.

7.10 Shirayama, S. and Kuwahara,K. Computation of Flow Past a Parachute by a Three-Dimensional Vortex Method.
AIAA-CP-86-0350. *Proceedings of the AIAA 24th Aerospace Sciences Meeting*, Reno, January 1986.

7.11 Shirayama, S. and Kuwahara,K. Superconductors and Fluid Dynamics. *Proceedings of the First Nobeyama Workshop,1985*, Edited by Kuwahara, Mendez and Orszag. Springer-Verlag, 1985.

7.12 Strickland,J.H. On the Utilization of Vortex Methods for Parachute Aerodynamic Predictions. AIAA-CP-86-2455. *Proceedings of the AIAA 9th Aerodynamic Decelerator and Balloon Technology Conference*, Albuquerque, October 1986.

7.13 Rehbach,C. Numerical Calculation of Three-Dimensional Unsteady Flows with Vortex Sheets. AIAA-CP-78-111. *Proceedings of the 16th Aerospace Sciences Meeting*, Huntsville, January 1978.

7.14 Meyer, J. and Purvis, J.W. Vortex Lattice Theory Applied to Parachute Canopy Configurations. AIAA-84-0795. *Proceedings of the AIAA 8th Aerodynamic Decelerator and Balloon Technology Conference*, Hyannis,April 1984.

7.15 deBernardinis,B., Graham,J.M.R. and Parker,K.H. Oscillatory Flow Around Disks and Through Orifices. *Journal of Fluid Mechanics*, 102, pp.279-299, 1981.

7.16 McCoy,H.H. and Werme,T.D. Axisymmetric Vortex Lattice Method Applied to Parachute Shapes. AIAA-CP-86-2456. *Proceedings of the AIAA 9th Aerodynamic Decelerator and Balloon Technology Conference*, Albuquerque, October 1986.

8. EXTRA-TERRESTRIAL APPLICATIONS OF PARACHUTES

During the ten years which began in 1976 intensive activities in both the United States of America and the Soviet Union have been directed towards exploring the characteristics of three other planets in the solar system, Mars, Venus and Jupiter. In separate missions during July and August 1976 two Viking instrument packages launched from the United States were soft-landed on to the surface of the planet Mars. Parachutes were used on both of these operations as a significant part of their deceleration phase. The entry capsules entered the Martian atmosphere at a Mach number of about 2.0, at which stage the parachutes were deployed in order to decelerate the system. They were then jettisoned as retropropulsion was responsible for the payloads' terminal descent. As the atmospheric characteristics on the planet Mars might well support life as we understand it, it was important to sterilise the entire descent systems, including the parachute canopies. This was done for 200 hours at a temperature of about 140 deg.C. (280 deg.F).

A mission whose purpose is to bring back to earth a selected 5 kg. set of sample materials from the surface of Mars had been planned by the United States. This was to have taken place in the late 1980's, but budgetary and other considerations have delayed this intended mission until the 1990's.

In September 1977 two United States Pioneer probes began their journey to the planet Venus, having been scheduled to arrive there in December 1978. For partial trajectory control over altitudes from 67 - 44 km in the Venus atmosphere the largest of these two probes was designed to employ a parachute. Though this mission was sufficiently successful for some data to be acquired, it is not known by the writer to what extent this larger probe and its parachute decelerator materially contributed to this success.

Reference 8.1 indicates that in March 1982 two Soviet probes which had been launched in 1981 safely landed on Venus. These probes, which were called Veneras 13 and 14, had parachutes which were jettisoned about 45 km (28 miles) above that planet's surface. Since the Venus atmosphere is hostile, having an atmospheric pressure some 90 times that on earth and an atmospheric temperature which is around 450 deg C. (850 deg. F.) the surface survival time would be small. However, it was long enough for chemical analyses to be made of the soil and for landing sites to be photographed, the relevant data being radioed back to the earth. By late 1982 a total of seven successful Soviet landings on Venus had been reported but it is not known for how many of these missions parachutes were employed to decelerate the probes.

A Galileo spacecraft designed to enter the atmosphere around the planet Jupiter in August 1988 was also planned. Although scheduled for an American launch in May 1986 this research programme has also suffered considerable delays.

Over this ten year period there has been a very considerable increase in knowledge concerning the physical characteristics of the planets which were being explored. Many writers report that at the time the Venus probes were launched the atmosphere around that planet was much better understood than was the atmosphere around Mars in the late 1970's.

For all of these planets the adopted parachute designs closely resemble those which have already been used for spacecraft recovery in the earth's atmosphere.

8.1 ATMOSPHERIC CHARACTERISTICS ON MARS, VENUS AND JUPITER

According to reference 1.9, little is known with any certitude about the characteristics of the atmosphere around Mars. At the surface it is certainly very cold and it has only about 0.01 times the density of the earth's atmosphere. The pressure there has been obtained from the Mariner space research programme. Darnell, Henning and Lundstrom[8.2] report data from Mariner IV which gives pressure at the surface of Mars as probably between 5 and 10 millibars. Moog, Bendura, Timmons and Lau[8.3] add that even with the data from the Mariner 9 mission large uncertainties still remain about the Martian atmospheric densities and scale heights. For landings on Mars high entry velocities are necessary, reference 8.2 quoting 3.7 to 4.9 m/sec. (presumably what was intended was 3.7 to 4.9 km/sec.) (12 000 to 16 000 ft/sec.) at altitudes of 4.6 to 6.1 km (15 000 to 20 000ft.). The corresponding entry Mach Number was believed to be a little above 1.0. Reference 8.3 states that the parachute must be capable of operating over a Mach number range from as high as 2.0 to a low subsonic Mach number and perform without damage in a range of dynamic pressures from 24 - 479 N/m^2 (0.5 to 10 lbf/ft^2). In this reference an entry dynamic pressure of 239 - 311 N/m^2 (5.0 to 6.5 lbf/ft^2) is claimed. In a much earlier paper Heinrich[8.4], quoting NASA[8.5] and General Electric Company[8.6] data, estimated the first stage of entry into the Martian atmosphere to be at a velocity of 0.93 km/sec. (3 056 ft/sec.) at an altitude of 7.35 km. (24 000ft) and a Mach number of 4 0. Even allowing for the undoubted rapid refinement of data on the atmosphere around Mars it is clear that there are very wide uncertainty bands present.

On the planet Venus reference 1.9 indicates that the atmospheric conditions are reasonably well established. The atmospheric density is about 100 times that of the earth's atmosphere and the surface temperature is close to 480 deg.C (900 deg. F.) Because of this hostile environment, life was not considered to be possible and thus a biologically clean exploratory system was not considered essential.

A source of relevant and up-to-date information about the properties of the atmosphere around these three planets is the Journal of Geophysical Research. For example, data on the Martian atmosphere are contained in references 8.7 and 8.8. Reference 8.9 is also to a model of the atmosphere around Mars, while reference 8.10 is to the atmosphere around Jupiter.

8.2 MISSION REQUIREMENTS FOR PARACHUTES

On the Viking Mars mission reference 1.9 explains that the capsules were designed to enter the Martian atmosphere at about 245 km (800 000 ft). At about 6.5 km (21 300 ft). above the surface and at a velocity of about 365 m/sec. (1 200 ft /sec.) a disc-gap-band parachute opened. This parachute was disconnected at an altitude of about 1.2 km (4 000 ft.) when the payload velocity was about 60 m/sec. (200 ft /sec.).

On the Pioneer Venus mission, reference 1.9 states that the planet's atmosphere was entered at about 67 km (220 000 ft), the 300 kg (670 lb) probe decelerating to a Mach number of about 0.8. At this altitude the dynamic pressure was 3 300 N/m^2 (69 lbf/ft^2). Using a guide surface pilot parachute the main conical ribbon parachute was then deployed. The prime function of this 5 m (16.2 ft) nominal diameter canopy, which had a drag coefficient of 0.52, was to stabilise the probe through the Venus cloud cover so that scientific examination of the atmosphere could be carried out. By 47 km (155 000 ft) the velocity of the parachute and its payload was so low that the parachute was jettisoned, the impact of the probe on the surface of Venus occurring 37 minutes later. The requirement for this parachute was thus much more limited than was that for the Viking mission to Mars. However, as the density of the atmosphere on Venus is large and the atmospheric temperature close to the planet very high, at a lower altitude than 47 km a parachute is neither needed nor would it have been a practicable proposition.

Corridan, Givens and Kepley[8.11] indicate that the purpose of the Galileo mission is to explore the planet Jupiter and its satellites by indirect measurements, made from an orbiting vehicle, as well as more direct by atmospheric measurements, made from an entry probe. This probe is designed to enter the atmosphere of Jupiter at 47 km/sec. (29 miles/sec.), then to be slowed by its blunt forebody to a transonic velocity. At a Mach number of between 0.91 and 1.01 and a corresponding dynamic pressure of between 4 850 and 7 650 N/in^2 (102 and 160 lbf/ft^2) a 20 deg. conical ribbon pilot parachute of 1.1 m (3.74 ft) nominal diameter is to deploy. When the entry Mach number decreases to between 0.87 to 0.97 the conical ribbon main parachute of 3.8 m (12.48 ft) nominal diameter is to be deployed. The purposes of this latter are to separate the instrumented descent module fom its heat shield and to provide drag for a controlled descent through the atmosphere. Further details of the Galileo mission to the planet Jupiter are given in references 8.12 and 8.13.

8.3 HEINRICH'S 1966 ANALYSIS OF EXTRA-TERRESTRIAL PARACHUTE AERODYNAMICS

In 1966, when considering the behaviour of parachutes descending in a Martian environment, Heinrich[8.4] stated that the most significant performance characteristics of a parachute system were:

(i). its rate of descent;
(ii). its dynamic stability characteristics in pitch;
(iii). its opening time and
(iv). its opening shock load.

These characteristics depend on the weight of the payload and on the parachutes's aerodynamic characteristics. These latter are functions of the canopy shape and attitude, its Reynolds number and its Mach number. Heinrich argued that the most significant way in which the parachute canopy shape would be altered when it descended through the atmospheric environment of a planet other than the Earth is through the changes which would occur in the effective porosity of the canopy.

Working from earlier research[2.13] which he had undertaken on the porosity of parachute canopies, Heinrich argued that at a given *dimensionless pressure ratio* across the canopy the variation in the effective porosity of the canopy from that at sea level in the earth's atmosphere could be expressed as a function of two variables, the ratio of the density of the fluid in which the canopy is immersed to that of air at sea level and the Reynolds number at which the parachute descends. Heinrich defined the dimensionless pressure ratio across the canopy fabric as the ratio of the actual pressure difference across the canopy to that which would establish sonic flow in the fabric interstices. Because the fluid density in the Martian environment is much lower than it is above the earth's surface, he established that the effective porosity of a parachute canopy descending on the planet Mars would be only between 15% and 30% of its value when descending above the earth's surface.

For the type of parachute canopy envisaged for high Mach number inflation in the Martian environment he argued that the variation of its aerodynamic characteristics with Reynolds number would be weak and that the Mach number was the dominating dimensionless parameter. He therefore recommended that in model tests the Mach number should be made equal to that of the prototype, defining the modelling conditions as follows:-

(i). the model Mach number should be that of the prototype;
(ii). the fluid density for the model tests should be that of the fluid in which the prototype is immersed;
(iii). the dimensionless pressure ratio, defined above, across the canopy fabric for the model tests should be the same as that for the prototype.

By establishing these three modelling conditions, Heinrich sought to establish values of aerodynamic coefficients on model canopies in the earth's atmosphere which would be identical to those on full-scale prototype canopies in the Martian atmosphere. Then, by making the fluid density for the model canopy equal to that for the full-scale prototype, the rates of descent V_D could be related through the respective sizes of canopy, the known gravitational accelerations in both environments and the known masses of the payloads which would be attached to the canopies.

Next, he considered a simplified expression for the motion of a parachute and its payload when oscillating in pitch. Using a relationship which was similar in form to equation 3.20, but taking the origin of the parachute and payload system to be at its centroid; by neglecting the gravitational moment of the canopy about the origin compared with that of the payload at bD from the centroid, he obtained:

$$mb^2D^2\dot{q} = {}^1/_2\rho V_D^2({}^\pi/_4)\, D^2 C_m \qquad (8.1)$$

and substituting for the descent velocity V_D

$$V_D^2 = mg \,/\, [{}^1/_2\rho({}^\pi/_4)\, D^2 C_D] \qquad (8.2)$$

produced:

$$\dot{q} = (C_m/C_D)(g/b^2D)\ . \qquad (8.3)$$

With identical aerodynamic characteristics in the two environments Heinrich thus established that for $\dot{q}$ to be the same in each, then:

$$(g/D)_{Earth} = (g/D)_{Mars}\ . \qquad (8.4)$$

Since the ratio of the gravitational accelerations, $g_{Mars}/g_{Earth} = 0.38$, this established that

$$D_{Mars}/D_{Earth} = 0.38\ . \qquad (8.5)$$

Thus, the size of the model would need to be 2.63 times the size of the prototype. Similarity in the rate of descent requirement, equation 8.2, then led to the ratio of payload masses:

$$m_{Mars}/m_{Earth} = 0.38\ . \qquad (8.6)$$

Thus, in order to achieve the same aerodynamic coefficients in the two different environments Heinrich sought to make tests on a model which was of the same shape as the prototype. To ensure the shapes were wholly identical he considered how to make the canopy porosity on the Earth similar to that on Mars. Although Heinrich's model canopy was tested at full-scale Mach number its Reynolds number was dissimilar to that of the prototype.

If model aerodynamic tests in the earth's atmosphere are performed under conditions in which the air density is equal to the fluid density in the atmosphere around Mars, equation 8.2 then indicates that the rate of descent for the model will be equal that of the prototype. This entails testing the model canopy in the earth's atmosphere at an altitude of about 32 km (105 000 ft) above the earth's surface. Under these circumstances, in the earth's atmosphere the Froude number F, shown in equation 2.39 to equal $V_D^2/D_e g$, will be about one-seventh of its value for the prototype descending in the Martian atmosphere.

Although the model test in the earth's atmosphere may meet all of Heinrich's specifications, because of differences in Reynolds number and of canopy porosity in these tests there is no possibility of ensuring total dynamic similarity. However, the prototype parachute in the Martian environment has to be deployed at high Mach numbers and in order to meet this requirement highly porous ribbon canopies are required. For these there will be minimal variation of aerodynamic characteristics with Reynolds number. Since a given parachute canopy is less porous in the Martian atmosphere than it is in the atmosphere surrounding the earth and as has been discussed in Section 2.2.1.4, reducing the porosity decreases the canopy stability in pitch, it is necessary to test in the earth's atmosphere, but at altitudes of some 32 km (105 000 ft) where the atmospheric density is of the order of that on Mars, parachutes intended for use within the Martian atmosphere. If under these conditions the ribbon canopies exhibit the required stability characteristics in pitch, then in the Martian environment they should be adequately stable.

8.4 TESTS ON PARACHUTES FOR EXTRA-TERRESTRIAL APPLICATIONS CONDUCTED IN THE EARTH'S ATMOSPHERE

Reference 1.5 describes the three experimental programmes which were devised to establish the characteristics of the parachutes for Viking Mars landings. Initially, the Planetary Entry Parachute Programme was established to select the most appropriate canopy shape. Disk-gap-band, ringsail and cross parachutes were deployed at altitudes in excess of 30 km (100 000 ft.) and at Mach numbers from 1.0 to 2.8 in these rocket and balloon-launched tests. As a consequence the disk-gap-band parachute was selected.

In the subsequent Low Altitude Drop Test Programme parachute opening loads and stresses at up to 1.5 times the predicted design loads were investigated as the canopies were deployed from a B-57 aircraft flying at 15 km (50 000 ft) altitude. Finally, in order to test the transonic interference effects produced by the large and blunt forebody and to check the stability characteristics, Moog, Bendura, Timmons and Lau[8.3] report that balloon-launched tests were conducted in which a simulated full-scale Viking vehicle attached to a 16 metre (53 ft.) nominal diameter parachute was tested over a Mach number range from 0.47 to 2.18.

From reference 1.9 it is seen that tests in the earth's atmosphere of the Pioneer-Venus probe vehicle and parachute occurred in two stages. In the first of these a bomb-shaped test vehicle was dropped from an F-4 aircraft flying at 12 km (40 000 ft) altitude. In the second stage a simulated probe test vehicle with a mass of 304 kg (670 lb) together with its entire parachute system was released from a balloon at 27.5 km (90 000 ft) and the parachute was deployed satisfactorily.

Tests in the earth's atmosphere devised to simulate the Galileo-Jupiter mission are reported by Corridan, Givens and Kepley[8.11]. Parachute deployment was required at 16.5 km (54 391 ft), a dynamic pressure of 6 000 N/m^2 (125 lbf/ft^2) and a Mach number of 0.92. At transonic speeds problems were encountered because of poor parachute performance in the wake of the blunt forebody and some wind tunnel deployment tests were initiated in the NASA Langley transonic dynamics wind tunnel. In these experiments freon 12 used as the test medium and one-quarter and one-half scale models of the pilot parachute were tested. Since the wind tunnel working section had a cross-sectional area of 23 m^2 (248 ft^2) the blockage area ratios, described in Section 6.6, for these tests were a negligible 0.4% for the one-quarter scale model and between 1% and 3% for the one-half scale model.

REFERENCES

8.1 Shefter, J. Survival on Venus. How the Russians did it. Aviation Week. November 1982.

8.2 Darnell,W.L., Henning,A.B. and Lundstrom,R.R. Flight Test of a 15-Foot-Diameter (4.6-Meter) 120° Conical Spacecraft Simulating Parachute Deployment in a Mars Atmosphere. NASA TN D-4266, December 1967.

8.3 Moog,R.D., Bendura,R.J., Timmons J.D. and Lau, R.A. Qualification Flight Tests of the Viking Decelerator System.*Proceedings of the AIAA Fourth Aerodynamic Deceleration Systems Conference*, Palm Springs,1973.

8.4 Heinrich,H.G. Model Laws Governing Parachute Performance in Martian Environment. *(Modellgesetze für Fallschirmversuche im Hinblick auf die Atmosphere des Planeten Mars)*. WGLR-DGRR-Tagung, Bad Godesberg, Federal Republic of Germany, October 1966.

8.5 Levin,G.M.,Evans,D.E. and Stevens,V. Engineering Models of the Mars Atmosphere for Entry Vehicle Design. NASA Technical Note TN D-2525, 1964.

8.6 Heinrich,H.G. Basic Aerodynamic Problems of Parachute Landings on the Planet Mars. Report 66 SD 238, Re-Entry System Department, General Electric Company, Philadelphia, USA, 1966.

8.7 Owen,T., Biemann,K., Rushnek,D.R., Biller,J.E.,Howarth,D.W. and Lafleur,A.L. The Composition of the Atmosphere at the Surface of Mars. *Journal of Geophysical Research*, 82, 28, pp.4635-9, September 1977.

8.8 Seiff,A. and Kirk,D.B. Structure of the Atmosphere of Mars in Summer at Mid Latitudes. *Journal of Geophysical Research*, 82, 28, pp.4364-4378, September 1977.

8.9 Model of Mars' Atmosphere (1974). NASA SP-8010, December 1974.

8.10 Williams,G.P. Planetary Circulations:1. Barotropic Representation of Jovian and Terrestrial Turbulence. *Journal of Geophysical Research*, 35, pp.1399-1426, 1978.

8.11 Corridan,R.E., Givens, J.G. and Kepley, B.M. Transonic Wind-Tunnel Investigation of the Galileo Probe Parachute Configuration. AIAA-84-0823. *Proceedings of the AIAA 8th Aerodynamic Decelerator and Balloon Technology Conference*, Hyannis, 1984.

8.12 O'Neil,W.J. and Mitchell,R.T. Galileo Mission Overview. AIAA-83-0096. *Proceedings of an AIAA Conference*, Reno, 1983.

8.13 Vojvodich,N.S., Drean,R.J., Schaupp,R.W. and Farless,D.L. Galileo Atmospheric Entry Probe Mission Description. AIAA-83-0100. *Proceedings of an AIAA Conference*, Reno, 1983.

9.FURTHER AERODYNAMIC RESEARCH INTO PARACHUTES

Knacke[1.11] has suggested three important milestones that have occurred in parachute development:

(i). Irvin's free-fall parachute jump in April 1919 as a member of Hoffman's U.S. Army team. After freefalling for a short distance Irvin pulled a ripcord and opened his parachute pack which had no static line connection between the pack and the aircraft;

(ii). the work by Madelung's team at the Flugtechnisches Institut, Stuttgart leading to the development of ribbon parachutes in about 1934. These were necessary in order to increase the stability and reduce the inflation loads on parachutes required for the in-flight and landing deceleration of aircraft;

(iii). manoeuverable gliding parachutes. These have a complex history of development, achieving designs capable of contemporary commercial development through Jalbert's 1961 ram-air design.

Parachute aerodynamics has correspondingly developed from its initial rôle, that of providing a service to aid the understanding and extension of full-scale flight trials, conducted on descending parachutes in the atmosphere. Instead, it has become the means whereby appropriate wind tunnel tests, together with the analytical prediction of parachute performance and stability characteristics, can supplement without supplanting these flight trials.

9.1 AERODYNAMIC PROBLEMS IN FULL-SCALE FLIGHT TESTING

As has been indicated in Section 6.1, the testing of parachutes during free flight in e atmosphere appears to be the most obvious experimental procedure. However, because the atmospheric environment is uncontrolled it can be a difficult medium in which to make aerodynamic measurements which, having been made, can be as difficult to interpret. Determination of the parachute drag is still a fundamental problem but this is given by equation 2.34 once the parachute's rate of descent is known. Near the ground a mean rate of descent can be determined, either crudely by a timing process or by more sophisticated kinétheodolite methods, but both of these techniques are limited to relatively low altitudes.

Measurement of the manner in which the canopy's aerodynamic coefficients vary with the angle of attack is limited by the difficulty in determining this angle in flight. It can only be estimated when the instantaneous direction of the relative airflow is known with certainty. Since the parachute canopy is bluff the flow around it is strongly influenced both by its own shape and that of its payload. The only known method of estimating the relative airflow is from frame-by-frame study of ciné-film records and as these are unlikely to include any means of flow tracing, at best such a technique can only be a very approximate process.

Much of the parachute's flight performance and stability analysis must be determined by visual inspection, supported by photographic records. Because of this limitation it is necessary to judge the stability or the instability in pitch of a descending parachute solely in terms of the angle through which the descending parachute oscillates. During its descent the variation of such an angle can be measured through the use of gyroscopically-controlled instruments. Although this angle's amplitude is of significance if the parachute is unstable in pitch, for a stable parachute, as has been indicated in Section 2.3.2, its amplitude may be as much a function of the local atmospheric instabilities as it is of the degree of the parachute's stability in pitch. The widespread practice of quoting average angles of oscillation, particularly for stable parachutes, can therefore be misleading.

Wherever possible, canopy inflation tests are best carried out in the atmospheric environment using full-scale parachutes. Depending on the parachute application, different designs of launchers are used to carry these parachutes up to their deployment altitude. As the parachutes deploy the required aerodynamic data is relayed back to the ground control station.

9.2 AERODYNAMIC PROBLEMS IN WIND TUNNEL TESTING

Although the ultimate criterion of a parachute's performance is its behaviour in the atmospheric environment, for a better appreciation of its aerodynamic characteristics it is clearly necessary to supplement performance data gathered there with information from appropriate wind tunnel tests. In order to perform these tests the difficulties in achieving geometric similarity between the wind tunnel model and the full-scale prototype parachute canopy, which have been described in Section 6.3, must be overcome. These include blockage constraints around the bluff parachute canopy imposed by the wind tunnel walls and which, Section 6.6 indicates, necessitate testing in a facility whose working section cross-sectional area is some twenty times the parachute canopy's projected area. Parachutes required for re-entry vehicles and for extra-terrestrial applications must be tested in wind tunnels operating at full-scale Mach number and, as has been outlined in Section 8.4, this is particularly important for parachutes operating in the transonic Mach number range.

Although procedures by which canopy inflation loads under finite mass conditions can be determined in wind tunnels have been outlined in Section 6.4.3.1, they are only appropriate for large scale wind tunnel models, because the dimensionless inflation force/time signature relationship described in Section 5.3.4 is dependent on the model shape and the smaller the wind tunnel model the more difficult it is to model its shape faithfully. Lee[6.5] has confirmed that when determining inflation loads the shape of the canopy includes its flexibility and that canopy

flexibility has a marked effect on the values obtained for both the dimensionless opening time and dimensionless opening force.

The only solution to these wind tunnel problems is to use costly test facilities that will be adequate for the proposed experimental programme.

9.3 AERODYNAMIC PROBLEMS IN THE ANALYTICAL DETERMINATION OF A PARACHUTE'S CHARACTERISTICS

Following the work of Rosenhead[7.2] and of others, as has been described in Section 7.3, a promising start to the development of a theoretical model capable of representing the continuous vortex sheet which is shed by parachute canopies has been made. Strickland[7.12] has made clear that applications of this technique to parachutes are, as yet, in their infancy. Currently, analytical solutions are sought for:

(i). the steady-state pressure distribution over an imporous canopy at zero angle of attack;
(ii). the effect of canopy porosity on these last solutions;
(iii). the steady-state pressure distribution as the angle of attack is varied, making the canopy asymmetric to the flow;
(iv). the corresponding pressure distributions when the flow is unsteady;
(v). the effect on these pressure distribution of the canopy shape varying with time, as occurs in the inflation process; and
(vi). compressibility effects on all of these solutions.

There would appear to be excellent prospects of achieving such solutions in the not-too-distant future.

9.4 EFFECTS OF GROWTH IN COMPUTER POWER

The single most significant factor in the contemporary development of parachute aerodynamics is the growth in computer power, made readily available through developments in both mainframe and mini-computers. The power that is now available makes possible the replacement of semi-empirical and strongly experimentally-orientated methods of analysis. Not only does the computer readily access a vast amount of experimental data so that these can be compared for design optimisation studies but it enables solutions to be made of arrays of non-linear equations where linearisation or special-case solutions were all that used to be available. It also demands a new type of experimental approach, since analysts now require the answers to different kinds of questions. Not only does the computer make it possible to achieve complete solutions to sophisticated problems, but through its data storage capabilities and its ability to achieve numerical solutions to differential equations, it can identify the major independent parameters in any investigation and determine how required dependent parameters vary as a function of any one of them. As a direct consequence of these computer-based parameter identification and optimisation techniques industrially-relevant predictive studies are now made.

9.5 REWARDING FIELDS IN CONTEMPORARY EXPERIMENTAL RESEARCH

For much contemporary wind tunnel research Section 9.2 has indicated that large, high-speed wind tunnels, available only at national or international levels, may be necessary. However, other problems can be identified which are capable of study in more locally-available experimental facilities.

9.5.1 The Aerodynamics of High Performance Gliding Parachutes

Lingard[9.1] states that the optimum performance for conventional ram-air gliding parachutes occurs at an aspect ratio of about 2:1 when the ratio of lift to drag is about 3:1. By developing a mathematical model for the aerodynamics of ram-air parachutes he has identified the factors which limit this gliding parachute's performance.

To obtain a higher lift to drag ratio it is first necessary to close the leading edge of the parachute, leaving a single open cell on the under surface. This leads to a substantial reduction in drag but, because the internal pressure of the wing is then somewhat less than the stagnation pressure, the leading edge of the parachute will now collapse inwards and, in order to maintain the inflated shape, it is necessary to sweep the leading edge backwards. Where this has been done, the resulting swept-wing closed-cell concept for the ram-air gliding parachute develops lift to drag ratios ratios which exceed 5:1. Ratios of up to 6:1 have been predicted, doubling the glide ratio from the maximum currently possible with the contemporary unswept ram-air parachutes.

In experiments conducted in the 7.3 m. (24 ft.) diameter low-speed wind tunnel at the Royal Aircraft Establishment, Farnborough, U.K., lift to drag ratios in excess of 5:1 have been measured on such gliding parachutes. Currently, experimental research into high performance gliding parachutes is continuing in order to obtain this performance improvement without impairment of either the parachute's inflation characteristics or its stability and controllability.

9.5.2 The Aerodynamics of Rotating Parachutes

An important application for rotating parachutes which was mentioned in Section 2.3.4 is to provide a facility by which submunitions can rotate about one of their body axes during their initial deceleration and subsequent steady descent. Ibrahim[1.1] has described the search pattern which is traced by certain forms of submunition during such a

descent. Pepper[9.2] shows how these canopies are designed to generate the necessary rotation, a component of the total aerodynamic force providing the torque which results in the canopy autorotation. He also describes other benefits which can follow from canopy rotation, these are increased canopy drag and improved stability characteristics in pitch. For the rotating parachute application which he describes, that of recovery of high performance re-entry vehicles, high rates of rotation are desirable and with these the drag coefficient developed on the autorotating parachute described was some four or five times the value that it would have had if this parachute did not rotate.

Doherr, Münscher and Saliaris[9.3] defined a rotor quality number R_Q in terms of the canopy drag coefficient C_D and the rotor coefficient C_r

$$R_Q = C_r\sqrt{C_D} \qquad (9.1)$$

where

$$C_r = f\,D_o\,/V_D \qquad (9.2)$$

and f is the autorotation frequency in revolutions per second, D_o is the canopy nominal diameter and V_D its rate of descent, so that $C_r = 1/J$, J being the advance ratio, as normally defined for propellors. The significance of this rotor quality number has been discussed by Doherr and Synofzik[9.4], who describe a series of wind tunnel experiments devised to measure R_Q for a rotating guide surface parachute. The methods of performance evaluation which they describe are recommended for more general application in wind tunnel tests on rotating parachutes.

9.5.3 Experiments to Further the Application of Vortex Sheet Theories to Parachutes

Writing of the development of vortex sheet theories, a quotation included in the introduction to Section 7 stated: "It is at this point that we are handicapped by the fact that experimental techniques are, at this moment, lagging behind the advance of theory". Given the desire and the facilities to perform these necessary experiments, what facts need to be discerned from them?

Much of the experimental work performed on parachutes in wind tunnels has been with a view to determining the mean values of the aerodynamic coefficients which are developed. Any observation that these coefficients might fluctuate in magnitude has been considered to arise from extraneous factors, such as poor wind tunnel design or the blockage constraint imposed by the model.

A deeper understanding is now required of the nature of the flow around bluff bodies in general and around parachute canopies in particular. A fundamental question is: when the canopy is set symmetrically in the flow, what is the frequency at which it sheds vortices and what determines this frequency? Can it be disassociated from the stiffness of the sting support? Is it a function of the properties of the canopy fabric? Is the oscillation in resonance with a much lower amplitude driving oscillation? Is it eynolds number dependent?

If this flow in the wake is periodic, then are the aerodynamic forces developed on the canopy correspondingly periodic and if they are, with what amplitude do they vary?

Since the purpose for which this information is required is the construction of a vortex sheet model, what is the simplest form in which these new physical insights can be expressed?

REFERENCES

9.1 Lingard,J.S. The Aerodynamics of Gliding Parachutes. AIAA-86-2427. *Proceedings of the AIAA 9th Aerodynamic Decelerator and Balloon Technology Conference*, Albuquerque, October 1986.

9.2 Pepper,W.B.,Jr. New, High-Performance Rotating Parachute. AIAA-84-0808. *Proceedings of the AIAA 8th Aerodynamic Decelerator and Balloon Technology Conference*, Hyannis, April 1984.

9.3 Doherr,K.-F., Münscher,D. and Saliaris,C. Steur- und Stabilisierungsmechanismen von Submunitionen. Internal Report IB 111-86/9, DFVLR Institut für Flugmechanik, Braunschweig, Federal Republic of Germany, 1986.

9.4 Doherr,K.-F. and Synofzik,R. Investigations of Rotating Parachutes for Submunitions. AIAA-86-2438. *Proceedings of the AIAA 9th Aerodynamic Decelerator and Balloon Technology Conference*, Albuquerque, October 1986.

10. POSTSCRIPT

There continue to be a number of fundamental and challenging problems in parachute aerodynamics, the reasons for which are very similar to what they were when W.D.Brown published *'Parachutes'* [1.4] in 1951, declaring as his aim that of selecting 'the principal aerodynamic characteristics of parachutes and the various known factors which affect these characteristics'. The bluff body of the conventional parachute canopy still possesses a non-rigid structure and has a mass which is of the order of mass of the air which it displaces. However, Brown could not have appreciated how the passage of 35 years would bring such a diversity of parachute application or, accompanying this diversity, the necessity for a deeper fundamental understanding of physical principles. One of the many benefits of trying to bring threads together in this AGARDograph has been a much deeper appreciation of the developments which have occurred in such a short period of time.

Twenty years later, in a review on aerodynamic decelerators written from the Sandia Laboratories at Albuquerque, Pepper and Maydew[1.7] remarked that Brown had written the only book on parachute technology that was known to them. At that time extensive ribbon parachute development work was taking place at the Sandia Laboratories. Although this AGARDograph might not have done justice to that particular activity, it does contain more than a dozen references to significant aerodynamic research performed subsequently by individuals working at the Sandia Laboratories.

What led to these developments has been both the circumstances and the individuals whose contributions to the subject have been demanded by these circumstances. Knacke[1.11] states that 'it was World War II, its forebearings and its aftermath, that started the widespread application of parachutes for the air drop of troops and supplies, for the retardation of ordnance, the in-flight and landing deceleration of aircraft and the recovery of missiles, drones and spacecraft' and although Brown wrote with direct experience of that war he could not have foretold all of this aftermath.

Brown mentions Heinrich and Knacke, the first of whom he describes as a German technician, who designed during World War II the 'mushroom' or 'beret' parachute, primarily for dropping heavy bombs and sea mines. He referred to Knacke as a German scientist who appears to have invented the "Taschengurt". In this AGARDograph there are nine separate refererences to Heinrich's work and the contribution made to parachute research and development by the Minneapolis postgraduate school which he established, has been outstanding. Similarly, through his research and teaching. Knacke has made a series of memorable contributions to this subject. Both have been honoured by the AIAA for the outstanding parts they have played in the development of parachutes.

Over these years the most significant contribution to the dissemination of information on parachute technology has been the AIAA Aerodynamic Decelerator Conferences, held in the United States every two and a half years. Most active participants in parachute aerodynamics throughout the world have been present and have contributed to these Conferences. Pepper and Maydew refer to the first and second ones, held in 1966 and 1969. Since that time these conferences have grown in significance. In October 1986 the 9th AIAA Aerodynamic Decelerator and Balloon Technology Conference took place in Albuquerque, New Mexico.

72.

REPORT DOCUMENTATION PAGE			
1. Recipient's Reference	**2. Originator's Reference**	**3. Further Reference**	**4. Security Classification of Document**
	AGARD-AG-295	ISBN 92-835-0422-4	UNCLASSIFIED

5. Originator Advisory Group for Aerospace Research and Development
North Atlantic Treaty Organization
7 rue Ancelle, 92200 Neuilly sur Seine, France

6. Title
THE AERODYNAMICS OF PARACHUTES

7. Presented at

8. Author(s)/Editor(s)	**9. Date**
D.J.Cockrell — Editor A.D.Young	July 1987
10. Author's/Editor's Address	**11. Pages**
See flyleaf.	78

12. Distribution Statement This document is distributed in accordance with AGARD policies and regulations, which are outlined on the Outside Back Covers of all AGARD publications.

13. Keywords/Descriptors

Aerodynamic characteristics
Parachutes
Inflating
Deployment
Extra-terrestrial bases

14. Abstract

This AGARDograph discusses the principal aerodynamic characteristics of parachutes and the factors which affect those characteristics. It takes into account many of the publications that were summarised in the 1963 and 1978 United States Air Force Parachute Design Guides, the proceedings of biennial American Institute of Aeronautics and Astronautics Aerodynamic Decelerator Conferences, the Helmut G.Heinrich Decelerator Systems Engineering Short Courses held in 1983 and 1985 and 'The Parachute Recovery System Design Manual', shortly to be published by the United States Naval Weapon Center.

It is anticipated that its main readers will be recent engineering graduates entering research establishments, parachute companies or related industries so some appreciation of basic mechanics, the principles of computing and elementary fluid mechanics on the part of the reader has been assumed.

Its content includes Steady-State and Unsteady Aerodynamics, Parachute Deployment and Inflation, Experimental Investigations, Methods of Analysis, Extra-Terrestrial Parachute Applications and Some Suggestions for Future Research.

This AGARDograph has been produced at the request of the Fluid Dynamics Panel of AGARD.

AGARDograph No.295 Advisory Group for Aerospace Research and Development, NATO THE AERODYNAMICS OF PARACHUTES by D.J.Cockrell Published July 1987 78 pages This AGARDograph discusses the principal aerodynamic characteristics of parachutes and the factors which affect those characteristics. It takes into account many of the publications that were summarised in the 1963 and 1978 United States Air Force Parachute Design Guides, the proceedings of biennial American Institute of Aeronautics and Astronautics Aerodynamic Decelerator Conferences, the Helmut G Heinrich Decelerator Systems Engineering P.T.O.	AGARD-AG-295 Aerodynamic characteristics Parachutes Inflating Deployment Extra-terrestrial bases	AGARDograph No.295 Advisory Group for Aerospace Research and Development, NATO THE AERODYNAMICS OF PARACHUTES by D.J.Cockrell Published July 1987 78 pages This AGARDograph discusses the principal aerodynamic characteristics of parachutes and the factors which affect those characteristics. It takes into account many of the publications that were summarised in the 1963 and 1978 United States Air Force Parachute Design Guides, the proceedings of biennial American Institute of Aeronautics and Astronautics Aerodynamic Decelerator Conferences, the Helmut G.Heinrich Decelerator Systems Engineering P.T.O.	AGARD-AG-295 Aerodynamic characteristics Parachutes Inflating Deployment Extra-terrestrial bases
AGARDograph No.295 Advisory Group for Aerospace Research and Development, NATO THE AERODYNAMICS OF PARACHUTES by D.J.Cockrell Published July 1987 78 pages This AGARDograph discusses the principal aerodynamic characteristics of parachutes and the factors which affect those characteristics. It takes into account many of the publications that were summarised in the 1963 and 1978 United States Air Force Parachute Design Guides, the proceedings of biennial American Institute of Aeronautics and Astronautics Aerodynamic Decelerator Conferences, the Helmut G.Heinrich Decelerator Systems Engineering P.T.O.	AGARD-AG-295 Aerodynamic characteristics Parachutes Inflating Deployment Extra-terrestrial bases	AGARDograph No.295 Advisory Group for Aerospace Research and Development, NATO THE AERODYNAMICS OF PARACHUTES by D.J.Cockrell Published July 1987 78 pages This AGARDograph discusses the principal aerodynamic characteristics of parachutes and the factors which affect those characteristics. It takes into account many of the publications that were summarised in the 1963 and 1978 United States Air Force Parachute Design Guides, the proceedings of biennial American Institute of Aeronautics and Astronautics Aerodynamic Decelerator Conferences, the Helmut G.Heinrich Decelerator Systems Engineering P.T.O.	AGARD-AG-295 Aerodynamic characteristics Parachutes Inflating Deployment Extra-terrestrial bases

Short Courses held in 1983 and 1985 and 'The Parachute Recovery System Design Manual', shortly to be published by the United States Naval Weapons Center.

It is anticipated that its main readers will be recent engineering graduates entering research establishments, parachute companies or related industries so some appreciation of basic mechanics, the principles of computing and elementary fluid mechanics on the part of the reader has been assumed.

Its content includes Steady-State and Unsteady Aerodynamics, Parachute Deployment and Inflation, Experimental Investigations, Methods of Analysis, Extra-Terrestrial Parachute Applications and Some Suggestions for Future Research.

This AGARDograph has been produced at the request of the Fluid Dynamics Panel of AGARD.

ISBN 92-835-0422-4

Short Courses held in 1983 and 1985 and 'The Parachute Recovery System Design Manual', shortly to be published by the United States Naval Weapons Center.

It is anticipated that its main readers will be recent engineering graduates entering research establishments, parachute companies or related industries so some appreciation of basic mechanics, the principles of computing and elementary fluid mechanics on the part of the reader has been assumed.

Its content includes Steady-State and Unsteady Aerodynamics, Parachute Deployment and Inflation, Experimental Investigations, Methods of Analysis, Extra-Terrestrial Parachute Applications and Some Suggestions for Future Research.

This AGARDograph has been produced at the request of the Fluid Dynamics Panel of AGARD.

ISBN 92-835-0422-4

Short Courses held in 1983 and 1985 and 'The Parachute Recovery System Design Manual', shortly to be published by the United States Naval Weapons Center.

It is anticipated that its main readers will be recent engineering graduates entering research establishments, parachute companies or related industries so some appreciation of basic mechanics, the principles of computing and elementary fluid mechanics on the part of the reader has been assumed.

Its content includes Steady-State and Unsteady Aerodynamics, Parachute Deployment and Inflation, Experimental Investigations, Methods of Analysis, Extra-Terrestrial Parachute Applications and Some Suggestions for Future Research.

This AGARDograph has been produced at the request of the Fluid Dynamics Panel of AGARD.

ISBN 92-835-0422-4

Short Courses held in 1983 and 1985 and 'The Parachute Recovery System Design Manual', shortly to be published by the United States Naval Weapons Center.

It is anticipated that its main readers will be recent engineering graduates entering research establishments, parachute companies or related industries so some appreciation of basic mechanics, the principles of computing and elementary fluid mechanics on the part of the reader has been assumed.

Its content includes Steady-State and Unsteady Aerodynamics, Parachute Deployment and Inflation, Experimental Investigations, Methods of Analysis, Extra-Terrestrial Parachute Applications and Some Suggestions for Future Research.

This AGARDograph has been produced at the request of the Fluid Dynamics Panel of AGARD.

ISBN 92-835-0422-4